ANNUAL REVIEWS

Annual Review of Genetics

Meiosis: Dances Between Homologs

Denise Zickler[1] and Nancy Kleckner[2]

[1]Institute for Integrative Biology of the Cell (I2BC), Centre National de la Recherche Scientifique (CNRS), Université Paris-Sud, Université Paris-Saclay, Gif-sur-Yvette, France

[2]Department of Molecular and Cellular Biology, Harvard University, Cambridge, Massachusetts, USA; email: kleckner@fas.harvard.edu

Annu. Rev. Genet. 2023. 57:1–63

First published as a Review in Advance on October 3, 2023

The *Annual Review of Genetics* is online at genet.annualreviews.org

https://doi.org/10.1146/annurev-genet-061323-044915

Keywords

meiosis, chromosome, pairing, recombination, crossover interference, evolution, mitosis versus meiosis

Abstract

The raison d'être of meiosis is shuffling of genetic information via Mendelian segregation and, within individual chromosomes, by DNA crossing-over. These outcomes are enabled by a complex cellular program in which interactions between homologous chromosomes play a central role. We first provide a background regarding the basic principles of this program. We then summarize the current understanding of the DNA events of recombination and of three processes that involve whole chromosomes: homolog pairing, crossover interference, and chiasma maturation. All of these processes are implemented by direct physical interaction of recombination complexes with underlying chromosome structures. Finally, we present convergent lines of evidence that the meiotic program may have evolved by coupling of this interaction to late-stage mitotic chromosome morphogenesis.

1. INTRODUCTION

Meiosis is the modified cellular program in which haploid gametes (e.g., sperm and egg) are produced from a diploid progenitor germ cell. Union of male and female gametes in a zygote then restores the basic cellular diploid state. A central component of this program is shuffling of genetic information such that each gamete genome receives a different combination of genes from the two parents. As such, meiosis is fundamental to sexual reproduction. The general view from outside the field is that meiosis is complicated. One goal of this review is to ameliorate this impression. Meiosis can essentially be viewed as the mitotic program with a very few modifications which allow (*a*) recombination between, and segregation of, homologous maternal and paternal chromosomes (known as homologs) followed by (*b*) an additional round of segregation of sister chromatids, which thus produces haploid gametes. We provide an overall conceptual framework and key references that readers can use as a tour guide for further, deeper investigation.

We hope this article will be useful both to newcomers, especially those from outside the classical genetic, molecular, and cytological communities, and to those who may be familiar with some, but not all, aspects of the process. We also note that meiotic functions are important not only per se but also because activation of meiosis-specific genes in somatic cells can play key roles in initiation and/or maintenance of malignant phenotypes in cancer cells.

Our approach necessarily involves (*a*) considerable oversimplification, particularly with regard to variations among different organisms, including nonmodel organisms (1, 211); (*b*) omission of citations of vast numbers of important primary publications and researcher contributions; and (*c*) speculative, idiosyncratic, and/or controversial suggestions that, nonetheless, aim to unify known phenomena and promote further discussion.

2. BACKGROUND

2.1. One Round of DNA Replication and Two Rounds of Segregation

In mitosis, a round of DNA replication is followed by segregation of sister chromatids to opposite poles, thereby restoring the original chromosome configuration (**Figure 1*a***). By contrast, during meiosis, a single round of DNA replication is followed by two rounds of chromosome segregation (meiosis I and meiosis II), as required to produce haploid gametes from a diploid progenitor cell. At meiosis I (MI), homologs segregate to opposite poles (a process that never occurs during the mitotic program). Meiosis II (MII) sister chromatids segregate as during mitosis (**Figure 1*b***).

During mitosis (and MII), movement of sister chromatids to opposite poles requires that the segregating entities be connected. This connection occurs specifically between centromere regions. When all sister pairs have achieved bipolar orientation, the spindle checkpoint is satisfied and anaphase is allowed to proceed. The same principle applies during MI (120): Movement of homologs to opposite poles is again ensured by connectedness between the segregating units. In most organisms, this connection is provided by the presence of one or a few reciprocal crossovers, each involving one chromatid of each homolog, in combination with linkage (cohesion) between sister chromatids along their lengths (397). The resulting configuration is visible cytologically at metaphase I, where the crossover-correlated linkages comprise chiasmata (**Figure 1*b–d***). At anaphase I, release of intersister arm connections allows homologs to move to opposite poles. Centromere/kinetochore regions of sister chromatids remain connected and are released later, in mitosis-like fashion, at MII. The meiotic process also requires appropriate modifications of kinetochore orientations and spindle function and suppression of DNA replication in the period between the two divisions.

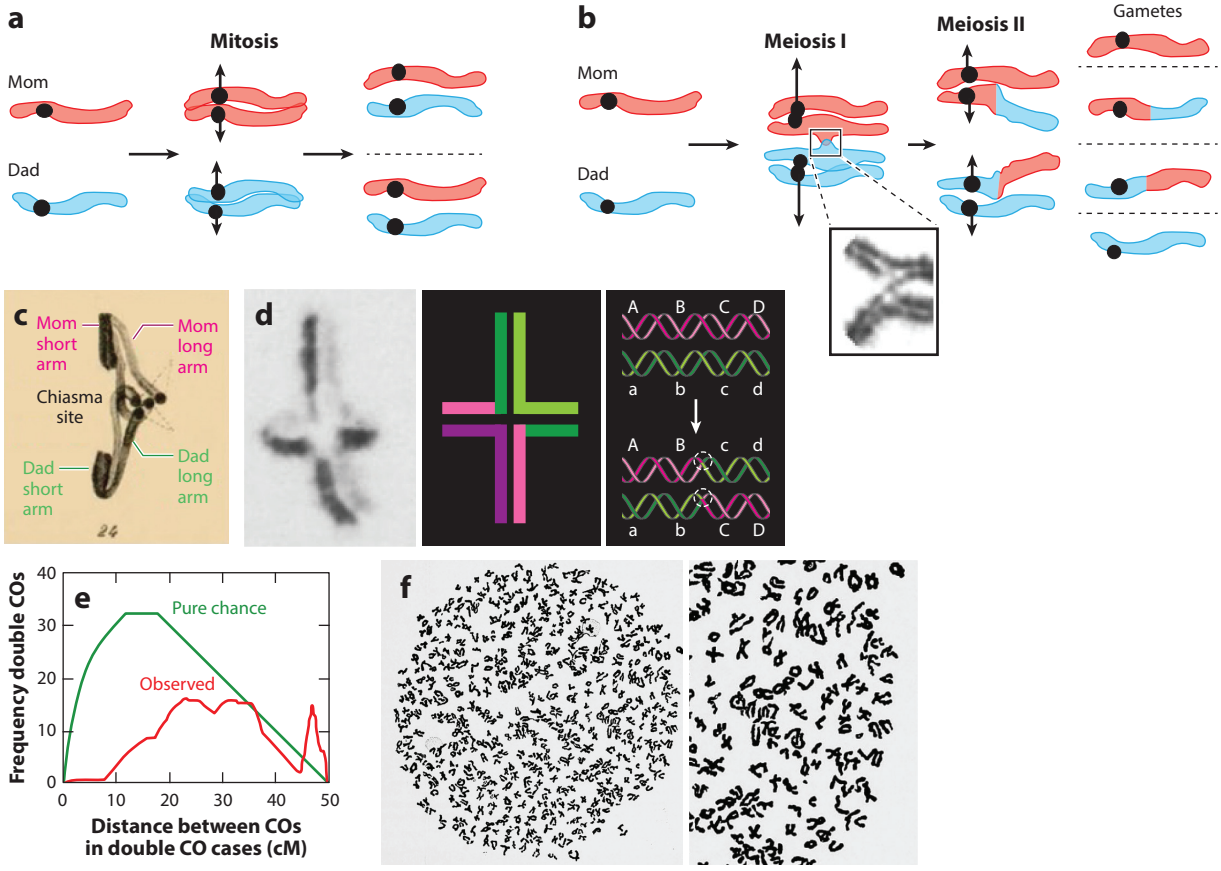

Figure 1

Meiosis: segregation and crossovers. (*a*,*b*) Comparison of the mitotic and meiotic programs. Meiosis uniquely involves segregation of homologs (Mom and Dad) at the first of two divisions (meiosis I). This process requires a physical connection between homologs, usually provided by one or more crossovers between nonsister homolog chromatids, each seen cytologically as a chiasma (*b*, *inset*). (*c*) The nature of a chiasma was first appreciated by Janssens based on figures seen at anaphase of the first division (193). Panel adapted from Reference 193. (*d*) Janssens's hypothesis was proven by differential BrdU labeling of sister chromatids, which directly revealed exchange of nonsister chromatids at chiasma sites. Panel depicts (*left*) a diagnostic image, adapted with permission from Tease & Jones (333); (*middle*) corresponding chromatid paths of homologs (*pink* and *green*, with BrdU-labeled chromatids in darker color); and (*right*) crossing-over at the DNA level. Panel *d* middle and right images adapted with permission from Martin White. (*e*) Panel depicts what was first described by Muller (249) as the tendency for genetic double crossovers to be fewer than expected by random distribution. Panel adapted from Reference 249. (*f*) Adder's tongue fern *Ophioglossum vulgatum* has a total of 2n = 1,260 chromosomes, every homologous pair of which exhibits at least one chiasma at meiosis I (*right*, *partly enlarged*), in accord with the strict requirement for the obligatory crossover. Panel adapted with permission from Reference 256 (CC BY-NC-SA 4.0). Abbreviation: CO, crossover.

2.2. Evolutionary Rationale: Genetic Shuffling

The fundamental raison d'être of sexual reproduction is the shuffling of genetic information, thereby creating favorable new combinations of alleles and/or disrupting unfavorable allele combinations (233, 347). The mechanics of the two meiotic divisions shuffle information at the whole-chromosome level. In accord with Mendel's laws, at MI, the homologs of a given chromosome segregate randomly to one or the other spindle pole, and this choice is made independently

for each chromosome. However, Mendelian segregation does not provide for shuffling of alleles along an individual chromosome. This effect requires crossover recombination between homologs at the DNA level.

This genetic consequence of crossing-over is the evolutionarily selected effect of recombination rather than its mechanical role in ensuring homolog segregation. Indeed, MI homolog segregation is sometimes achieved by connections that do not involve crossing-over (famously, in *Bombyx mori* females and *Drosophila melanogaster* males) (3, 169, 291). However, this effect is only ever observed in one sex of a given organism, usually the heterogametic sex [perhaps in relation to limited homology between the maternal and paternal chromosomes (211)], in accord with an essential evolutionary role for crossing-over.

Along any given chromosome, crossovers occur at different positions in different nuclei but, nonetheless, always tend to be evenly spaced. This phenomenon, known as crossover interference, was originally discovered genetically (249) (**Figure 1*e***). It is also seen cytologically in the even spacing of chiasmata and, at earlier stages of meiosis, of chromosome-associated recombination complexes along prophase chromosomes (see Section 6).

Interference is of central importance from an evolutionary perspective. Total crossover levels can be a critical parameter for evolutionary success, and crossover interference is often a primary determinant of total crossover number (although other effects can also be prominent) (141, 143). If interference operates over longer or shorter distances, the result is fewer or more crossovers, respectively, and thereby less or more shuffling. Additionally, the tendency for crossovers to be evenly spaced, per se, increases genetic shuffling (347), perhaps providing an additional rationale for the existence of interference. Notably, even though chiasmata mediate homolog segregation, large increases in chiasma numbers do not detectably affect chromosome stability, at least in plants (67, 188), suggesting that the evolutionary role of interference lies elsewhere.

The mechanical role of crossing-over for MI homolog segregation does have one specific implication: Each homolog pair must acquire at least one crossover. This requirement is referred to as the obligatory crossover (166), and the mechanisms by which it is achieved collectively comprise crossover assurance (317). This is especially notable because a given homolog pair usually acquires only one or a few crossovers. Several features are involved in obligation and assurance. As described in Section 6, the substrate for crossover interference is an array of a large number of recombination intermediates. The number of such intermediates and the parameters of the patterning process usually ensure that at least one intermediate will be designated a crossover. Thereafter, progression of designated interaction(s) through subsequent biochemical steps must be efficient enough that at least one finally yields a mature crossover product. In aberrant situations where one or more of these effects is compromised, compensatory effects come into play (see Section 4.2).

Some organisms lack crossover interference. In these cases, crossover number per homolog pair is Poisson distributed among different nuclei, but the average frequency is high enough to ensure that zero-crossover pairs are rare.

Additionally, when the obligatory crossover is absent, backup connection mechanisms are present to ensure that homologs still segregate properly much of the time. Such connections often involve specialized localization of the synaptonemal complex (SC) to centromeres and/or heterochromatin associations (81, 97, 153, 281).

The importance of the obligatory crossover is dramatically illustrated by adder's tongue fern, whose chromosome complement comprises 630 homolog pairs, every one of which is connected by a single chiasma (256) (**Figure 1*f***).

2.3. Four Fundamental Challenges for Interactions Between Homologs

The most fundamental and unique feature of the meiotic process is a highly programmed series of interactions between homologs, which, in aggregate, set the stage for their segregation at MI. One important component, of course, is the occurrence of biochemical recombination at the DNA level (see Sections 3 and 4). However, centrally important events must also occur at the level of whole chromosomes. Three such effects can be recognized.

First, homologous chromosomes must find each other, and become coaligned along their lengths, without being entangled in other chromosomes. That is, homologs must be regularly paired (see Section 5).

Second, crossover interference is a phenomenon of spatial patterning and thus requires communication along the lengths of whole chromosomes (see Section 6).

Third, local crossing-over at the DNA level must be accompanied by an analogous exchange at the chromosome level to provide continuous structure along the paths of the two involved chromatids (see Section 7).

Completion of this program requires hours in budding yeast but days or weeks in some organisms, especially vascular plants, which have very long chromosomes. Since DNA recombination per se can be completed in minutes, this dramatic prolongation of meiotic prophase likely reflects the complexities of whole-chromosome events, most notably homolog pairing (301).

Together these considerations raise a fundamental question: How are the DNA events of recombination and whole-chromosome processes locally coordinated in time and space? The answer lies in the facts that (*a*) meiotic interhomolog interactions occur when chromosomes are in an organized state, with chromatin loops displayed along structural axes, and (*b*) throughout the program, DNA recombination complexes are physically associated with those axes, with functional interplay between local and whole-chromosome events at every stage. These effects are integrated by nucleus-wide progression factors provided by global cell cycle control. In Section 8, we propose a rationale for the evolution of meiosis from the mitotic program that can account for these basic features.

2.4. Basics of the Meiotic Program

Several fundamental features of meiosis underlie all basic processes.

2.4.1. Classical stages. The meiotic interhomolog interaction program (396) is implemented after DNA replication during a prolonged prophase-like period, so called because at this stage chromosomes are long, thin individualized units (**Figure 2*a*,*c*,*e***) as during mitotic prophase (213). At the light microscope level, the two homologs (each comprising a pair of sister chromatids) are initially separate entities. They progressively come into spatial coalignment at a significant distance (pairing), after which they become progressively juxtaposed into a single morphological unit comprising all four chromatids (synapsis) (**Figure 2*a*,*c*,*e***). These events define the classical meiotic stages of leptotene (culminating in coalignment), zygotene (partial synapsis), and pachytene (complete synapsis). Then, in a prometaphase-like transition (diplotene), chromosomes become short and compact and all connections between homologs are lost except at chiasmata to give the final metaphase I configuration (**Figure 2*b*,*d***). The DNA events of recombination occupy the entire period from leptotene to/through diplotene (270) (**Figure 2*f***; Sections 3–6).

2.4.2. Chromosome axes. Throughout prophase, each homolog is organized as a cooriented sister linear loop array with a single conjoined sister-chromatid axis (**Figure 3*a*,*b***). Along this structure, loops are closely packed with an evolutionarily conserved density (~20 per micron) (184). Loop lengths are relatively uniform, for example, varying by less than twofold in a given

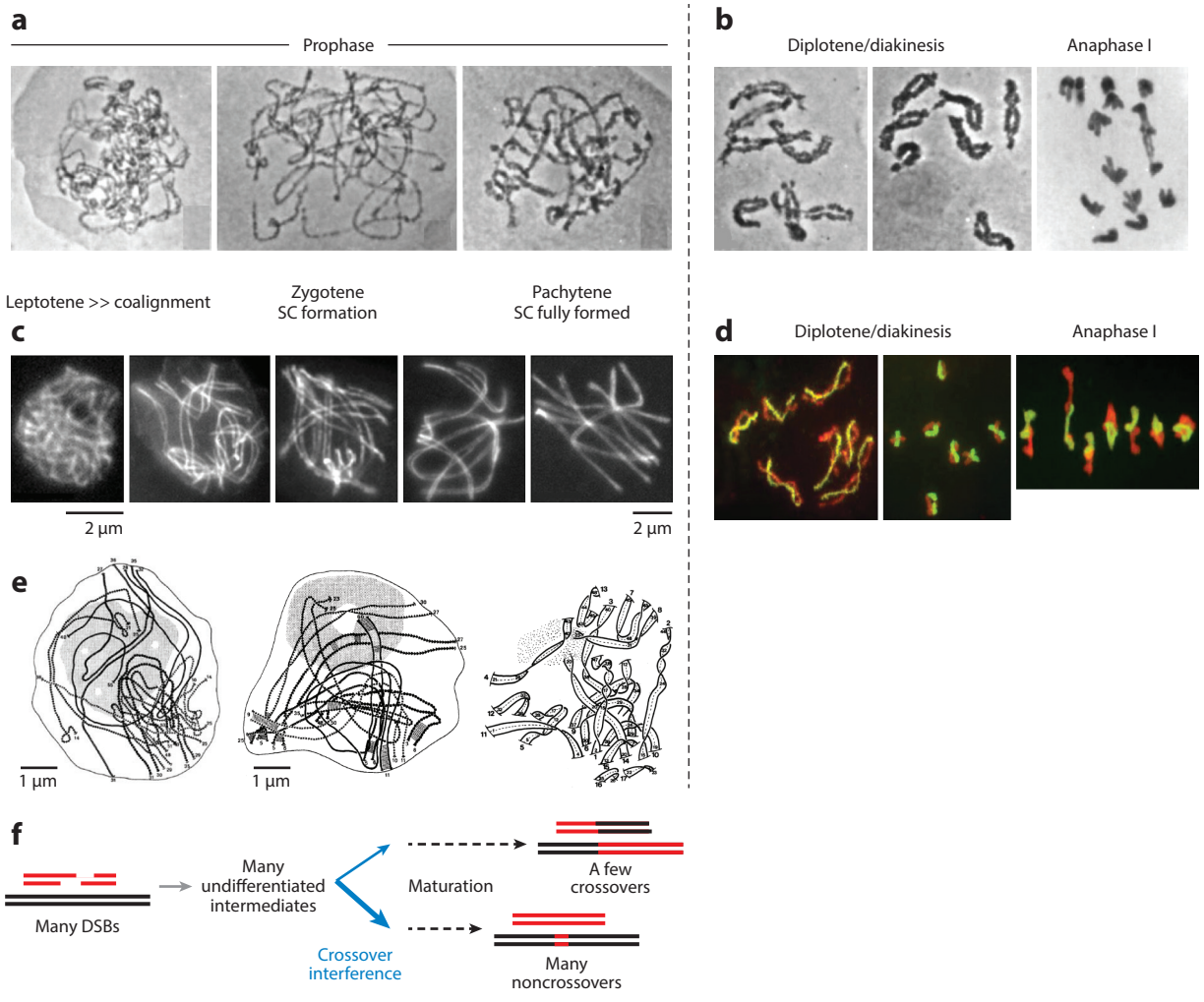

Figure 2

Classical cytologically defined stages of meiosis (*a–e*). (*a*,*b*) Light microscope images of squashed rye chromosomes from (*a*, *left*) early prophase through (*b*, *right*) anaphase I. Panels *a* and *b* adapted from Reference 396. (*c*) Fluorescence imaging of *Sordaria macrospora* chromosomes illustrates the progression of pairing including (*middle*) coalignment and (*right*) synapsis. Axes are visualized by cohesin Spo76/Pds5-GFP. Panel adapted from Reference 91. (*d*) Differential fluorescence labeling of the genome complements of an F1 hybrid of *Festuca pratensis* (turfgrass; *red*) × *Lolium multiflorum* (ryegrass; *green*) indicates the sites of chiasmata between the red and green chromosomes from (*left*) diplotene to (*right*) anaphase I (A. Lukaszewski, D. Kopecky & G. Linc, personal communication). Panel obtained by method described in Reference 190. (*e*) Electron microscopy reconstructions of serial sections through *Sordaria* nuclei at the (*left*) coalignment stage and (*middle*) early zygotene stage. Segments of bars between homolog axes indicate SC initiation sites; the nucleolus is indicated in gray. Serial sections through a budding yeast pachytene nucleus (*right*) show full synapsis. The left and middle images of panel *e* are adapted from Reference 394, and the right image is adapted with permission from Reference 35. (*f*) DNA events of recombination occupy all of prophase. Abbreviations: DSB, double-strand break; SC, synaptonemal complex.

region (397). Sister loop modules are in phase at the structural level (397); however, loops at corresponding positions along sister axes do not always contain exactly corresponding DNA sequences (368), which is also seen for mitotic chromosomes (264). Because loop density is conserved, changes in axis length are accompanied by reciprocal alterations in loop size, with shorter/longer loops resulting in longer/shorter axes, without any change in basic axis structure (e.g., 128, 258).

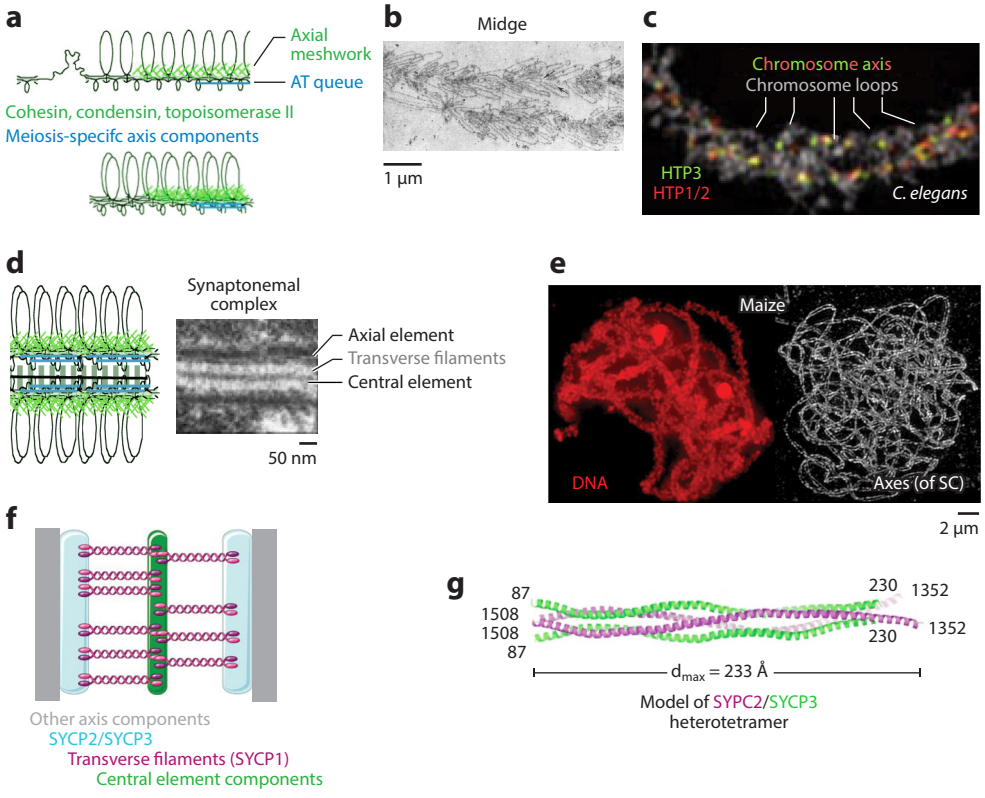

Figure 3

Axes and the SC. (*a*) Schematic of meiotic chromosome organization. (*Top*) Along each chromatid, chromatin is organized into a linear array of loops that are spaced at an evolutionarily conserved density along a structural axis, the assembly of which creates the linear array. (*Bottom*) Sister chromatid linear loop arrays are cooriented and tightly juxtaposed via a morphologically single conjoined axis. Panel adapted from Reference 184. (*b*) Direct visualization of cooriented sister linear loop arrays along coaligned midge homologs displayed by surface spreading. Panel adapted with permission from Reference 178. (*c*) Organization of HORMA-domain axis components HTP1/2 and HTP3 along worm pachytene chromosomes seen in high-resolution microscopy. Panel adapted from Reference 368. (*d*) The SC, showing (*left*) a schematic of the homolog axes (*blue* and *green*) linked by SC central region components (*black*) and (*right*) corresponding electron microscopy picture of the *Sordaria* SC. (*e*) SIM images of maize pachytene chromosomes illustrating (*left*) compact chromatin along (*right*) axes of SCs. Panel adapted from Reference 356. (*f*) Schematic of SC middle region organization. Panel adapted from Reference 399 (CC BY 4.0). (*g*) Model for tetramer organization of meiotic axis components SYCP2/SYCP3. Panel adapted from Reference 364 (CC BY 4.0). Abbreviation: SC, synaptonemal complex.

Mitotic prophase axis structure is directly analogous to that of meiosis, with cooriented linear loop arrays and the same (conserved) loop density (184, 213, 306). Indeed, in muntjac, mitotic and meiotic prophase axes are identical in length (184).

Axes in both programs comprise a queue of locally AT-rich sequences that are cohesin-binding sites (22, 302), plus a meshwork of structural components that include cohesin(s), condensin(s), and topoisomerase II (TopoII) (124, 132, 149, 189, 303, 345, 368) (e.g., **Figure 3*c***). For cohesins and condensins, mitotic and meiosis-specific versions often collaborate. Meiosis-specific axis components (e.g., HORMAD proteins and others) are also present (107, 129, 189, 283). Cohesins, condensins, ubiquitination, SUMOylation, chromatin modifications, phosphorylation/

dephosphorylation, and transcription have all been implicated in determining axis assembly and/or axis length (45, 140, 345, 362, 378). Nonetheless, in both programs, how close-packed linear arrays of loops arise remains an important mystery (124).

2.4.3. Pairing, synapsis, and separation. Leptotene pairing comprises coalignment of homolog axes at a distance of ~400 nm, and synapsis during zygotene/pachytene comprises the installation of the SC between those axes (335, 394, 396) (**Figure 2*d***). The SC is a nearly universally meiosis-specific structure that brings homolog axes together at a distance of ~100 nm (109, 121, 157, 198, 299, 393) (**Figure 3*d***). Chromatin loops emanate outward from the two axes (242) (**Figure 3*e***). Within the SC, sister chromatid arrays are stacked one above the other (189, 254). In the electron microscopy (EM)-defined SC structure, homolog axes are linked by a central region comprising a close-packed array of coiled-coil transverse filaments that emanate outward in both directions from a specialized central element to contact meiosis-specific components of the corresponding axes (**Figure 3*d*,*f*,*g***). If appropriate nucleation is provided and/or normal homology-dependent interactions are absent, the SC can form between axes of unrelated chromosomes (219, 397).

Diplotene involves longitudinal chromosome shortening and compaction plus global loss of the SC, with resultant separation of homologs, except at chiasmata (**Figure 2*b*,*d***). By analogy with mitotic prometaphase (55, 113), shortening likely involves a reduction in the number of chromatin loops with a concomitant reciprocal increase in chromatin loop length. However, meiotic diplotene and mitotic prometaphase differ significantly with respect to sister chromatid cohesion. In meiosis, cohesion is maintained along the lengths of chromosomes, as required for MI segregation. By contrast, in mitosis, sisters become well individualized, although they do remain linked by periodic intersister bridges (55).

2.4.4. Recombination. Meiotic recombination is highly programmed, with tight regulation at every step, and occurs specifically between homolog chromatids (see Sections 3 and 4). This contrasts dramatically with recombinational repair in mitotic cells, which occurs in response to spontaneous chromosome damage and usually between sister chromatid partners (36, 165). In addition, in mitotic cells, double-strand breaks (DSBs) are often repaired in the alternative process of nonhomologous end joining (165), but, during meiosis, this latter option is avoided or repressed, except in special circumstances (4, 136, 207, 210, 224, 319, 383).

Just as for structural features, meiotic recombination recruits molecular components from mitotic DNA processes, along with meiosis-specific paralogs and uniquely meiotic proteins (155). Type I and type II topoisomerases, helicases, RecA homologs and their collaborators, and components of the DNA mismatch repair system have all been co-opted and/or repurposed to serve the specialized challenges of meiosis.

In brief (**Figure 2*f***), recombination initiates by programmed DSBs at early leptotene (see Section 3). One of the two DSB ends identifies and interacts with its allelic partner on a homolog chromatid. After this step, a select few interactions are designated to become (evenly spaced) crossovers. The remaining majority are fated to mature without an exchange of flanking regions, as noncrossovers. Most organisms exhibit one or a few crossovers per homolog pair, while the numbers of DSBs and of noncrossovers increase with genome size. For example, crossover:noncrossover ratios can be 1:50 or more in polyploid plants (265). The two types of recombination interactions then undergo further processing during zygotene/pachytene and are finally completed during pachytene/diplotene.

2.4.5. Recombination/structure association. Recombination complexes occur in direct physical association with longitudinal structures (e.g., axes and/or SCs) at every stage (160, 184, 397)

(**Figure 4**). This association is required for virtually every step of DNA recombination and for every recombination-related whole-chromosome process.

Existence of this association emerged from EM observations. Dense nodules were found to occur along the SC at late pachytene, with numbers and spacing predicted for crossovers (42) (**Figure 4*a*,*b***). Additional nodules, associated with individual axes or SCs and more numerous, were observed at earlier stages (leptotene to mid-pachytene) and inferred to represent earlier recombination complexes (397, 398) (**Figure 4*b***). Recombination complexes are also visible as discrete molecular ensembles (foci) via fluorescent or EM-visualized immunogold tags (240, 241, 367, 398) (**Figure 4*c*,*d***; see Section 4).

Recombination complexes associate with individual chromosome axes prior and prerequisite to initiation of recombination (**Figure 4*e*, subpanels *i*,*ii***, and **4*f***; Section 3). Recombination initiation occurs at genomic positions that lie between sites involved in axis formation, leading to the idea that recombination complexes form in chromatin loops and are indirectly tethered

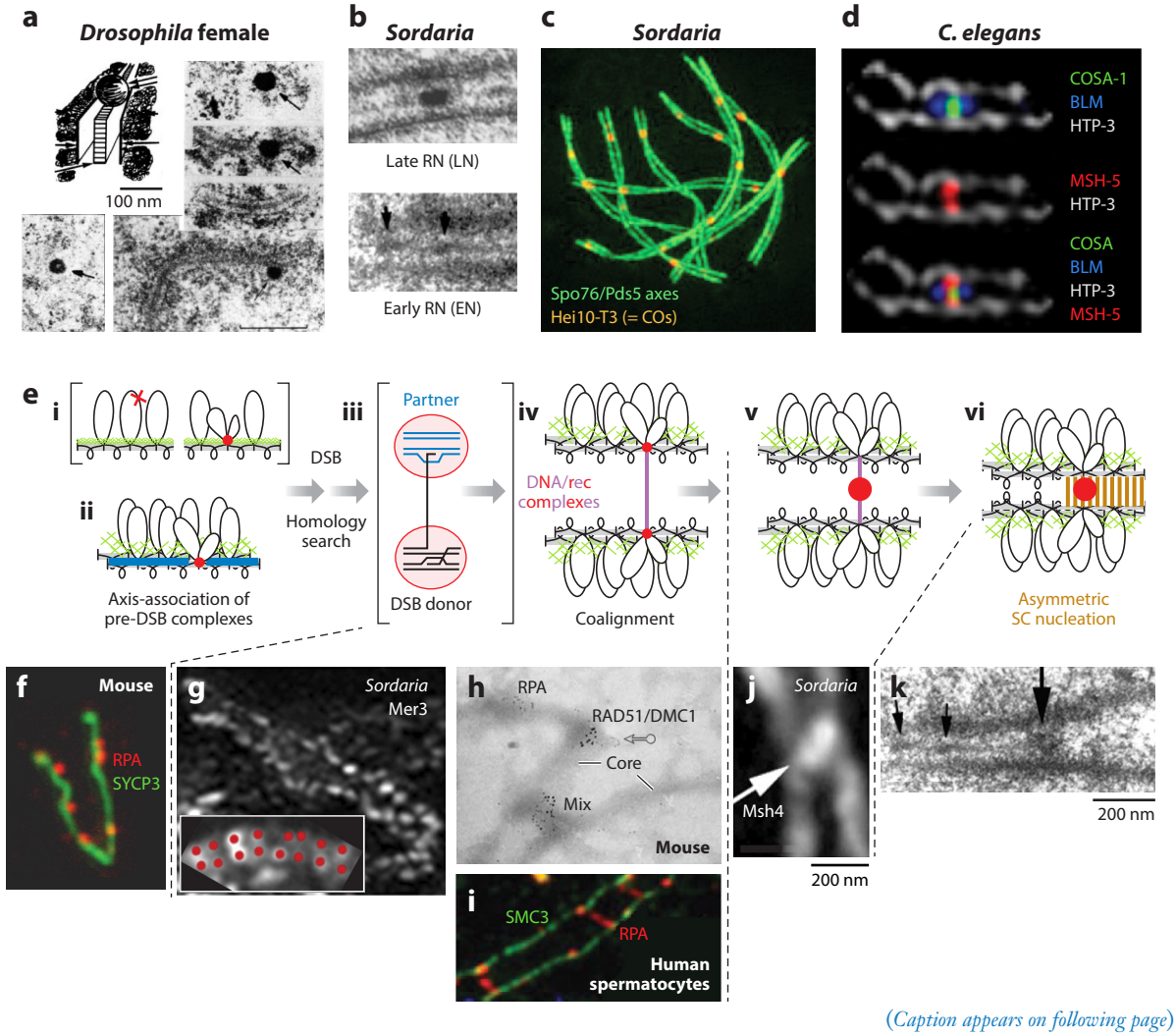

(*Caption appears on following page*)

Figure 4 (*Figure appears on preceding page*)

Axis/SC-association of recombination complexes. (*a*, *right*) EM serial sections of *Drosophila melanogaster* female SC with associated nodular structures (now called recombination nodules) and (*left*) schematic reconstitution. Panel adapted with permission from Reference 42. (*b*) Pachytene SCs exhibit both (*top*) large crossover-correlated nodules and (*bottom*, *arrows*) smaller nodules, which represent a subset of noncrossover complexes. Panel adapted from Reference 388. (*c*) SIM fluorescence image of *Sordaria* pachytene chromosomes. Axes are visualized by cohesin Spo76/Pds5-GFP and sites of crossovers by foci of the E3 ligase Hei10. Panel adapted from Reference 84 (CC BY-NC 4.0). (*d*) *Caenorhabditis elegans* crossover recombination complexes (*green*, *blue*, and *red*) colocalize between the two homolog axes (HTP-3; *gray*), with which they are in direct contact. Panel adapted with permission from Reference 367. (*e*, *i–vi*) Diagram of the progression from early leptotene through zygotene SC nucleation. (*i*) Recombination complexes (*red*) are first associated with chromatin loop sequences (*red X*), which are next (*ii*) physically associated with chromosome axes (*blue* and *green*). (*iii*) DSB formation occurs in these complexes: One DSB end identifies the corresponding sequence on the homolog, which it engages in a nascent D-loop. (*iv*) The new nascent D-loop complex is associated with its corresponding axis. Unknown events then bring homolog axes into coalignment juxtaposition, linked by DNA/recombination complexes, which are displayed on and/or between the two axes (*purple*). (*v*) Interaxis bridges, now also containing structural components, allow axis-associated recombination complexes (*red*) to relocate to a between-axis position. Bridges then shorten, thereby (*vi*) nucleating SC formation (*gold bars*), which proceeds asymmetrically from the former bridge position. (*f–k*) Illustrations of chromosomes corresponding to subpanels *i* to *vi* in panel *e*. (*f*) Single-strand binding protein RPA (with axis component SYCP3). Panel adapted with permission from Reference 241. (*g*,*h*) Coaligned homolog axes are linked by DNA/recombination complexes. (*g*) Mer3 helicase foci are in matching pairs on invisibly linked axes. Panel adapted from Reference 325. (*h*) EM image of immunogold-labeled RAD51/DMC1. Panel adapted with permission from Reference 240. (*i*) Paired RPA foci link homolog axes. Panel adapted with permission from Reference 263. (*j*) Contracting bridges marked by Msh4. (*k*) EM picture of *Sordaria* asymmetric SC formation nucleated at the site of a crossover-correlated recombination complex (*large arrow*; *small arrows* indicate smaller nodules). Panels *j* and *k* adapted from Reference 91. Abbreviations: CO, crossover; DSB, double-strand break; EM, electron microscopy; EN, early nodule; LN, late nodule; rec, recombination; RN, recombination nodule; SC, synaptonemal complex.

to underlying axes (22, 171, 201, 238, 274, 303, 374) (**Figure 4*e*, subpanels *i*,*ii***). Other, more dynamic scenarios for association involving adjustment of loop base positioning are also possible, as inferred for mitotic DSB repair (13, 124).

DSBs identify and then interact with corresponding partner sequences on their homologs and mediate axis coalignment (**Figure 4*e*, subpanel *iii***; see Sections 4 and 5). During this process, DSB/partner interactions also become axis associated. The outcome of this process is a configuration in which matching pairs of recombination complexes occur along the lengths of the axes, with one DSB end in each complex (**Figure 4*e*, subpanel *iv***, and **4*g*,*h***).

Next, crossover interference is implemented. In some organisms, it is known to be imposed upon the array of coalignment connections, with concomitant SC nucleation; in other cases, it is suggested to be imposed after SC formation (see Section 6). In either case, SC formation is accompanied by movement of recombination complexes from an on-axis to a between-axis position on SC central regions. This process first involves relocalization to interaxis bridges, which then contract to give close juxtaposition of axes and SC nucleation (91) (**Figure 4*e*, subpanels *v*,*vi***, and **4*j*,*k***).

Crossover products arise within prominent SC-associated complexes (see Section 7) at late pachytene or possibly during diplotene, when small bits of SC plus associated crossover complexes often remain at the sites of emerging chiasmata (see Section 7). By contrast, as defined in budding yeast, noncrossover products arise around mid-pachytene (8), and, in all organisms, corresponding recombination complexes are released from the SCs at or before this stage as indicated by reductions in the number of recombination-correlated nodules and foci (e.g., 84, 240, 241).

3. DNA RECOMBINATION PART I: INITIATION

3.1. DSBs via Axis-Associated Transesterase Complexes

Meiotic recombination is initiated by DSBs, catalyzed by a transesterase mechanism derived from that of a topoisomerase (TopoVI) (rather than by hydrolysis, as for restriction enzyme cleavage)

(199, 297, 374) (**Figure 5*a***). In accord with this topoisomerase-like mechanism, Spo11 protein, which catalyzes DSB formation, remains covalently bound to the 5′ ends of the DSB, where it directs ensuing events. The 5′ strand termini are specifically resected by the combined effects of endo- and exonucleases to give long (0.5–1 kb) overhanging single-stranded tails with 3′ ends, suitable for invading an intact partner duplex and eventual extension by a DNA polymerase

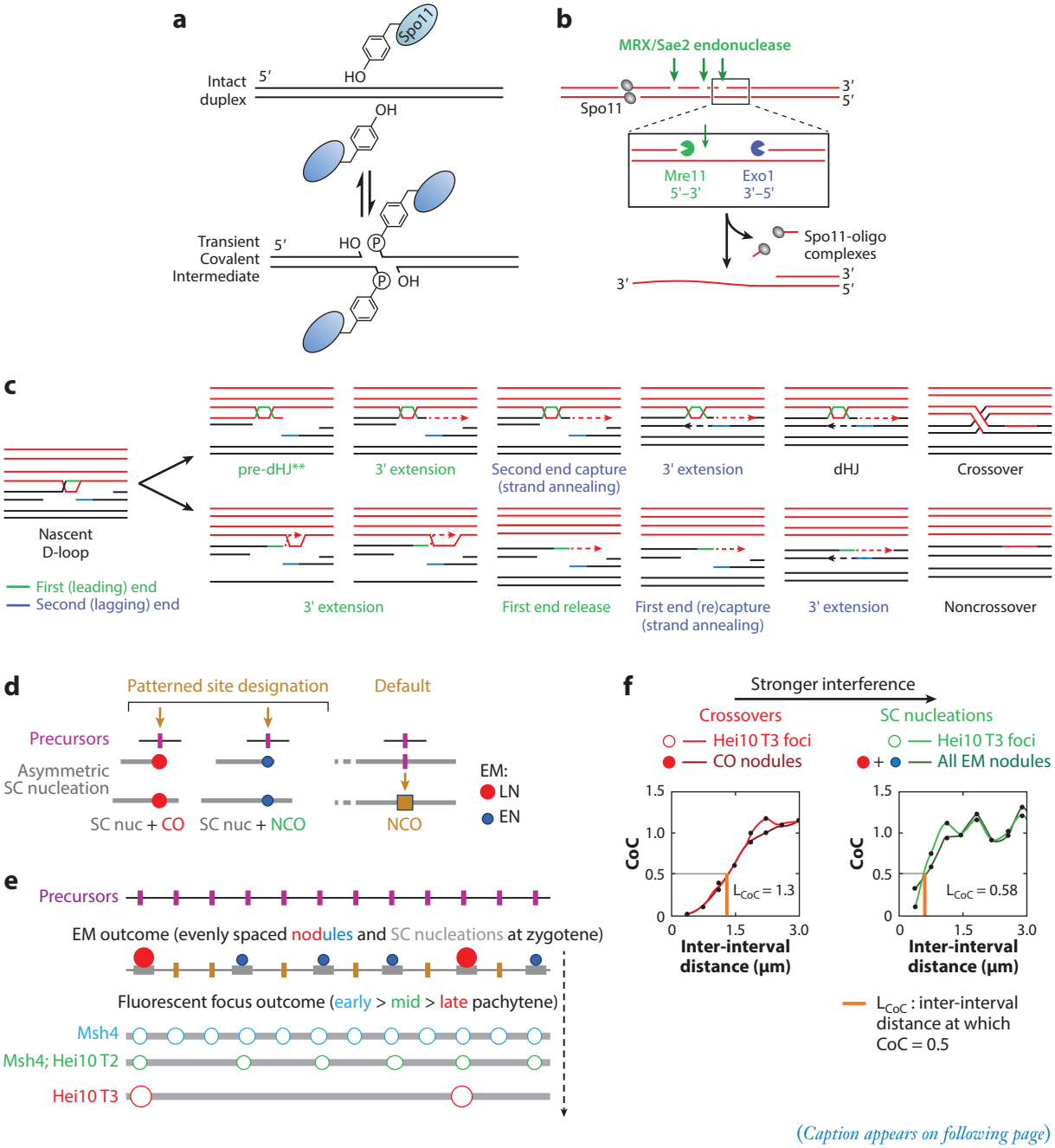

(*Caption appears on following page*)

Figure 5 (*Figure appears on preceding page*)

Recombination. (*a*) Spo11 cleaves DNA by a transesterase mechanism, with nucleophilic attack by an −OH group on the protein. As a result, the protein remains covalently attached to the 5′ strand ends at the cleavage site. Panel adapted from Reference 174. (*b*) Endo- and exonucleolytic cleavage produce Spo11-oligo products and result in the resection of 5′ ends to give 3′ single-stranded DNA tails. Panel adapted from image provided by Soonjoung Kim and Scott Keeney. (*c*) A current model for canonical events of meiotic recombination, emphasizing sequential events at first (leading) and second (lagging) DSB ends and distinctions between the (*top*) crossover and (*bottom*) noncrossover pathways. (See Section 4.1.3.1 for complexities.) (*d–f*) Interference-mediated designation of SC nucleations with embedded crossover interference. (*d*) Undifferentiated recombination interactions (precursors to patterning) undergo three fates. Some give rise to SC nucleations which exhibit interference (*gray*). A minority subset of these SC nucleation sites are also designated to mature as patterned (interfering) crossovers (*red*); the remainder are matured as noncrossovers (*blue*). A third set of precursor recombination interactions do not undergo SC nucleation and mature into noncrossovers as the default option. (*d*,*e*; *top*) The leptotene/zygotene events depicted in panel *d* are manifested directly in EM SC and recombination nodule patterns (ENs and LNs as in **Figure 4*b***). (*e*, *top*) These leptotene/zygotene events are also manifested in the patterns of recombination-complex foci that emerge later, sequentially, during pachytene. At early pachytene, Msh4 foci (*blue open circles*) mark all recombination sites, regardless of the fact that patterning has already differentiated the corresponding interactions into three types. By mid-pachytene, observable foci correspond only to the subset of interactions that exhibited EM nodules at zygotene and are seen as medium-sized foci of E3 ligase Hei10 (T2 type, *green*), which colocalize also with a reduced number of Msh4 foci. By late pachytene, a subset of these foci transiently acquires large Hei10 foci (T3 type, *red*) that specifically mark the sites of crossovers. Panel *e* adapted from Reference 388. (*f*) Interference distributions of the (*left*) indicated recombination complexes and (*right*) SC nucleation sites defined by Coefficient of Coincidence (CoC) analysis. (*Filled circles* represent EM nodules; *open circles* represent Hei10 foci as in panel *e*.) Interference is weaker for complexes that correlate with (*right*) SC nucleations and stronger for (*left*) crossover-correlated complexes, which represent a subset of those nucleations. Note that for CoC analysis, chromosomes are divided into intervals; for each pair of intervals, the number of chromosomes that exhibit crossovers in both intervals is divided by the number expected if crossovers occur independently in the two intervals. These ratios are then plotted as a function of inter-interval distance. A lower ratio at smaller inter-interval distance implies interference. Vertical orange lines indicate inter-interval distance at which CoC = 0.5, a convenient metric for the strength of interference. Panel *f* adapted from Reference 392. Abbreviations: CO, crossover; CoC, Coefficient of Coincidence; dHJ, double Holliday junction; DSB, double-strand break; EM, electron microscopy; EN, early nodule; LN, late nodule; NCO, noncrossover; nuc, nucleation; SC, synaptonemal complex.

(29, 43, 155, 253, 375) (**Figure 5*b***). In budding yeast, resection is tightly coupled to DSB formation, with the Mre11-Rad50-Xrs2 (MRX) complex, which mediates DSB resection, also being required for DSB formation (155). Interestingly, due to its transesterase nature, the Spo11 reaction is intrinsically reversible (**Figure 5*a***). Thus, onset of resection could be an important determinant of DSB frequency.

Spo11 cleavage appears to favor bent DNA, as well as entrapment of two duplexes, as part of the formation of an appropriate higher-order complex (59, 374). If the two duplexes are from sister chromatids, this configuration could ensure that a DSB occurs at a given site on only one of the two sisters. Other findings raise the possibility that DSB formation might require prior direct contact between coaligned underwound DNA/DNA duplexes adjacent to the actual DSB site (164, 282), which could explain how interhomolog interactions influence DNase hypersensitivity at recombination hot spots (373).

DSB formation requires the interdependent action of many proteins (354, 374). In budding yeast, 10 such components comprise 3 subgroups: the core complex (Spo11, Rec102/TopoIVB, Ski8, and Rec104), the MRX complex, and the RMM proteins (Rec114, Mei4, and Mer2), most or all of which have homologs in other organisms. The yeast RMM complex plays a key role. In vitro, it binds DNA with high cooperativity to form condensates that contain hundreds or thousands of protein molecules and recruit Spo11 (58).

DSB formation also requires association of Spo11 complexes with chromosome axes [whose formation, in contrast, is DSB independent (334)]. Correspondingly, mutations in axis components universally reduce DSB frequencies. RMM component Mer2 is particularly critical for association of pre-DSB complexes to axes components (274, 300, 361). Additionally, transcription

can modulate DSB patterns by modulating the localization of axis components (328). Association of pre-DSB recombination complexes with axes is also critical for mediating the timing of DSB formation, which is coupled globally to cell cycle progression and locally to DNA replication, via CDK and CDK-dependent DDK-mediated phosphorylation of Mer2 (24, 176, 251, 280). Similarly, in *Caenorhabditis elegans*, DSB levels are controlled by the opposing activities of PP4PPH-4.1 phosphatase and ATR kinase on DSB-1, the homolog of budding yeast Spo11 collaborator Rec114 (131).

3.2. DSB Landscapes

DSBs occur at a large number of positions along the genome and at a wide range of frequencies. Multiple chromosomal features work combinatorially, hierarchically, and over multiple size scales to determine DSB landscapes (22, 73, 204, 216, 223, 252, 273, 338, 351). Globally, DSBs tend to occur more and less abundantly in GC-rich and AT-rich regions, respectively (corresponding to A-type and B-type domains in mammalian chromosomes). They are somewhat rarer in centromere and telomere regions (34) and can vary on a per-chromosome level (252).

In many organisms, breaks tend to occur in nucleosome-depleted regions (273). In mouse and human [but not all mammals (15)], DSB formation is targeted to specific sequences by PRDM9 via its array of zinc fingers (223). These zinc finger domains undergo rapid evolution to new specificities (9, 279, 369) with implications for evolution and speciation. Interestingly, PRDM9 has potent nucleosome remodeling activity, and when PRDM9 is absent, DSBs again occur in nucleosome-depleted regions (30). DSB formation also involves local DNA sequence bias and, aside PRDM9, modifications of chromatin structure (73, 374).

3.3. DSB Patterning In *Cis* and In *Trans*

Global modulation aside, DSBs do not occur randomly either along or between chromosomes (223, 338, 374). Several phenomena, not necessarily independent of one another, have been described.

3.3.1. Hot spot competition. Occurrence of a hot spot reduces the activity of a nearby hot spot (176, 262). This effect could arise prior to DSB formation by competition for required components or during DSB formation (by DSB interference; below).

3.3.2. DSB interference in *cis*. On a per-DNA-molecule basis, the formation of a DSB at one locus reduces the chance of another DSB occurring in its vicinity, strongly over the distance of a single loop and detectably over distances of ~100 kb (~10 loops) (110). In budding yeast, this effect requires the DNA damage-response kinase Tel1(ATM) (223).

3.3.3. One DSB per pair of sisters. At a single DSB hot spot, the frequencies of nuclei that exhibit 0, 1, or 2 interhomolog recombination events are incompatible with a random distribution of DSBs and ensuing events among the four chromatids. DSBs are thus inferred to occur on only one of two sister chromatids (389).

3.3.4. Even spacing of DSB complexes. DSB-associated recombination complexes occur with even spacing along leptotene chromosomes, perhaps reflecting constraints during DSB formation (322, 334) (see Sections 3.3.1–3.3.3).

3.3.5. Double DSBs. Irrespective of constraints on DSB spacing, Spo11-mediated DSBs tend to occur in concerted pairs along a single chromatid (164, 224, 282). This effect may involve

coalignment of the DNA duplexes of the two involved segments in regions of topological stress. Such events likely provide a significant source of genome instability, potentially including translocation of the excised segment.

3.3.6. *Trans* interactions between homologs. In budding yeast, DSB patterns can also be influenced by interactions between homologs that precede DSB formation (175, 373), consistent with the DSB-independent pairing observed in that organism (see Section 5.3.3). Additionally, recombination events occur only once per four chromatids, that is, once per pair of homologs, by processes dependent on Mec1/Tel1 (ATR/ATM) (389). This effect could operate at the level of either DSB formation and/or ensuing DSB/partner interactions (see Sections 3 and 4).

3.4. Ensuring Enough DSBs for at Least One Crossover

If a pair of homologs does not have a sufficient number of DSBs, it will be at risk for not having even the single crossover required for MI segregation (see Section 2.4). Several factors mitigate this risk.

3.4.1. Extra DSBs. DSB formation is normally shut off by a feedback mechanism that operates in early/mid-pachytene, likely by the modulation of axis status and resultant release of DSB complexes (248). When early interhomolog interactions are defective, this shutoff does not occur and DSB formation continues to give additional (compensatory) DSBs (176, 209, 248, 336). As an independent but interrelated effect, DSB shutoff requires the induction of the mid-/late prophase program, which, when defective or delayed, also results in extra DSBs (176). Related effects also occur in mouse and *C. elegans* (63, 176, 380).

3.4.2. Length compensation. Very short chromosomes (studied mostly in budding yeast) and the very short region of homology between mammalian XY chromosomes (PAR) are at particular risk due to a paucity of DSBs. In both cases, DSB formation is enhanced by increased axis length and additional genetically encoded *cis* effects, as well as prolongation of DSB formation because of late homolog engagement (172, 252, 327).

3.5. The Hot Spot Paradox

When a DSB occurs at a preferred hot spot, recombination with a homolog template lacking the corresponding hot spot sequence will sometimes eliminate the hot spot determinant, thus extinguishing the hot spot. As this occurs throughout the genome, it should progressively reduce DSB formation and thereby, ultimately, crossing-over and fertility (27). However, genomes maintain sufficient numbers of DSB hot spots over evolutionary time. In mammals in which hot spot specificity is defined by PRDM9, erosion is thought to be counteracted by mutation of the PRDM9 zinc finger domain, resulting in frequent invention of new hot spots (123, 385). Hot spot erosion may also be minimized by constraints on the lengths of heteroduplex DNA tracts (62, 93, 349). On the other hand, in many organisms, for example, in Saccharomycetes over millions of years and in birds, hot spot erosion simply does not occur, perhaps because Spo11 targets functional genomic elements that are evolutionarily constrained (e.g., promoters) (200, 321) in contrast to organisms with PRDM9 (30). And yet, snakes have active PRDM9 and appear to undergo rapid hot spot evolution despite the fact that recombination is localized preferentially to functional regions (311). Interestingly, in fission yeast, environmental control of recombination rates at multiple classes of DSB hot spots could largely explain rapid PRDM9-independent changes in recombination landscapes (284).

4. DNA RECOMBINATION PART II: PROGRESSION TO CROSSOVERS AND NONCROSSOVERS

4.1. Differential DNA Events at the Two DSB Ends Initiate a Bifurcating Recombination Pathway

Due to the availability of physical and biochemical assays, of synchronous meiotic populations, and of sophisticated sequencing-based genetic analyses, DNA events of meiosis have mainly been directly defined in budding yeast (5, 17, 26, 49, 155, 228, 269, 270). In other organisms, the molecular nature of events is inferred from cytological studies of recombination complex–correlated foci, genetic and DNA sequencing analysis, the effects of mutations in conserved recombination proteins, and, in mouse, analysis of crossover and noncrossover products in physical assays (62, 130, 155). **Figure 5*c*** summarizes a current model for the recombination process as discussed below.

4.1.1. Partner interaction via ends-apart nascent D-loops. Following DSB formation and resection, one DSB end (the leading end) engages the corresponding sequence on a homolog chromatid duplex in a nascent (and not yet physically observable) D-loop. The other DSB end remains associated with its originating chromosome where it may form an analogous nascent D-loop with its still-intact sister chromatid duplex (155). This ends-apart configuration comprises the initial DNA linkage between homologs. The fundamental asymmetry between leading- and lagging-end events manifested at this stage, which might be established during DSB formation (253), governs events thereafter (180).

4.1.2. Bifurcation and postbifurcation maturation. At the ends-apart nascent D-loop stage, the recombination pathway bifurcates into crossover-fated and noncrossover-fated branches as governed by the rules of crossover patterning (25, 155). The critical DNA change that signals and comprises crossover designation is not known. After bifurcation, crossover- and noncrossover-fated strand invasion intermediates progress to their respective final products (155).

4.1.2.1. Crossover-fated single-end invasions. The earliest crossover-specific intermediate detected thus far by physical analysis is a single-end invasion (SEI) in which one resected DSB end can be stably cross-linked to a partner duplex in a stable, discrete state. An SEI forms without accompanying DNA synthesis (156; N. Hunter, personal communication) and could be a doubly branched structure with a protruding 3′ end [a so-called predouble Holliday junction (predHJ) (206)]. Recombination-related synthesis then extends the leading-end 3′ single-stranded tail. Noncrossover-fated D-loop intermediates also undergo extension by 3′ end–primed DNA synthesis (but without a discrete detectable SEI).

4.1.2.2. Second end capture/release. In both branches of the pathway, the extended 3′-end single-stranded DNA (ssDNA) tail anneals with the 3′ tail of its corresponding lagging DSB end. [Notably, this commonality does not correspond to the sequence of events proposed in the long-standing canonical DSB repair pathway (5, 206).] However, the crossover and noncrossover pathways are fundamentally different in the details of this transition. For crossover-fated intermediates, the lagging DSB end from the DSB-forming chromosome is captured by the extended leading-end complex. This second end capture gives a more robust interhomolog connection. For noncrossover-fated intermediates, the leading DSB end is released from its new linkage to the homolog partner and reanneals with the lagging end, now eliminating the previously established interhomolog linkage.

4.1.2.3. Completion. After the second end capture, crossover-specific intermediates undergo additional DNA synthesis and give rise to interhomolog double Holliday junctions (dHJs). These,

in turn, are resolved specifically to mature crossover products in a process that includes migration of the strand exchange junctions (5, 261). Noncrossover-fated intermediates are unbranched and are matured by further DNA synthesis and ligation, giving an overall process of synthesis-dependent strand annealing (SDSA) (8, 155). Interestingly, some late joint molecules are involved in topological linkages with other molecules that require decatenation by a type I topoisomerase (332). The nature of these linkages remains mysterious.

4.1.3. Additional factors. Meiotic recombination is significantly more complicated than outlined in the above-described pathway.

4.1.3.1. Complexities. Marker patterns defined by sequence analysis suggest that, not infrequently, both ends of a DSB interact with a homolog partner and, also, that multiple rounds of strand invasion often occur, for example, with a DSB end switching templates between the homolog and the sister (5, 230). In addition, not infrequently, the two DSB ends interact with different partners to create multichromatid joint molecules (mcJMs), which are resolved into noncanonical arrays of products by structure-specific nucleases with the help of SMC5/6 (260, 332, 372). These complexities likely arise after establishment of the ends-apart configuration (which is clearly manifested in paired recombination complexes at the coalignment stage and in the fact that SEIs form without DNA synthesis).

4.1.3.2. Type II crossovers. Canonical crossovers exhibit interference and are resolved by MutLγ (155); these are called Type I. However, a significant fraction of crossovers, called Type II, do not exhibit interference and are resolved by structure-specific nucleases (e.g., Mus81/Mms4) rather than the canonical resolvase MutLγ (155). In budding yeast, Type II events largely arise via mcJMs in both wild type and aberrant situations where they occur at elevated levels (332, 384). Type II events comprise 10% of crossovers in plants and mammals and 20–40% of crossovers in budding yeast. In budding yeast, Type II resolution also provides a minority of noncrossovers (332). In some organisms (e.g., *Schizosaccharomyces pombe*, *D. melanogaster*, *C. elegans*, and *Tetrahymena thermophila*), all crossovers form without MutLγ (discussion in 221, 384).

4.1.3.3. Ectopic recombination. DSBs may interact with homologous or nearly homologous sequences located at nonallelic (i.e., ectopic) positions (215, 312).

4.2. Molecular Implementation

Progression of recombination after DSB formation is mediated by a large constellation of molecules that, together, accomplish a complex array of DNA and whole-chromosome events.

4.2.1. The nascent D-loop stage. D-loop formation is mediated by RecA homolog(s) (32, 155). Most plants and animals, and budding yeast, utilize a meiosis-specific homolog, Dmc1, which, together with several specific partners, is responsible for strand invasion and ensuing events at the leading DSB end (32, 206, 235, 294, 343). The RecA homolog Rad51, which is primary in the mitotic cell cycle, is recruited into auxiliary roles (48, 60, 145, 179, 202, 205). Some organisms, for example, *C. elegans*, *Sordaria macrospora*, and *Neurospora crassa*, utilize Rad51 alone. Strand invasion also requires complex interplay among accessory factors (e.g., for Dmc1: RPA, Rad51, Rdh54/Tid1, Mei5-Sae3, and Hop2-Mnd1) (46, 145, 235, 316, 339, 340).

4.2.1.1. Homolog bias. The evolutionary and mechanistic roles of meiotic recombination dictate that it should occur preferentially between nonsister (homolog) chromatids, a feature known as homolog bias. In budding yeast, the ratio of interhomolog to intersister crossover interactions

is ~5:1 (versus the 2:1 ratio expected for random partner choice), and sister events are also rare in *C. elegans* (10). Bias is established during nascent D-loop formation and, accordingly, requires specific effects of RecA homologs and their modulators. In organisms that specify both meiosis-specific Dmc1 and mitotic Rad51, the latter molecule is recruited to the task of homolog bias (32, 150, 205). Axis components are also involved in homolog bias, including cohesins and meiosis-specific axis proteins, dependent on phosphorylation by meiotic and ATR/ATM checkpoint kinases (32, 57, 147, 150, 155). The logic and mechanism of homolog bias are mysterious. Sister-specific inhibition zones could be involved (117). The axis could be a barrier to use of the sister chromatid (review in 33, 147), or homolog bias might actually be the default option for mitotic DSB repair. In this case, cohesins would promote sister bias in both mitosis and meiosis, and the role of the meiotic recombination apparatus would be to eliminate this cohesin-mediated channeling (150).

4.2.1.2. DSB-mediated coalignment. Nascent D-loops identify matching sequences in loops of the homolog partner. The resulting complexes concomitantly become associated with the underlying partner axes. This association results in axis coalignment to ~400 nm (33, 325) (**Figure 4*e*, subpanel *iii***). Bridges that include recombination complexes are observed at this stage in many organisms (91, 325, 398, and discussion therein) (**Figure 4*h*,*i***). Interestingly, coalignment-mediating interactions tend to be quite regularly spaced (e.g., **Figure 4*g***). Such a pattern is not consistent with independent formation of DSBs on the two homologs. Thus, there must be some type of feedback between the formation of one interhomolog pairing contact and that of another contact nearby. For example, a DSB-mediated interaction at one location could inhibit another interaction (or even occurrence of another DSB) nearby. The relationship of such a process to DSB interference (see Section 3) remains to be determined.

In *Sordaria* (325), two key recombination proteins are required for proper coalignment. Mer3 is a DNA helicase that stabilizes and modulates D-loops via catalytic and noncatalytic activities (11, 93, 101, 155). MutSγ (Msh4/Msh5) embraces and stabilizes strand exchange junctions. It is related to the bacterial mismatch repair protein MutS but has no role in mismatch repair (138, 139, 155). Mer3 is present in axis-associated complexes on both DSB ends at the coalignment stage, presumably stabilizing interhomolog and intersister D-loops at the two ends (**Figure 4*g***). However, ensuing coalignment actively requires Mer3 as well as MutSγ, which acts downstream of Mer3, likely via effects at the leading DSB (325). Coalignment also requires Zip2 and Zip4 (91), which, together with Spo16, comprise a tight complex that binds both axes and branched DNAs and mediates the recombination complex/structure interface (14, 83, 91, 285, 342) (see Section 4.2.3.2).

4.2.2. Pathway bifurcation by crossover designation: timing and effects. During crossover patterning, a small subset of undifferentiated precursor interactions is designated to become crossovers, with the rest fated mostly to become noncrossovers as the default option. Each crossover designation sets up a spreading inhibitory signal that reduces the probability of another designation occurring nearby. The final number of crossovers is thus determined by the relative strengths of the designation and interference processes. Importantly, in order for this differentiation process to work, the recombination process must be arrested at the critical precursor stage such that progression is dependent on regulation. The nature of this arrest and the molecular events that comprise crossover designation are not known for any organism, but available information is discussed in this section and the next. The nature of the spreading inhibitory interference is similarly mysterious (see Section 6).

At present, a general conundrum pertains to understanding crossover patterning. In budding yeast and *Sordaria*, crossover designation is concomitant with SC nucleation and is independent

of SC polymerization or complete SC formation. It has been suggested in other organisms that crossover patterning requires the SC and, more specifically, occurs in the context of fully formed SC (see Section 6). Such proposals notwithstanding, there are close analogies between the patterns of events in these latter organisms and those defined in *Sordaria*, consistent with the operation of a single paradigm in all cases.

4.2.2.1. Budding yeast. In this organism, crossover designation occurs at the ends-apart nascent D-loop stage, with extension of leading DSB end strand invasion and/or pre-dHJs as the immediate DNA outcome (155). In accord with such timing, during leptotene, pairs of Rad51/Dmc1 cofoci occur at the ~400-nm separation expected for coalignment (33). Also, crossover designation at the DNA level and SC nucleation at the structural level are tightly coupled. The two events occur at the same sites; they both exhibit interference; and they are coordinately disrupted by mutations in key proteins (the ZMMs), which act downstream to implement both crossover formation and SC formation (25, 108, 316, 317). Moreover, the SC central region is not required for interference (see Section 6).

4.2.2.2. Sordaria. In this organism, after homolog axes are coaligned by invisible links (DNA connections) at ~400 nm (**Figure 4*g***), they progress to ~200-nm separation, with concomitant emergence of robust bridges comprising DNA, cohesin complexes, and the same proteins involved in mediating coalignment (MutSγ, Mer3, Msh4, Zip2, and Zip4) (91) (**Figure 4*b***). Patterning occurs at (or is concomitant with) this ~200-nm bridge stage. Thus, crossover designation appears to occur at the nascent D-loop stage, before SC forms, as in budding yeast. Furthermore, crossover patterning is accompanied by patterning of SC nucleation sites as part of a single-coordinate process (84, 388) (**Figure 5*d–f***). An intermediate number of recombination precursor/bridge sites (less than the total but larger than the number of crossovers) undergo a designation process that gives evenly spaced SC nucleations, and a subset of these SC nucleation sites are also, concomitantly, designated to become crossovers. This is shown directly by EM studies (388). SC nucleations are marked by two types of nodules, smaller and larger, referred to for historical reasons as early and late, respectively (**Figure 4*b***). The sum of both types of nodules, and thus SC nucleations, represents a subset of total recombination/coalignment interactions and exhibits interference (**Figure 5*f–h***); among these, the larger (late) nodules correspond to the totality of crossovers and also exhibit interference, which is more robust than that for the totality of all nodules/SC nucleations (**Figure 5*g,h***). A third subset of early recombination interactions are not marked by nodules and presumably also mature to noncrossovers (**Figure 5*f,g***). These conclusions are extended by fluorescence microscopy, which defines the same number of SC nucleations seen in EM and reveals the subsequent emergence, during pachytene, of recombination foci marked by E3 ligase Hei10 and MutSγ Msh4, which correspond in number and interference distribution to total EM nodules (**Figure 5*g,h***). Also, thereafter, MutSγ foci disappear and a smaller number of recombination complexes emerge that correspond specifically to crossovers in number and interference pattern (**Figure 5*g,h***).

This nested patterning effect can be explained mechanistically by a progressive designation process in which the first events occur at more sensitive precursor sites to give both SC nucleations and crossover designation while later events give only SC nucleations (and maturation of the corresponding interactions to noncrossovers as the default). These findings could be explained alternatively by two successive, independent rounds of interference (e.g., 80); however, the two rounds would have to occur essentially simultaneously during an extremely transient period (91). Patterning in budding yeast is easily mapped onto this *Sordaria* scenario by specifying that all designation events give both crossovers and SC nucleations.

4.2.2.3. Mouse. Prior to SC formation, mouse and human chromosomes exhibit large numbers of interaxis bridges that include recombination and cohesin proteins (discussion in 91) (**Figure 4*b***). Then, an intermediate number of recombination complexes emerge that contain Mer3, MutSγ, TEX11(aka Zip4), and RPA (241, 288, 289). It has been proposed that crossover designation is imposed on this intermediate set of complexes (80, 289). Alternatively, however, these complexes could be the downstream outcome of coordinate patterning of crossovers and SC nucleations at the leptotene/zygotene transition, just as in *Sordaria* and budding yeast. Several observations are in accord with this possibility. The mouse intermediate complexes appear concomitant with SC nucleation and are associated with sites of SC nucleations (263, 289, 295). SC nucleations in mouse occur not only at sites of crossovers but also at a number of other sites (126). The pattern observed in mouse is similar to that observed in *Sordaria*, where an intermediate number of recombination foci containing MutSγ are initially stabilized by an E3 ligase activity and then diminish to the crossover number (84) (**Figure 5*e***). But in *Sordaria*, these intermediate complexes are known to reflect only the subset of recombination interactions that underwent interference-mediated crossover designation/SC nucleation at a previous stage, at the leptotene/zygotene transition (84, 388) (**Figure 5*e*,*f***). Finally, in budding yeast, foci of MutSγ and several other molecules present in mouse intermediate complexes only appear, and/or are specifically stabilized, as downstream outcomes of crossover patterning (25, 138, 139).

4.2.2.4. Plants. Early pachytene chromosomes of plants also exhibit an intermediate number of MutSγ recombination complexes, which is reduced to a small number of crossover-correlated complexes by late pachytene (47, 144), as in *Sordaria* and mouse (see Sections 4.2.2.2 and 4.2.2.3). This progression, together with other findings, has been interpreted to mean that the early pachytene complexes are undifferentiated precursors and crossover designation acts on these complexes after SC has formed, in the context of the SC (Section 6). However, as in mouse, existing data are also compatible with a *Sordaria*-like process: (*a*) Plants also exhibit interaxis bridges at leptotene, some of which are sites of SC nucleation (7); (*b*) strikingly, in tomato, crossover-correlated recombination complexes, marked by Mlh1 foci, emerge concomitant with SC formation and during zygotene and are already present in their full number by early pachytene (212); (*c*) analysis of maize inversion heterozygotes suggests that crossover designation nucleates SC formation (225); (*d*) the overall patterns of MutSγ foci and Hei10 foci in plants are very similar to those in *Sordaria* (see Section 4.2.2.2); (*e*) Zip4 is required for normal SC formation in *Arabidopsis thaliana* (47) as in *Sordaria*; and (*f*) SC nucleations occur in excess over crossovers (143).

4.2.2.5. Caenorhabditis elegans. In this organism, a number of MutSγ foci are present at early pachytene and are generally inferred to be precursors of much smaller numbers of crossover-correlated foci present at later pachytene (177, 367, 380). However, the fact that the earlier MutSγ foci are present in their full number already at early pachytene raises the possibility that they have already developed during zygotene, leaving open the possibility of an earlier designation process in this organism as well.

These uncertainties are significant in part because they bear on whether crossover interference does or does not depend on the SC (see Section 6). Resolving them is an important future challenge.

4.2.3. Crossover designation, progression, and maturation. The bifurcation decision is implemented and followed by an elaborate series of effects as required to ensure the appropriate final outcomes.

4.2.3.1. Crossover designation. The activities that directly promote nascent D-loop extension/pre-dHJ formation for crossover designation are unknown. In budding yeast, the absence of

helicase Rdh54, the direct partner of Dmc1, allows efficient formation of crossover and noncrossover products and SCs, but the crossovers exhibit no interference (318). Perhaps this complex is required to arrest recombination at the precursor stage and then undergoes a conformational change in response to crossover designation.

From another perspective, a family of related meiosis-specific E3 ligases has been discussed as a possible mediator of crossover designation. In *Sordaria* and budding yeast, this is not the case: Such molecules, Zip3 and Hei10, respectively, act downstream of patterning (25, 84, 317). In mouse, two such molecules, Hei10 and RNF212, modulate intermediate complexes (288, 289) whose significance is not yet clear (155). However, in plants, in the context of scenarios that invoke the occurrence of patterning at pachytene, Hei10 is proposed to mediate interference by undergoing Ostwald ripening, with molecules moving from a larger number of smaller (precursor) complexes to a smaller number of large crossover-fated complexes in a process driven by decreased surface tension (115, 244) (see Section 6). And in *C. elegans*, an E3 ligase–mediated reaction–diffusion process has been proposed (390) (see Section 6). In general, it can be very difficult to critically distinguish effects that comprise crossover designation from those that immediately ensue to stabilize crossover-fated interactions and/or prepare them for progression to the next stage.

4.2.3.2. Postbifurcation progression. In budding yeast, postbifurcation DNA events of crossover formation are mediated by MutSγ and Mer3, with an early handoff from Dmc1 and later release of Rad51 (likely from lagging DSB ends) (155). MutSγ uses its ability to bind strand exchange junctions to stabilize SEI-to-dHJ intermediates and, concomitantly, to protect these intermediates from D-loop dissociation by the helicase/decatenase activity of Sgs1/TopoIII/RmiI (STR) (82, 173, 332, 384). The exact role of Mer3 in these events is not established. Second end capture for crossing-over is directly promoted by strand annealing protein Rad52 (206), assisted by single-strand binding protein RPA (267; K.P. Kim, personal communication). During noncrossover formation, in contrast, the STR complex is responsible for dissociating the leading DSB end from its partner (173, 332). Other events (e.g., DNA replication) and information from other organisms are discussed elsewhere (155).

In budding yeast, crossover-specific SEI formation and SC nucleation are coupled. The two processes are coordinately mediated by an ensemble of molecules known as the ZMMs. All ZMMs have homologs or relatives in other organisms with corresponding and/or related roles (155). Operation of this complex has been elucidated to some degree in budding yeast with two branches of effects. One branch comprises the biochemical components MutSγ and Mer3. The other branch comprises the axis-linking Zip2/Zip4/Spo16 (ZZS) complex. This branch directly nucleates SC formation, first recruiting SC central region components and then transverse filament component Zip1, with the help of prominent SUMOylation (19, 139, 285, 286). Both branches require SUMO E3 ligase Zip3 (49, 108, 139, 317). However, the structural branch seems to be primary because the ZZS complex can load without MutSγ (108). Coupling of the recombination branch to the structure branch likely requires the ZZS complex, which is needed for loading MutSγ and Mer3 (316). In addition, coupling requires SC component Zip1, potentially prior to SC formation per se: Zip3 first binds axes independent of Zip1 and then binds recombination sites dependent on Zip1 (315); furthermore, Zip1 recruits Zip3 to the recombination ensemble via its associated 9-1-1 complex (316). This early role of Zip1 could correspond to an early role specific to phosphorylated Zip1 (50). Zip1 and Zip3 are also required for stabilization of MutSγ complexes in two different, independent processes involving phosphorylation and SUMOylation, respectively (138, 139) (see Section 5).

Budding yeast studies also reveal direct roles of DDK (Cdc7-Dbf4) for the ZMM transition. After pathway bifurcation, Cdc7 is physically associated with the ZMM ensemble (83) and

promotes crossover formation by effects on Zip1, Rec8, and MutSγ (50, 138, 381). Since the action of Cdc7 is primed by cell cycle kinases, these effects are directly linked to cell cycle progression, as is also true for Cdc7-mediated DSB formation (138, 250). DDK is also important for mediating the interaction of telomeres with/through the nuclear envelope (290) as required for end-led motion.

4.2.3.3. Crossover-biased dHJ resolution by the Mutlγ complex. dHJs are resolved to crossovers by the endonuclease activity of MutLγ (Mlh1/Mlh3), which acts on branched structures as part of a tightly regulated complex. MutLγ is recruited to developing dHJs by proliferating cell nuclear antigen (PCNA) and its loader replication factor C (RFC) and nicks dHJ intermediates, codependent upon EXO1 (in a noncatalytic role) and MutSγ, which binds Holliday junctions (39, 155, 194, 226). MutLγ also participates in mismatch repair (72). Importantly, a dHJ has the potential to yield either a noncrossover or a crossover, according to whether junctions are resolved in the same or different senses, but during meiosis, the majority of dHJs are resolved to crossovers. Recent studies suggest a possible mechanism (194, 228). Crossover specificity can arise by PCNA-mediated targeting of MutLγ to the strands that contain single-strand gaps prior to the formation of covalently closed dHJ intermediates, in analogy with initiation steps of DNA mismatch repair. Moreover, resolution would occur only when each of the two Holliday junctions adopts one of two different coaxially stacked-X conformers. Exactly how the two appropriate conformers are created, and in such a way as to be different, remains to be determined. Internal factors, such as MutSγ (39, 194, 367), and/or external geometric constraints, such as the association of flanking arms to homolog axes or via association with SC central regions, could be involved. This model is also consistent with indications that dHJ resolution requires STR helicase/decatenase activity: MutLγ-mediated nicking occurs some distance from the actual strand exchange junctions, thus necessitating branch migration (194). Noncanonical resolvases work by other mechanisms (155).

4.2.3.4. Stringency roles for helicase/decatenase activity. Branch migration by STR helicase/decatenase not only is required along the normal crossover and noncrossover pathways but also serves as a stringency factor that channels mcJMs and other aberrant joint molecule structures into the canonical noncrossover and crossover pathways, inhibits ectopic recombination, and is required for recombination to be biased toward homologs rather than sisters (82, 332, 384). A second helicase, FANCM, also serves a stringency function in budding yeast (304). Analogous effects can be inferred for diverse helicase/topoisomerase activities in other organisms (155, 320). Notably, in the absence of this activity, most recombination interactions are resolved by structure-specific nucleases to give a mixture of noncrossovers and crossovers. As a result, in plants and mammals, where most recombination interactions normally produce noncrossovers (versus crossovers), the absence of such activities can result in a dramatic elevation in the number of crossovers (67, 86, 99).

4.2.3.5. RNA. An intriguing mystery for future study is the recent finding that excessive accumulation of RNA-DNA hybrids around DSBs competes with Rad51/Dmc1, impairs homolog bias, and decreases crossover and noncrossover recombination. On the other hand, precocious removal of RNA-DNA hybrids by RNase H1 overexpression also impairs meiotic recombination, raising the possibility of a positive role (379). More generally, involvement of noncoding RNAs in meiotic recombination is an area of future interest (114, 152, 313).

4.2.3.6. The synaptonemal complex. The intimate association of crossover recombination complexes and the SC throughout pachytene points to important interplay. The SC is clearly

required for the efficient recruitment of late-stage crossover-specific complexes (e.g., 83, 367). Other diverse roles have been suggested (155).

4.2.4. Posttranslational modifications. Phosphorylation plays diverse roles in the meiotic program. DNA damage kinases ATR and ATM are recruited from roles in mitotic recombination and repair; mitotic and meiotic cyclin-dependent kinases directly affect recombination and chromosome structure components; and cell cycle–linked kinases (DDK/Cdc7 and polo-like kinase) link recombination progression to the cell cycle (84, 122, 137, 138, 147, 155, 170).

Recent studies have also revealed important roles for both SUMOylation and proteolysis:

- SUMOylation is a pervasive modification. Its importance was originally appreciated in budding yeast via the identification of ZMM protein Zip3 as a SUMO E3 ligase and its involvement in SC assembly (52, 151, 217, 341). A specific role has also been elucidated for MutSγ, which is stabilized by polySUMOylation of its Msh4 subunit. This effect may act as a rheostat to provide optimal levels of MutSγ complexes just as homolog engagement ensues (139). More generally, SUMO affects virtually every molecule involved in the meiotic interhomolog interaction program (19).
- SUMOylation has also been implicated in the regulated turnover of recombination complexes. In mouse, at leptotene/zygotene, SUMO E3 ligase RNF212 promotes SUMOylation along axes and colocalizes to a subset of recombination complexes (288, 289, 295). This modification makes progression of recombination dependent upon Hei10, a SUMO-targeted ubiquitin ligase (STUbL), which targets the substrate molecule for degradation by the proteasome. This SUMO-ubiquitin relay also affects axis SUMOylation. Similarly, *Sordaria* E3 ligase Hei10 mediates both development and turnover of two sequential types of recombination complexes, each demarked by characteristic amplified Hei10 foci, as well as integrating these inputs with CDK/cyclin inputs (84). E3 ligases also mediate the stabilization and turnover of recombination complexes in *C. elegans* but without involvement of SUMO (255, 390). And in plants, E3 ligase Hei10 accumulates sequentially in different types of recombination complexes, analogously to *Sordaria*, and promotes crossing-over in a dosage-dependent manner (47, 314). The general presumption is that analogous effects occur in all systems but with differences in molecular details (155). Critical differences may or may not exist with regard to the roles of such effects in crossover designation (see Section 4.2.3.1).
- Opposing effects of stabilization and proteolysis can also occur by a different mechanism. In budding yeast, the MutSγ subunit Msh4 is subject to proteasome-mediated degradation via a ubiquitin-independent N-terminal degron motif, and this effect is opposed by (Cdc7-mediated) phosphorylation of that motif. The relevant effect of phosphorylation is to provide an appropriate steady-state level of MutSγ as manifested in the formation of corresponding recombination foci. This modulation comes into play during implementation of ZMM effects and remains relevant through dHJ formation/resolution for crossover formation (138). Association of proteasomes to prophase axes is also observed in budding yeast (6).

4.2.5. Crossover/chiasma landscapes. In many/most organisms, crossovers/chiasmata do not occur uniformly along the lengths of the chromosomes. In barley and wheat, DSBs and earlier recombination intermediates occur regularly along the lengths of the chromosomes, whereas crossover-correlated foci show more localized distributions (142, 143, 265). These effects are not explained by crossover interference but instead suggest that the probability of crossover designation is globally modulated. In these organisms, and also in mouse (280), this pattern corresponds to a temporal program in which DNA replication, early events of recombination, and SC formation

all occur first near chromosome ends and then progress through middle regions. Crossovers then occur differentially in the earlier-progressing regions, with recombination in middle regions presumptively biased to give noncrossovers. The relative proportion of crossover versus noncrossover outcomes also varies significantly from one DSB site to another even within a given region. Factors contributing to global modulation include chromatin modification status and proximity to an axis association site (51, 79, 89, 112, 315). Centromere regions and heterochromatin also exhibit specific effects (133).

4.3. Some Broader Implications

Meiotic recombination involves specific modulations that are of integral importance for its evolutionary role in genetic shuffling and/or for MI homolog segregation.

4.3.1. Crossover levels are adjusted by modulations of axis length. Total crossover levels are proportional to chromosome axis length. This relationship is robust because (*a*) DSBs and DSB-mediated interhomolog interactions tend to be evenly spaced and are proportional in number to chromosome axis length (325, 357) and (*b*) interference then acts on this array of DSB-mediated interhomolog interactions to give crossovers the same average spacing all along the chromosomes.

Importantly, this proportionality holds even when axis lengths vary due to a genetic perturbation (e.g., 323) or within a single organism or even a single nucleus (359). This is because the density of loops along the axis is the same in the different cases (184) so that all axis-associated aspects of recombination always occur with the same length-dependence. Modulation of axis length has thus emerged as an important simple and general mechanism for modulating crossover frequency (without perturbation of any other, more complicated processes). For example, (*a*) axis length differences underlie differences in crossover levels between males and females in several organisms (e.g., 116, 128, 358). (*b*) They can also explain heritable differences in crossover levels among different gamete-producing individuals (61, 185, 348). (*c*) Changes in crossover levels in different environmental conditions can reflect corresponding changes in axis length [e.g., temperature (220, 247)]. (*d*) Crossover levels covary across chromosomes on a nucleus-to-nucleus basis in several organisms (359). Some nuclei have especially low levels of crossovers on all chromosomes, while others have especially high levels of crossovers. This effect results from global nucleus-to-nucleus variation in chromosome axis length. Such covariation is evolutionarily important. It increases the frequencies of hypo- and hypercrossover gametes. And this effect, in turn, confers a selective advantage when environmental conditions fluctuate, in so-called gametic bet hedging: Hypocrossover gametes are favored when conditions are constant (and new combinations are disfavored), while hypercrossover gametes are favored when conditions have changed (and new combinations confer a selective advantage) (359).

4.3.2. Post-DSB crossover homeostasis. In several situations, chromosomal perturbations result in compensatory effects that help to maintain a normal or near-normal level of crossovers. Some of these effects act to increase DSBs (see Section 3). Other effects appear to come into play at a later stage:

- If DSB formation is reduced below its normal level, the frequency of crossovers is reduced, but to a less-than-proportional extent, at the expense of noncrossovers (231, 392). This effect arises because crossover designation at a given DSB site is affected by interference from already-designated crossovers at nearby DSBs. When DSB density is reduced, flanking DSBs will be further away, and thus interference effects will be reduced, leading to an increased likelihood that a given DSB will give rise to a crossover.

- In *Drosophila* and *C. elegans*, structural heterozygosities impede crossover formation within the heterozygous region but result in an increase in crossover levels in other regions (known as the interchromosomal effect) (41, 70, 168). Similarly, in *Sordaria* and *A. thaliana* mutants where homolog pairing is compromised, crossover levels tend to be maintained but with crowding of crossovers into regions where pairing could still occur normally (162, 334).

4.3.3. Human meiosis. Intriguingly, although recombination in the two human sexes proceeds analogously and efficiently through most stages, there is a dramatic difference in the number of gametes with abnormal numbers of chromosomes (aneuploidy) between female and male, and, moreover, this difference is age dependent.

4.3.3.1. Female. Human female meiosis is characterized by high levels of aneuploidy as compared to that of human males or other species. Oocyte aneuploidy occurs at especially high levels in very young women, at somewhat lower (but still elevated) levels in women of prime child-bearing age, and then it dramatically and progressively increases with increasing maternal age (i.e., the maternal age effect) (127, 134, 135, 363).

For women of child-bearing age, a key contributor to elevated aneuploidy is inefficient maturation of crossovers (357). Crossover sites are determined correctly, for example, as in male meiosis, but some of the resulting crossover-designated interactions fail to ultimately give crossovers. In effect, a subset of crossovers is subtracted from the total array that would normally have occurred. One consequence of this subtraction is an increased frequency of homolog pairs that lack even the one obligatory crossover. In addition, there is an increase in the frequency of pairs that exhibit only distal crossovers. Both types of configurations predispose chromosomes to missegregation by compromising the tension-sensing process that ensures regular bipolar alignment. The mechanistic basis for this crossover maturation inefficiency (CMI) is not known. It might reflect an intrinsic defect in the crossover recombination process (e.g., a defect at the critical intermediate step of second end capture). Alternatively, human oocytes exhibit very high levels of interlocking (23). Such configurations can sometimes be held in place by recombination interactions that normally would give rise to crossovers (Section 4), and elimination of the involved DNA linkages would allow prophase progression but with loss of the corresponding crossover products.

The proximate cause of increased aneuploidy with increasing age is the reduction in cohesion between sister chromatid arms (which is required to keep homologs connected until anaphase I onset; see Section 2.4.3). This cohesin fatigue could, in turn, result from age-dependent metabolic or physiological changes (127). CMI cannot be the primary basis for the maternal age effect because recombination is completed in oocytes prior to the birth of the mother. However, the resultant increase in chromosomes with only distal crossovers should sensitize those chromosomes to cohesin fatigue: Since homolog connectedness at MI is maintained by cohesion distal to the most centromere-proximal crossover, chromosomes with only distal crossovers are held in place by only the short regions of cohesion and thus will be more susceptible to loss of cohesins. Such complications could also contribute to interesting effects: not only MI segregation but also the fate of sister chromatids at MII (268). Overall, CMI is a major contributor to the fact that occurrence of both missing crossovers and aberrant crossover positioning is correlated with aneuploidy (135).

Importantly, aneuploidy is also elevated in very young women, the basis for which is not understood (127).

4.3.3.2. Male. In the male germline, very young men (and mice) have a higher frequency of aneuploid gametes, perhaps because of defective crossover maturation (386). In mature men, the frequency of aneuploidy does not increase with increasing paternal age (as in women; see above).

However, the frequency of mutations in sperm does increase with age. In the male germline, mitotic divisions that precede spermatogenesis occur throughout the lifetime of the parent. Mutations may accumulate during successive rounds of DNA replication during these divisions (for a recent discussion, see 370).

4.3.4. Speciation. Studies of meiotic recombination provide two inputs into the discussion of what ensures speciation. One factor is that heteroduplex DNA formed between homologous genomes is specifically detected and rejected by interplay between the DNA mismatch repair system and the meiotic recombination machinery (28). A second factor is the discovery that heterozygosity for the zinc finger histone methyl transferase PRDM9, which defines DSB hot spot preferences in some mammals (including human), is also a speciation gene (e.g., 75, 76, 102). In hybrid crossovers, infertility results when PRDM9 does not interact with the same positions on homologs, indicated by DSB asymmetry (76, 102, 385). This effect occurs after DSB formation and results in defective synapsis and crossover formation, implying that it must occur during coalignment pairing and/or implementation of crossover designation. PRDM9 might be important for DSB/partner homology searching, or it might be required to create a nucleosome-free region on the partner duplex to allow the formation of a DSB/partner D-loop complex (324). Or, as PRDM9 also interacts directly with chromosome axes (20, 272, 337), it might be required for robust association of the nascent D-loop complex with the partner axis.

4.3.5. Recombination-associated mutation and gene conversion. The DNA synthesis that accompanies meiotic recombination tends to be error prone, resulting in an elevation of mutation rate in meiosis versus mitosis (12). In addition, local sequence shuffling between homologs can arise due to the local DNA events at sites of recombination (64). When such events occur with a noncrossover outcome, they are often referred to as gene conversions. Formally, however, gene conversion is non-Mendelian segregation of a single marker, irrespective of whether the outcome is a crossover or noncrossover. In their evolutionary consequences, these localized changes are more analogous to mutation than to the genetic shuffling resulting from crossing-over (63, 112, 347).

4.3.6. Increasing crossover levels for plant breeding. The creation of new genetic combinations in plants underlies efforts to optimize food-providing crops. As a result, factors that increase the frequency of crossing-over or allow it to occur in otherwise silent regions (e.g., heterochromatin) are emerging (142, 143, 195, 234, 314, 329, 344; but see also 330). Prominent among these are increases in the dosage-sensitive crossover-promoting factor Hei10 and mutations in helicase/topoisomerase complexes (e.g., 67, 86, 99, 314, 320). Such mutations allow noncrossover-fated interactions (which are in great excess over crossover interactions) to give rise efficiently and aberrantly to crossovers.

5. HOMOLOG PAIRING

5.1. Background

How do homologs manage to identify one another and become closely juxtaposed regularly along their lengths on a biologically relevant timescale without producing a tangled mess? These challenges are especially dramatic for organisms with very long chromosomes, even as they achieve full synapsis in very crowded states (**Figure *6a,b***).

5.1.1. DSB-mediated axis coalignment leading to synapsis. Homolog identification at the DNA level produces the ends-apart nascent D-loop configuration that comprises a first linkage

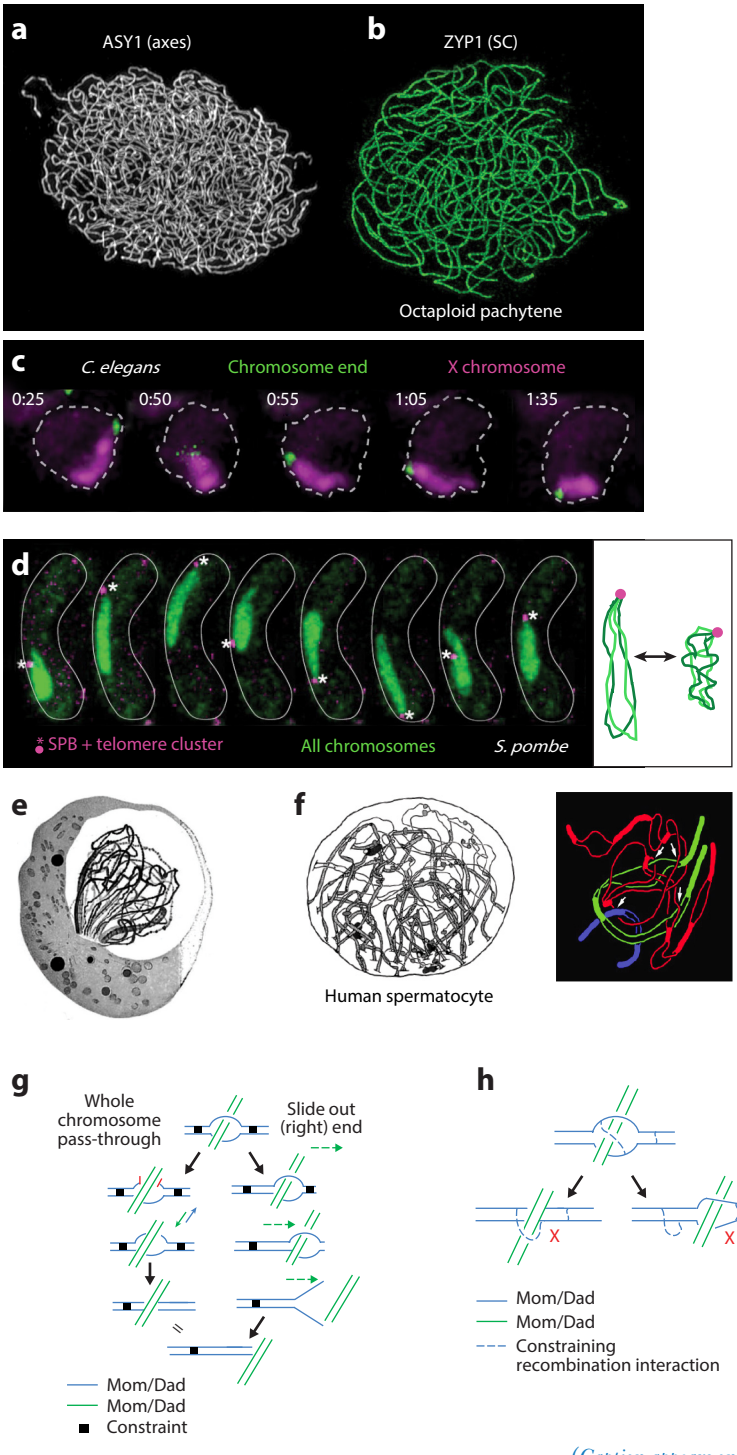

(*Caption appears on following page*)

Figure 6 (*Figure appears on preceding page*)

Homolog pairing. (*a*,*b*) *Arabidopsis arenosa* illustrates the complex paths of chromosomes not only (*a*) before coalignment when no SC is present but also (*b*) after SC formation. Panels *a* and *b* adapted from illustrations provided by Chris Morgan. (*c*) End-led motion of a *Caenorhabditis elegans* single-chromosome trajectory (ends in *green*) is depicted, as promoted by cytoskeletal dynein moving along microtubules. Panel adapted with permission from Reference 371. (*d*) In *Schizosaccharomyces pombe*, all chromosome ends are clustered at the spindle pole body (SPB; *magenta* and *white asterisk*), which is moved back and forth along an elongated cell by dynein motors. (*Right*) Homologous loci typically pair when the SPB is at the cell pole and the nucleus is elongated, whereas they unpair when the SPB is in the cell center and the nucleus is rounder. Panel adapted with permission from Reference 44. (*e*) The classical bouquet in flatworm is depicted. Panel adapted from Reference 111. (*f*) Interlockings at zygotene in human spermatocytes are depicted. Panel adapted with permission from Reference 293. (*g*,*h*) Fundamental requirements for the resolution of interlocks are shown. (*g*) Two ways that whole-chromosome relationships can be regularized are depicted. (*h*) Recombination interactions constrain interlock resolution (*red X*) regardless of how whole-chromosome relationships are regularized, by pass-through (*left*) or sliding out the end (*right*). Abbreviations: SC, synaptonemal complex; SPB, spindle pole body.

between homologs (**Figure 4*e***). However, regular spatial coalignment along the lengths of the chromosomes cannot be achieved by DNA/DNA contacts within diffuse chromatin. Accordingly, it is the association of recombination complexes with axes that allows these links to mediate regular spatial juxtaposition along chromosome lengths, after which SC can be installed (**Figure 4*e***).

5.1.2. DNA/DNA homology searching. How a DSB carries out homology searching is unclear. One model suggests that the leading DSB end is released from its DSB–donor axis association to create a homology-searching tentacle (181, 274). Alternatively, both DSB ends may remain associated with their original sister chromatid during the search. The latter scenario would imply a strong dependence on factors that bring homologous regions into close proximity.

The search process itself is subject to the same general requirements as all other RecA (homolog)-mediated searches. A RecA homolog/ssDNA filament searches proximate chromosomal regions in one, two, and three dimensions (i.e., sliding, intersegmental transfer, and collision), aided by simultaneous multivalent interactions (16, 278). The search process must also solve the speed-stability paradox. In brief, if pseudohomologous interactions are stable (and thus long-lived) enough to allow efficient discrimination between perfect and imperfect homology, it will take too long to sort through all of the alternative partners, but if the interactions are weak enough to allow rapid searching, they will not be adequate to sensitively discriminate perfect from imperfect matches (236). Suggested solutions to this paradox involve multistep kinetic effects (377). Interestingly, however, the speed of homology searching is unlikely to be the rate-limiting step in partner identification, as shown by the speed with which a RecA-bound oligonucleotide identifies its correct partner in vitro (376).

5.1.3. Atypical pairing and segregation. In *D. melanogaster* and *B. mori* female, as well as in *C. elegans* meiosis, SC forms between homologs before, in the absence of, or independent of recombination, respectively (85, 98, 169, 301). By contrast, in *S. pombe* and *T. thermophila*, there are many recombination interactions but no SC (221, 303).

5.2. How to Think About Pairing

If pairing of long, thin chromosomes began with those chromosomes randomly distributed and intermingled throughout the nucleus, the challenges to both homolog searching/identification and achieving acceptable topological relationships would be severe. Many different processes act synergistically to both avoid and overcome this situation, but they can be understood as the sum of two basic components.

First, multiple effects tend to place corresponding (allelic) regions of homologs in correlated dispositions. Any such process, in turn, will confer several concomitant advantages: (*a*) It will facilitate homology identification because the dimensionality, volume, and genomic complexity of the search process will be reduced. (*b*) Partner identification at the whole-chromosome level will be facilitated because of reductions in the extent to which a DSB must drag the rest of the chromosome along during the search process and in the number of chromosomes that might lie between the searching DSB and its corresponding partner region to complexify the search process. (*c*) The topological complexity of the chromosome milieu will be simplified, thereby reducing the chance that unacceptable relationships (e.g., entanglements/interlocks) will arise. A constellation of such processes act to increasing effect as the pairing process progresses, finally allowing a regular outcome (398).

Second, despite many facilitating effects, topologically unacceptable relationships nonetheless do arise. These must be (and are) actively eliminated. Other types of inappropriate contacts must also be eliminated. These processes, discussed below, have been reviewed (e.g., 187, 395, 398).

5.3. Nonrandom Chromosome Positioning Facilitates Homology Searching and Promotes Regular Topology

In many organisms, specific relative dispositions of different chromosomes facilitate homolog pairing. Some features are common to all studied organisms while others are organism-specific.

5.3.1. Clustering and coupling of centromeres or chromosome ends. Many organisms exhibit spatial clustering of centromeres or pericentric heterochromatin, often reflecting the persistence of the Rabl orientation created by anaphase of the preceding mitotic division. This organization places allelic regions at similar latitudes with respect to the cluster, thus simplifying spatial relationships between homologs (21, 307, 308, 396). Pairwise, homology-independent associations between centromeres (aka coupling) also likely contribute to pairing (discussed in 196). In some organisms, pairwise homology-independent and/or homology-dependent associations of telomeres also occur early in the pairing process (e.g., 118).

5.3.2. Telomere–nuclear envelope association. In most organisms analyzed so far, chromosome ends (telomeres) are associated with the nuclear envelope throughout the pairing period (105, 309, 396) (**Figure 2*e***). This feature allows homology searching among regions close to chromosome ends to occur in two dimensions rather than three. Indeed, in budding yeast, the farther that dispersed sequences are from their nearest telomere, the less likely they are to engage in ectopic recombination, a proxy for recombination-mediated pairing (312). Nuclear envelope association also prevents ends from threading through the matrix of internal chromosome regions, thereby minimizing one potential source of entanglements. Finally, this association allows cytoskeleton-mediated telomere-led chromosome motion.

5.3.3. DSB-independent pairing. Homologs can pair without the involvement of DSBs or RecA homologs (Dmc1 and/or Rad51). In meiosis, such pairing occurs prior to the initiation of recombination and can be genome wide or localized to, for example, centromeres or telomeres (398). In *S. pombe*, such pairing occurs globally and involves RNA-mediated phase separation (87). In *C. elegans*, pairing occurs in specific regions at chromosome ends (called pairing centers) and involves zinc finger proteins (which, however, do not specify all of the necessary information) (298). Recombination-independent pairing can also occur globally, as seen in budding yeast, mouse, and *D. melanogaster* (398). Interestingly, in *Drosophila*, recombination-independent pairing is famously present in somatic cells but is then lost in the germline before being reestablished in early meiosis (37, 167). And in budding yeast, pairing might occur in two phases: globally and

then in direct association with DSB formation (373). Finally, in many filamentous fungi, homologous sequences present at two or more dispersed positions in the genome can be silenced in the recombination-independent process of repeat-induced point mutation/methylation induced premeiotically (RIP/MIP) before karyogamy and thus meiosis. Sequences that are present on only one of the two homologs are similarly silenced at onset of meiosis in the process of meiotic silencing by unpaired DNA (MSUD) (232, 296). Several types of direct DNA–DNA interactions have been proposed to explain such phenomena (197, 296), as has a structure-based bar code (159).

5.3.4. Co-orientation of unrelated chromosomes by pulses of end-led motion. Universally, specifically during the pairing period, nuclear envelope–associated chromosome ends are actively moved by cytoskeletal motors via robust linkage to and through the nuclear envelope (via SUN/KASH proteins) (e.g., **Figure 6*c*,*d***). Chromosome ends are transported along nucleus-associated actin or tubulin filaments via cognate motor proteins (146, 192, 208, 218, 259, 301, 310) with correspondingly rapid motion (259, 371). End-led motions are important not only in the canonical program but also in *D. melanogaster* male meiosis, where both recombination and SC are absent (301). Interestingly, similar motions are triggered by telomere defects in mitotic cells (53). End-led motions are accompanied by chromosome deformations, often with correlated nuclear deformations, and/or are enabled by weakening of nuclear lamins (192, 275, 310, 387). Cytoskeleton-mediated whole-nucleus rotations also occur (218).

Disruption of chromosome end motion by chemical or genetic intervention can result in defects or delays in spatial association of homologs, increased association of unrelated chromosomes via ectopic recombination, promiscuous DSB-independent pairing interactions, and increased levels of interlocks (e.g., 218). Thus, overall, motion promotes partner identification, helps to avoid and/or eliminate topologically inappropriate relationships, and serves as a stringency factor to eliminate unwanted linkages.

A central effect of end-led motion is that groups of ends tend to move coordinately. This is dramatic in *S. pombe*, an exceptional case in which all telomeres are stably grouped into a tight cluster associated with the spindle pole body (fungal centrosome equivalent), which is moved back and forth along the length of a highly elongated cell in a so-called horsetail motion (44, 146) (**Figure 6*d***). This movement has critical implications. Each phase of motion tends to align all chromosomes, nonspecifically, thereby placing allelic regions at corresponding positions relative to the telomere cluster to favor both homolog identification and topological regularity. At each change of direction, relationships are disrupted and recreated, providing new opportunities for pairing of still unpaired homologs. Interestingly, in this organism, back-and-forth motion is initially accompanied by the establishment of recombination-independent pairing, with recombination-mediated interactions occurring later (87, 88). Thus, substantial pairing with regular topology can be achieved by easily adjustable phase separation interactions before more permanent recombination-mediated linkages are established.

The same principle may pertain to many organisms. In budding yeast and *C. elegans*, ever-changing groups of chromosome ends undergo directed movement in different directions at different times (191, 366). Coordinately moving ends may be directly associated (as in *C. elegans*) or linked indirectly to a directly transported chromosome end, for example, by localization to the surrounding region of nuclear envelope deformation (as in budding yeast). Sequential coordinate movements involving different sets of ends will again allow pairing to propagate throughout the genome. In this context, whole-nucleus rotation, which coordinately affects all chromosome ends throughout the nucleus, should tend to promote the propagation of co-orientation inward from the ends of the chromosomes along their lengths.

The ciliate protist *T. thermophila* exhibits a related effect: Pairing is promoted by dramatic elongation of the nucleus at the onset of meiosis with concomitant elongation and co-orientation of chromosomes that are nuclear envelope–associated along their lengths (221, 222).

Interestingly, in budding yeast, dynamic motions occur during pachytene when pairing is substantially completed, pointing to postpairing roles for motion (66, 191, 310).

5.3.5. Pairing should promote pairing. In *Sordaria*, where ends-apart nascent D-loop/axis complexes are marked by Mer3 helicase, the absence of that activity results in a woven-basket configuration of axes (325). Thus, some aspect of the act of homolog juxtaposition is, per se, important for regular coalignment. As one possibility, rapid juxtaposition of homolog axes at the site of one coalignment interaction will, because of axis stiffness, tend to draw adjacent homolog regions into closer proximity, concomitantly promoting both rapid and efficient homology identification in those regions and withdrawing the involved segment from the pairing pool, thus minimizing entanglements (119, 325). Also, coordinate end-led movement of chromosomes paired in end-proximal regions should promote pairing of downstream regions (246).

5.3.6. The bouquet. The bouquet configuration, in which all chromosome ends are clustered in a restricted region of the nuclear envelope, is a common feature of meiotic prophase, described in detail more than a century ago (111) (**Figure 6*e***). Although this configuration is widely assumed to favor speed and regularity of homolog pairing (307), this view is likely too simple. Sets of chromosome ends tend to colocalize throughout leptotene/zygotene; however, the classical tight bouquet configuration is a transient state that appears at late leptotene/zygotene, after coalignment pairing is mostly complete, and disappears at early pachytene, pointing to a late role (395, 397). Cytoskeleton-mediated end-led motion likely underlies movement of chromosome ends into the bouquet state, but what causes all ends to cluster is not known. Interestingly, however, the formation of a tight bouquet is part of an overall reorganization of the nuclear envelope, including massive clustering of nuclear pores in regions separated from telomere clusters (396). Perhaps this nuclear reorganization drives chromosome ends into a tight bouquet formation. What causes the bouquet configuration to be lost at early pachytene, when chromosome ends redistribute around the nuclear periphery, is also not known.

5.3.7. Nuclear volume. A universal feature of meiosis is an increase in nuclear volume throughout the pairing/synapsis period (e.g., 394). It is tempting to link this increase to the need for space for chromosome movement during chromosome coalignment and interlock resolution.

5.4. Topological Chromosome Entanglements/Interlocks Are Actively Eliminated

An early finding from light microscopy, since confirmed by EM and fluorescence imaging, was the observation of interlocks: configurations in which SC has formed on either side of an entrapped chromosome or pair of chromosomes (293, 397) (**Figure 6*f***). Topologically inappropriate chromosome configurations also occur at earlier stages, among axes that are not yet linked by SC (325). Nonetheless, by mid-pachytene, no such configurations are observed (292, 325), implying that they are actively removed. Effects that result in removal of interlocks are targeted to two main interrelated challenges (**Figure 6*g*,*h***).

5.4.1. Regularization of whole-chromosome paths. Removal of an unacceptable topological relationship between/among whole-chromosome paths necessarily requires movement of the entrapped and entrapping chromosome regions relative to one another. Such an outcome can be achieved in three possible ways (293). (*a*) An entrapping whole chromosome can be broken and an

entrapped chromosome or chromosomes passed through the break (**Figure 6*g***). (*b*) An entrapped chromosome (or pair of connected homologs) can move outward to an end of the entrapping chromosome (**Figure 6*g***). (*c*) An entrapped bivalent may be released from the nuclear envelope and withdrawn through the open entrapping region.

The first possibility arose because, in a classical interlock configuration, the entrapped chromosome region is flanked on both sides by SC (e.g., **Figure 6*f***). Since the SC was assumed to be a stable structure, the only way to resolve the situation would be to break one entrapping chromosome, allowing the entrapped chromosome to slide through the gap. Accordingly, it was proposed that disassembly of axes locally at the interlocked site (as is observed) would be followed by appropriately directed TopoII-mediated duplex/duplex passage, after which axis continuity could be restored (353). And more recently, an increase in interlockings in the absence of TopoII has been reported (229). However, it is now known that the SC is a highly dynamic structure (299) and can therefore be expected to undergo adjustment in response to external forces. Thus, in an interlock where SC segments surround an entrapped chromosome(s), the SC could undergo depolymerization and repolymerization to allow that chromosome to move outward for resolution. In this scenario, TopoII would have other roles.

The second possibility has arisen because configurations involving splayed ends of a homolog pair can be observed, suggestive of recent release of an entrapped chromosome (292). The required outward movement could be promoted by cytoskeleton-mediated end-led motions without detachment of end(s) from the nuclear envelope. Alternatively, interlock resolution could be related to the fact that the bouquet configuration dissipates at early pachytene, when chromosome ends redisperse around the nuclear envelope. The outcome of this transition will be a concerted springing apart of ends, which would intrinsically tend to promote movement of any entrapped chromosome outward through the entrapping chromosomes. Such an effect could explain why interlocks are finally resolved specifically during early pachytene. The third possibility has arisen due to observation of configurations in which an entrapped chromosome seems poised to withdraw through an entrapping hole (325).

5.4.2. Removal of constraining recombination linkages. Interlocks are formed during the process of homolog coalignment, which is mediated by recombination interactions that link homolog axes (Sections 3 and 4). Thus, topologically inappropriate configurations will be locked in by recombination interactions. These interactions are molecularly stable links; moreover, each homolog undergoes many such interactions. Thus, removal of constraining recombination interactions is a major challenge for interlock resolution. This challenge persists regardless of how whole-chromosome relationships are resolved (**Figure 6*b***). Any or all of the mechanisms discussed below are possible.

5.4.2.1. Crossover interference. Crossover interference causes most DNA intermediates to be directed toward the noncrossover fate, with concomitant loss of homolog linkages. Removal of these interactions would allow movement of the entrapped chromosome out through the ends of the entrapping chromosomes. This could be a powerful effect, especially if coalignment and interference are occurring concurrently (see Section 6). Such interplay has been suggested for *Arabidopsis arenosa* tetraploids (246).

5.4.2.2. Sensing stalled recombination. In a region involved in an entrapment, recombination interactions between widely separated homologs may be stalled at some intermediate stage. Such interactions could be removed by a damage response pathway, with resolution to interhomolog noncrossover or intersister outcomes. In accord with this idea, interlock frequency is increased in the absence of Mlh1, which resolves dHJs during meiosis but participates in recognition and

regularization of nonnative DNA structures during mismatch repair (325). Type I topoisomerase/helicase complexes should also participate in such effects via their ability to dissociate off-pathway recombination intermediates.

5.4.2.3. Topoisomerase-mediated decatenation. Absence of TopoII increases interlocking in *A. thaliana* (229). This could reflect a direct role for topoisomerase activity in the passage of one pair of sister chromatids through another (see Section 5.4.1). Alternatively, TopoII-mediated breakage and rejoining of a recombination bridge between entrapping homologs might allow the release of an entrapped chromosome, and/or TopoII might remove catenations among unrelated chromosomes that otherwise would block interlock resolution.

5.4.2.4. Local diffuseness. Sites of entanglements/interlocks tend to undergo axis disassembly, with diffuse chromatin at the involved location (148). This could potentially be a sign of a damage checkpoint response that enables resolution of recombination intermediates.

5.4.2.5. Conclusion. Unresolved interlocks will entrap unrelated chromosomes at metaphase I, inhibiting their correct segregation. Thus, interlock removal is a critical process, whatever its component mechanism(s).

5.4.3. Disruption of other unwanted contacts. Inappropriate pairing contacts can occur between partially homologous sequences; between perfectly homologous regions that are located in nonallelic positions (ectopically); and, in *C. elegans*, between nonhomologous chromosome ends that share binding of the same zinc finger pairing protein (298). Additionally, contacts between chromatin and the nuclear envelope and/or topological catenations between unrelated chromosomes can impede regular pairing. Pulses of end-led motions will tend to disrupt such unwanted linkages, either directly or by providing directionality to dissociation/reassociation reactions (see Section 6).

5.5. Pairing and the Synaptonemal Complex

The SC is a cytologically prominent pairing structure (**Figure 3*d***). Nonetheless, it is not responsible for either homolog recognition or juxtaposition. Correspondingly, in aberrant situations, SC can be installed independent of homology to link any two axes that come close enough together, for example, between nonhomologous regions or chromosomes, between the two arms of the same chromosome that fold back on one another, and in structural aggregates (polycomplexes) that occur inside or outside the nucleus (257, 397).

5.5.1. Is the full-length synaptonemal complex a structure for interference-dictated pairing maintenance? The SC was traditionally thought to have evolved in order to promote the biochemical events of recombination, for example, by stabilizing crossover recombination complexes. And, indeed, the SC clearly is important for the recruitment of molecules and execution of the final stages of crossover formation (155). We have, however, previously suggested that the fundamental evolutionarily driven role for extension of SC along the lengths of the chromosomes may be to maintain homolog pairing (183). Once crossover interference has been implemented and noncrossover-fated interactions have sufficiently progressed, crossovers will comprise the only remaining connections between homologs. Moreover, due to the effects of interference, crossovers are generally few and far between, especially along long chromosomes. Thus, the SC will be essential in maintaining a neat and regular relationship between homologs throughout pachytene, specifically because of the effects of crossover interference. This relationship could explain, for example, why *S. pombe* and *Aspergillus nidulans* lack both the SC and robust crossover

interference (96, 303): In the absence of interference, crossovers occur along all chromosomes in large numbers, thus bypassing the need for an SC (183).

5.5.2. Two-stage evolution of the synaptonemal complex? The above scenario has the corollary implication that the presence of an SC all along the chromosomes might have evolved in response to the evolution of crossover interference. Crossover interference may have evolved first because of the advantages it confers in determining crossover number and genetic shuffling (see Section 6). Its emergence would, in turn, have driven evolution of full-length SC. This scenario would imply that the SC is not required for crossover interference, in accord with the situation in at least some organisms (see Section 6). It is also opposite of the idea that, in organisms that lack both features (e.g., *S. pombe* and *A. nidulans*), it is the absence of the SC that is responsible for absence of interference (95) (see Section 6).

Alternatively, SC formation along the chromosomes might have evolved first, as a primordial pairing process, thereby creating conditions permissive for the subsequent evolution of recombination connections and crossover interference. The existence of organisms that have SC but no recombination (e.g., *B. mori* females) could support this alternative possibility.

Finally, the SC might have evolved in two stages, first to promote events specifically at sites of crossovers and later to ensure postinterference pairing. The first stage would explain the widespread nucleation of SC formation at crossover sites (see Section 6), the persistence of the SCs at crossover sites throughout the diplotene stage when most SCs have been disassembled (see Section 7), and the fact that some organisms only install SCs locally at crossover/chiasma sites, without extension along the lengths of the chromosomes (e.g., 69, 350).

In the second stage, once crossover interference emerged, SC nucleation at recombination sites would be expanded to include also other (noncrossover-fated) sites, thus allowing SC propagation along the lengths of chromosomes. This possibility is supported by the finding in *Sordaria* that the primary effect of interference is to produce evenly spaced SC nucleation sites, a subset of which are also (interfering) crossover sites and the remainder of which are a subset of noncrossover-fated sites (388). Interference-mediated SC nucleation thus has the dual function of promoting efficient installation of SC all along the lengths of homologs and allowing for special local relationships between crossover sites and the SC. It has also been suggested that "CO control in most species has been adjusted such that synapsis is initiated efficiently, but CO formation is limited to a relatively low level" (143, p. 37).

5.5.3. Summary. Despite its complexities, the meiotic pairing process can be boiled down to two components. First, multiple sequential processes tend to bring corresponding regions on homologs into close proximity, with two concomitant effects: (*a*) simplification and acceleration of DSB-mediated homology searching and (*b*) reduction of the probability that coalignment pairing will entrap entanglements. Second, additional processes eliminate unwanted contacts and inappropriate topologies.

6. CROSSOVER INTERFERENCE

Despite (or perhaps because of) considerable progress, current discussions of crossover patterning and related events are primarily dominated by questions rather than answers (103, 186, 276, 352, 358, 360) (see Sections 3 and 4).

6.1. Basics of Crossover Interference

As described above, crossover patterning involves (*a*) the creation of an array of undifferentiated precursor interactions, poised to undergo regulated fate determination; (*b*) the designation of a

subset of those precursor interactions to be crossovers, with noncrossover formation as the default option; and (*c*) each designation event triggering an inhibitory signal that spreads along the chromosomes and reduces the probability that subsequent designation(s) will occur nearby. Thus, the final array of crossovers is determined primarily by the balance between the strength of the designation activity and the distance over which the interference signal acts. An increase (or decrease) in the number of crossovers with a corresponding decrease in spacing can be achieved by either increasing (or decreasing) the strength of designation activity or decreasing (or increasing) the distance over which the inhibitory signal spreads. This general framework can accommodate diverse specific mechanisms for patterning. One logical framework that illustrates these effects invokes a fill-in-the-holes process (**Figure 7*a***).

6.1.1. Vocabulary note. From a mechanistic perspective, the term interference refers specifically to the spreading inhibitory signal. However, many perturbations other than an alteration in that signal per se can alter crossover patterns and thus appear phenomenologically as alterations in crossover interference.

6.1.2. The obligatory crossover. Occurrence of at least one crossover designation per homolog pair (see Section 4) is likely ensured as an intrinsic feature of the crossover patterning process (358, 392).

6.1.3. Chromatid interference. A long-standing question is whether the choice of homolog chromatids at one crossover site is influenced by which chromatids were involved in nearby crossover(s). Thus far, such influences can be observed, but appear to be modest, even in budding yeast where crossovers are especially close together (49, 100, 305).

6.1.4. Even spacing of precursors. Several lines of evidence suggest that undifferentiated precursor interactions tend to be evenly spaced, although this has not been extensively documented. One outcome of this feature is that crossovers can exhibit a residual tendency for even spacing even when the canonical interference process is not functioning (94).

6.1.5. When is crossover patterning implemented? Definition of the timing of crossover patterning in any particular organism is limited by the earliest time at which a crossover-specific marker is experimentally detectable. The first model for crossover interference was made at the time of Janssens's insight that diplotene chiasmata are sites of reciprocal crossovers between nonsister chromatids (reviewed in 193) (**Figure 1*c***). At that time, chiasmata were the only cytological marker for crossover formation. Darlington (74) thus proposed that interference is the result of mechanical effects that arise during diplotene compaction when chiasmata emerge, reasoning that closely spaced chiasmata would be incompatible with (and thus eliminated by) the compaction process. The availability of earlier markers for crossovers has since revealed that patterning is imposed much earlier, during early/mid-prophase. As described above, the patterning occurs at leptotene/zygotene in budding yeast and *Sordaria* and might occur at that same stage or later, during pachytene, in other organisms.

6.2. Crossover Interference Spreads Along Prophase Structures: The Metric of Interference Spreading Is Physical Distance Along Chromosomes

Crossover interference was originally discovered by genetic analysis, with effects therefore measured in genetic distance [centiMorgans (cMs)] (249) (**Figure 1*e***). However, subsequent work has shown that the actual metric for spreading of crossover interference is physical distance along the chromosome, measured in microns, rather than either genetic distance or genomic distance

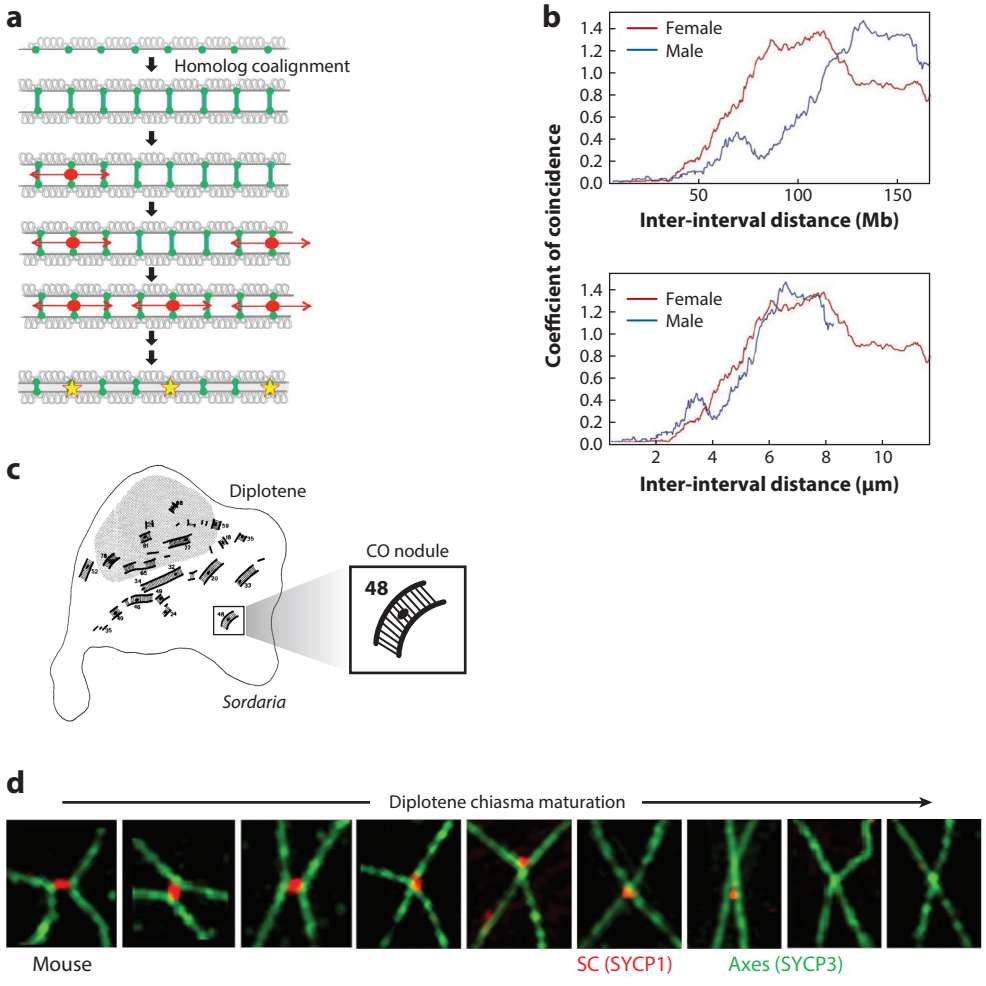

Figure 7

Crossover interference and chiasma maturation. (*a*) Simple fill-in-the-holes logic for crossover patterning. Precursors (*green*) are acted upon by crossover designation (*red balls*), which nucleates spreading crossover interference (*red arrows*). Sequential designation events fill in the holes between prior events to give evenly spaced crossovers (*yellow stars*). Panel adapted from Reference 357. (*b*) Crossover interference assayed by Coefficient of Coincidence analysis (see **Figures 1*e*** and ***5f***) in male and female mouse meiosis. If the genomic positions of crossovers are used as the distance metric, interference appears to be stronger in males than in females (*top*) but if physical positions of crossovers along prophase chromosomes are used as the metric, interference is the same in both sexes (*bottom*), implying that the true metric for spreading of the interference signal is physical distance along the chromosome. Panel adapted with permission from Reference 277. (See discussion in Reference 392.) (*c*,*d*) Chiasma maturation. (*c*) EM reconstitution of a serially sectioned diplotene *Sordaria* nucleus. Chromosomes exhibit remaining short SC segments, each marked with a crossover-correlated recombination nodule (e.g., detail in inset), in a number corresponding to the number of chiasmata (numbers indicate the section number). Panel adapted from Reference 394. (*d*) Axis (*green*) remodeling, including axis fusion, at sites of last SC segments (*red*), during diplotene chiasma maturation in mouse spermatocytes. Panel adapted from Reference 287. Abbreviations: CO, crossover; EM, electron microscopy; SC, synaptonemal complex.

[megabases (Mbs)]. For example, in mouse and human, chromosomes are longer in females than in males, but the spacing of crossovers along pachytene SCs (and thus the interference distance) is the same in both sexes, with analogous effects in plants (90, 357). By contrast, if the interference distance were defined in cM or Mb, it would seem as though interference was lower in

females versus males even though, mechanistically, the situation is identical in the two sexes (277) (**Figure 7*b***).

Such comparisons further suggest that interference spreads along the axial structures of the chromosomes rather than through the chromatin loops. Longer (shorter) chromosomes exhibit the same interference distance in micron axis length even though they exhibit (shorter/longer) loops and thus lower (higher) longitudinal chromatin density (128, 357). Similarly, interference spreads smoothly across centromeres despite their notably different chromatin compositions (and very small number of crossovers) (65). In tomato, the interference distance is relatively constant along the chromosomes despite variations in chromatin packing (aka loop size) (391).

6.2.1. Chromosome axes or SCs? The question then arises as to whether interference spreads along the homolog axes alone, involves polymerization of the SC, or spreads along the already-formed SC.

6.2.2. Budding yeast and *Sordaria*. Several lines of evidence identify chromosome axes, and not the SC, as the conduit for the interference signal in both budding yeast and *Sordaria*. Thus, the SC is not involved in crossover patterning in these organisms. This conclusion is supported by additional evidence beyond that discussed in Section 3. In budding yeast, (*a*) foci of ZMM protein Zip2, which mark crossover sites, exhibit an interference distribution along coaligned axes in a mutant lacking SC transverse filament protein Zip1 (108); (*b*) interference, as defined genetically, is robust in the absence of full SC formation in the *zmm* mutants *spo16* and *spo22* (317); and (*c*) mutations that directly affect interference spreading affect axis components (392). In *Sordaria*, where SC formation is also a consequence of patterning, the interference distributions of recombination nodules are seen even when the SC has just formed locally at nucleation sites (388).

6.2.3. Other organisms. In accord with the idea that interference might occur during pachytene, it is also often argued that the fully formed SC is a direct participant in interference-mediated patterning, particularly in plants and *C. elegans* (38, 68, 92, 121, 163, 214, 245, 299, 352, 390). Nonetheless, critical roles of the SC for patterning in these and other organisms remain to be established. In this regard, it is particularly notable that in budding yeast and *Sordaria*, the SC transverse filament protein (Zip1/Sme4) is important for crossover formation even in the absence of or prior to SC formation, respectively (91, 326).

Crossover interference is still present in *D. melanogaster* females when SC is discontinuous along the chromosomes and in mouse when the SC-promoting axis component Sycp3 is absent (78, 271).

- In *C. elegans*, the SC is proposed to comprise a spatial compartment, within which diffusion is constrained to create a crossover pattern (390). Partial depletion of SC transverse filament protein SYP-1 results in discontinuous SCs and more closely spaced crossover-correlated COSA-1 foci (214). While this has been interpreted as supporting a role for the SC in interference, in other situations, failure of synapsis on one chromosome is known to result (as an indirect effect) in increased numbers of crossovers and aberrant crossover patterning on other chromosomes (41). This could explain crossover patterns seen in the SYP-1 depletion case. In addition, a key characteristic of *C. elegans* crossover patterning is the occurrence of only one crossover per bivalent, and this same constraint is seen in mutants devoid of the SC, leading to the suggestion that the SC is not required for interference (367).
- In *A. thaliana*, deletion of both SC transverse filament ZYP1 proteins results in robust formation of Type I crossovers that do not exhibit interference as defined by genetic criteria (40, 92, 104). This observation may again point straightforwardly to a role of the SC in

mediating the spread of interference, for example, within a per-bivalent compartment. However, an equally viable possibility is that the ZYP1 proteins are required in an earlier role, for example, to arrest recombination complexes as is required to make them sensitive to patterning regulation. In the absence of arrest, recombination complexes could undergo unregulated crossover designations that would not only lack interference but would also occur in simple proportion to the concentration of crossover-promoting factors. These effects would explain why, in the absence of ZYP1s, Type I crossovers still occur but are no longer proportional to axis length in males and females [which is characteristic of normally patterned events (40)] and instead vary in frequency in correlation with the dosage of crossover factor Hei10 (92). Also, in the absence of both ZYP1s, coalignment pairing never reaches the 400-nm or 200-nm stages upon which crossover interference is imposed in budding yeast and *Sordaria* (92, 104), while in single *zyp1* mutants, the SC is again absent but coalignment is more normal and the distribution of diplotene chiasmata is consistent with operation of interference (266). Finally, in *Sordaria*, Sme4/Zip1 is known to have a pre-SC role in initiating the interference/SC nucleation transition (91).

6.3. Who Is Driving the Bus?

Crossover patterning involves molecular events targeted to recombination complexes (e.g., back migration of a pre-dHJ at the DNA level, phosphorylation of MutSγ, and/or accumulation of a critical level of SUMOylated MutSγ (see Section 4). These DNA events might comprise the only manifestations of patterning, with axes/SCs playing a passive platform role. Alternatively, axes/SCs could be more directly involved in the patterning process. Regardless of mechanism, crossover designation might involve a local change in an underlying structure at a recombination precursor site, which would then trigger a corresponding molecular change in the associated recombination complex plus an inhibitory signal at the structural level that propagates through the structure to disfavor crossover designations at encountered structure-associated precursors.

Several considerations support active involvement of structures. (*a*) The interference signal in budding yeast involves dynamic proteolytic turnover of axis components (392). (*b*) In *Sordaria*, interference-mediated patterning has SC nucleation as its primary outcome, with or without embedded crossover designation (388), suggesting that the basic effect of designation may occur at the structural level, with effects on recombination complexes as an accompanying downstream outcome. (*c*) Crossover designation in *C. elegans* induces a local expansion and elongation of the chromosome, implying that crossover designation is accompanied by a correlated structural effect (214). (*d*) The SC is intrinsically a highly dynamic structure (307), allowing the possibility of dynamic spreading effects within the structure. (*e*) Spatial patterns occur by transmission of mechanical stress along mitotic prophase chromosome axes, from which meiotic prophase axes are derived (Section 8).

6.4. What Is the Mechanism of Interference Spreading?

Since Darlington's original idea (74), many specific models for interference-mediated communication have been proposed.

6.4.1. Earlier models. Several explanations and models for crossover interference have been proposed. They fall into different categories, which are not mutually exclusive but which remain to be distinguished from one another experimentally before possible reconciliation.

6.4.1.1. Polymerization. Ultrastructural identification of SCs and recombination nodules led to an early model in which crossover designation triggered polymerization of an unknown

molecule along the SC (182). In this model, the distance between crossovers is determined by kinetic effects, that is, the relative rates of crossover designation and polymerization.

6.4.1.2. Inchworm oozing. Heterochromatin also exhibits a tendency for spreading. The current view is that modifications at one position promote analogous modifications at adjacent positions (71). An analogous effect could apply to meiotic crossover interference.

6.4.1.3. Precursor counting. Genetic considerations provoked a model in which crossover patterning proceeded sequentially along the chromosome by counting precursors, with crossovers separated by a nonrandom number of precursors that give rise to noncrossover products (203). This model has not been supported in budding yeast, most notably because variations in the density of precursors (DSBs) do not alter the distance over which interference spreads (231).

6.4.1.4. Chromosome oscillation. Hultén (154), inspired by twisting of SCs and convergence of homolog axes near sites of crossovers in chromosome spread preparations, proposed that oscillatory movements generated by telomere motion would generate waves along the lengths of individual homologs, with crossing-over promoted by the proximity of parental homologs arising at the nodal regions of these waves.

6.4.2. More recent models. Current discussions of crossover patterning consider two general categories of models in which communication along chromosomes is provided by either (*a*) redistribution of mechanical stress along structures or (*b*) diffusion of a crossover-promoting factor. Models based on either of these processes can explain crossover patterns. The two different scenarios remain to be critically distinguished from one another experimentally (but see Section 7), and combinations of effects are always possible.

6.4.2.1. Mechanical stress. Mechanical stress comprises the deformation of an object out of its equilibrium position and is measured in force exerted per unit area. An intrinsic feature is that any change in mechanical stress tends automatically to spread along/through an object and, moreover, tends to dissipate with distance (in imperfectly elastic systems) as the effects of force are absorbed by encountered components. In physical systems (where, obviously, ATP is absent) all spatial patterning is accomplished by such effects. Such an effect could underlie crossover interference (25, 186). In this case, a stress-promoted event (resulting in crossover/SC nucleation designation) would automatically result in local relief of stress. This effect, by its intrinsic nature, would automatically tend to redistribute in the vicinity, dissipating with distance, thereby reducing the probability that subsequent stress-promoted events (i.e., crossover designations) would occur in the nearby affected area. Significant support for the involvement of mechanical stress in crossover patterning is given by analogies between meiotic chromosomes and mitotic chromosomes, which exhibit clear evidence of stress-mediating patterning along chromosome axes (54, 55) (Section 8).

6.4.2.2. Diffusion. In biological systems, patterning can arise by reaction–diffusion mechanisms, for example, for even spacing of partitioning plasmids in *Escherichia coli* (161, 239). Such mechanisms have been proposed to underlie crossover patterning (106, 390).

The emergence of condensate formation as a pervasive phenomenon in biological systems has recently led to another idea: A critical factor might occur in a larger number of smaller complexes (aka precursors) and then undergo diffusion to form a smaller number of stable assemblies (aka crossover-fated complexes) by the process of Ostwald ripening or coarsening (103, 115, 244). This change would be driven by a reduction in surface-to-volume ratio with competition among available sites resulting in interference. Condensate-driven assembly is an attractive basis for the

emergence of recombination complex foci, particularly in light of biochemical studies of DSB complexes (374) and the identification of important roles for SUMOylation, which is known to promote aggregation. However, even accepting that accumulation and Ostwald ripening occur, a critical unanswered issue remains: Is this effect alone the cause of crossover patterning, as usually proposed, or is it the consequence of other signals that directly comprise crossover designation and secondarily target the observed effects?

6.4.2.3. Integration? It is possible to combine the imposition of crossover patterning by mechanical effects with condensate-mediated recombination complex formation. Focal assemblies in subcellular systems can be driven by condensation of protein complexes onto surfaces (237). This is an attractive model for formation of recombination ensembles on axes/SCs. Furthermore, the Tau protein, which seems to localize to microtubules by surface condensation, tends to be targeted to specific sites of microtubule deformation (i.e., flaws) (331), and in a mechanical model for crossover patterning, precursor sites comprise stress-sensitive flaws (25, 186). Thus, diffusion, condensation, and Ostwald ripening might all follow instructions provided by mechanical effects. Alternatively, in a different logic, the condensation process itself might generate stress along the surface of the substrate, which, by propagation outward, could preclude condensation at nearby positions.

6.4.2.4. Summary. The nature of interference-mediated patterning remains substantially mysterious in virtually every aspect. Further understanding will require moving beyond current approaches to biochemical and biophysical methods that directly address the underlying bases of different possible mechanisms.

7. CHIASMA MATURATION

Crossing-over results in new paths along the two involved chromatids at the DNA level. However, regular segregation of whole chromosomes requires that new paths be also created across the crossover site at the level of chromosome structure. That is, DNA exchange must be accompanied by axis exchange. Homolog axes generally exhibit no sign of discontinuity at pachytene. Thus, axis exchange likely occurs during diplotene compaction. This makes sense mechanistically because diplotene is, by its nature, a period of altered longitudinal axis organization. By analogy with mitotic prometaphase (55, 113), diplotene chromosome shortening likely occurs globally by modulation of the loop/axis structure to give shorter axes and longer loops.

During progression from pachytene to diplotene, short segments of the SC persist at sites of emerging chiasmata, accompanied by late-stage crossover recombination complexes, for example, EM nodules, Hei10 and/or Mlh1 foci, and axis component Hop1 plus cohesins (**Figure 7*c***). This ensemble appears to be important for chiasma maturation. The short SC segments initially connect separate homolog axes and progressively diminish as chiasmata emerge (287) (**Figure 7*d***). Moreover, component SC segments are required to prevent unregulated fusion of homolog axes at these positions, implying an active role in ongoing events (287). For example, a short SC segment might somehow guide the formation of new loop/axis paths by providing a barrier to loop extrusion. A role for the SC in stabilizing and guiding chiasma maturation at crossover sites could potentially have been the original driving force for the evolution of this structure (Section 5.5).

Given the presence of late-stage crossover recombination complexes, it is possible that resolution of dHJs to crossovers also occurs at this postpachytene stage, in coordination with axis exchange. Close coupling of axis exchange and crossover finalization could help to ensure a regular outcome.

8. EVOLUTION OF THE MEIOTIC PROGRAM

How meiosis might have evolved has been extensively discussed from many perspectives (e.g., 18, 158, 183, 365).

8.1. Intersister to Interhomolog Progression

We have previously suggested that meiotic interhomolog interactions might have evolved from mitotic intersister interactions (183). This possibility is sensible a priori and gains support from several observations.

8.1.1. At the DNA level. First, in meiosis, the mitotic DSB repair process is diverted from intersister to interhomolog bias. Then meiotic DSBs are catalyzed by Spo11, a TopoVI homolog. It has been proposed that, during mitosis, the role of TopoVI is to decatenate replicated sister chromatids (31). The Spo11/TopoVI complex binds and cleaves one duplex while binding and passing a second duplex through the gap without cleavage. In meiosis, analogous binding of the complex to duplexes from sister chromatids could explain why a DSB occurs on only one of two sister chromatids (see Section 4).

8.1.2. At the whole-chromosome level. Meiotic prophase chromosomes have the same structure as mitotic mid-prophase chromosomes, with sister linear loop/axis arrays closely conjoined into a single morphological unit (55, 213). During mitotic (intersister-biased) DSB repair, local DNA damage recruits, and is then repaired in the context of, cohesin and other structural proteins (13). The meiotic program of recombination-mediated interhomolog interactions is mediated by recombination complex/axis association, which might have evolved from this process. Mitotic chromosomes exhibit evenly spaced bridges between chromatid-sister axes from late prophase onward (55), and meiotic chromosomes exhibit evenly spaced bridges between homolog axes at late leptotene (91), an apparently analogous stage (186) (see Sections 2–4). Homolog segregation at MI utilizes the same connection-based tension logic as segregation of sister chromatids during mitosis. Moreover, crossovers between sister chromatids can cause them to segregate to opposite poles in mitosis. Finally, in *Sordaria*, when premeiotic karyogamy is blocked, the entire interhomolog interaction program, including crossover interference and SC formation, still occurs, but now between sisters rather than between homologs (346).

8.1.3. A general hypothesis. The above idea can be expanded into a general framework for how the meiotic interhomolog interaction program might have evolved from the mitotic program (**Figure 8*a***). This framework has four components. (*a*) The meiotic program could have evolved from the prophase-G1 period of the mitotic cell cycle. (*b*) Throughout this period, mitotic chromosomes are undergoing macroscopic morphogenetic changes. The same effects could drive the meiotic interhomolog interaction program. (*c*) More specifically, morphogenetic changes in mitotic chromosomes are likely mediated by mechanical effects. The same could be true for meiotic events with the important modification that the desired outcomes are achieved by targeting stress to, and transducing its effects via, axis/SC-associated recombination complexes. (*d*) Correspondingly, acquisition of recombination complex/axis association is the critical feature that has enabled the evolution of meiosis. Convergent observations that lead to this general hypothesis are described in the next section.

8.2. Mechanical Stress: From Crossover Interference to Chromatin Pressure

We have suggested that meiotic crossover patterning is governed by mechanical effects along chromosome axes, with redistribution of mechanical stress providing the requisite communication

along chromosomes (186). That idea raised an additional question: What could be the source of this stress? In response, we proposed that mechanical stress arises within chromosomes via chromatin pushing. Mechanical stress is measured in units of pressure (pascals) or, equivalently, force per unit area (newtons per square meter or pounds per square inch). A segment of chromatin free in solution, in a particular state and solvent condition, will occupy a particular envelope

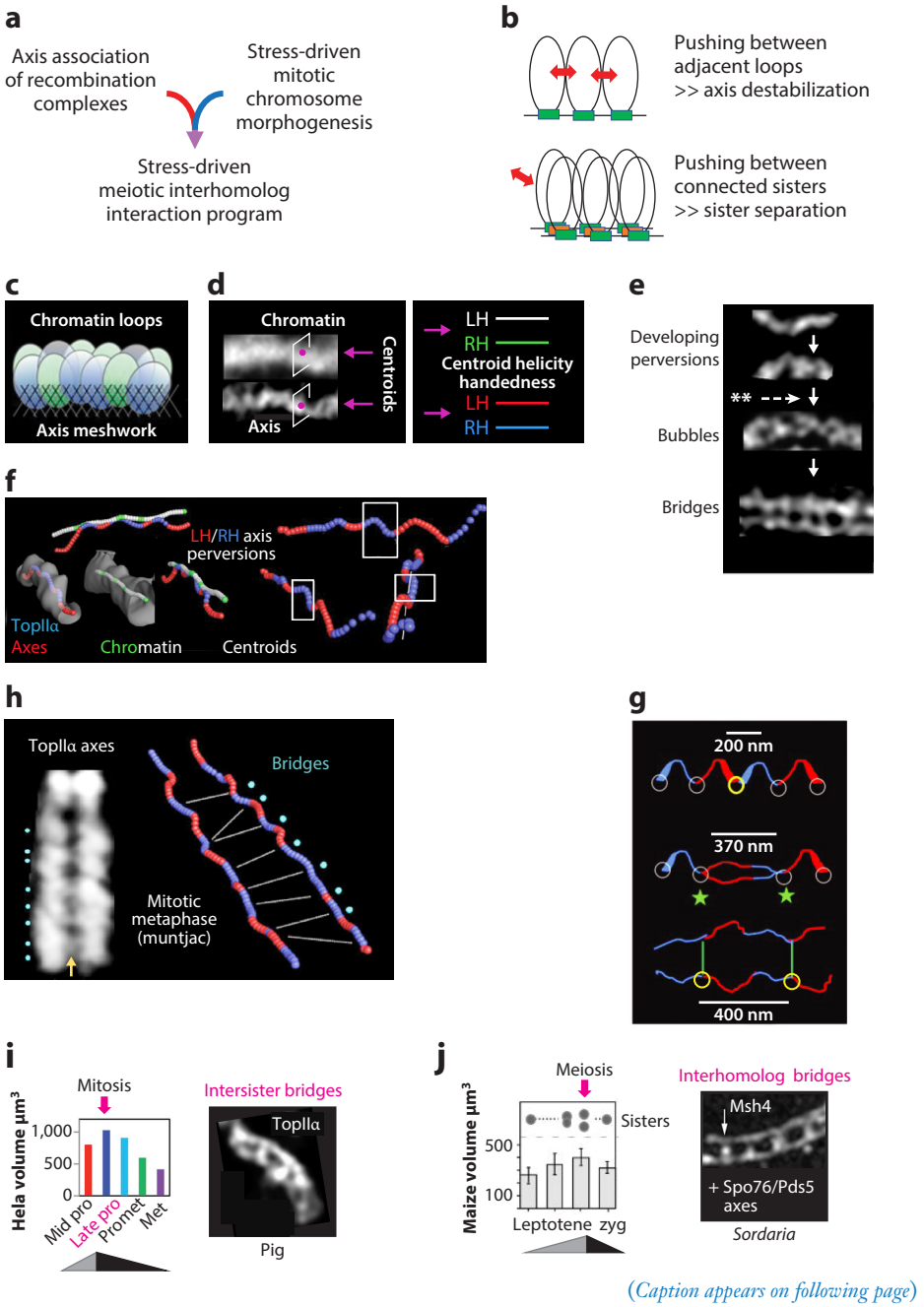

(*Caption appears on following page*)

Figure 8 (*Figure appears on preceding page*)

Meiotic and mitotic chromosomes. (*a*) Hypothesis for evolution of the meiotic interhomolog interaction program. (*b*) Effects of pushing between adjacent chromatin loops along an axis. Panel adapted with permission from Reference 186. (*c–h*) Mitotic chromosome morphogenesis. (*c*) Mitotic prophase chromosomes are cooriented sister linear loop arrays, analogous to meiotic chromosomes. (*d*) Intensity-weighted centroid paths of axes (TopoIIα) and chromatin (H2B-mCherry) are defined and analyzed for LH and RH helicity. (*e*) Mitotic mid-prophase chromosome axes become progressively more deformed by (*top*) development of perversions. At late prophase, concomitant with loss of bulk cohesin, (*middle*) sister axes split in evenly spaced bubbles with (*bottom*) interaxis bridges developing at positions between bubbles. (*f*) Perversions along axes (*red/blue*) and chromatin (*green/white*) of mid-prophase chromosomes showing half-helical segments of alternating handedness. Panels *c–f* adapted from Reference 55. (*g*) Proposed explanation for late-prophase bridge emergence in panel *e*. Sister axes split and interaxis bridges arise at positions of handedness changes, likely via coordinate effects of pushing stress along axes and between sister chromatid chromatin arrays. Panel adapted from Reference 54. (*h*) Bridges between sister chromatids remain throughout prometaphase/metaphase. Apparent helical coiling is, in fact, a consequence of the presence of perversions. Panel adapted from Reference 55. (*i,j*) Strong similarities between (*i*) mitotic late prophase/prometaphase and (*j*) meiotic leptotene/zygotene (*pink arrows*). Chromatin volume increases and then decreases in mitotic chromosomes (*i*, *left*) and meiotic chromosomes (*j*, *left*). Volume increase is accompanied by permanent sister separation in mitotic chromosomes (*i*, *right*) and a transient tendency for sister separation in meiotic chromosomes (*j*, *right*). Morphologically and compositionally analogous interaxis bridges emerge concomitantly in both programs, between sisters in mitotic chromosomes (*i*, *right*) and between homologs in meiosis (*j*, *right*). Grey and black triangles correspond to chromatin expansion and compaction, respectively, at the indicated stages. Panel *i* adapted from References 55 and 213; panel *j* adapted from References 91 and 186. Abbreviations: LH, left handed; RH, right handed; TopoIIα, topoisomerase IIα.

volume. If that segment is constrained in some way, for example, by intersegment tether(s) or because it is surrounded by other chromatin, it will tend to push against the constraining feature(s) (e.g., 227). Such pushing forces comprise mechanical stress.

The chromatin of organized mitotic or meiotic chromosomes will be constrained along their lengths by loop/axis organization and between sisters by their close juxtaposition. Within such a structure, chromatin-pushing forces between adjacent loops can promote axis deformation and pushing forces between sister arrays can promote a tendency for sister axis separation (**Figure 8*b***). Pushing forces will also sensitize the chromosomes to molecular changes that weaken the constraining features, which can lead to autocatalytic release of such features (213).

The above effects can, of course, also be modulated by changes in basic chromatin composition, solvent conditions (e.g., Mg^{++} or Ca^{++} concentrations) or other factors such as molecular crowding. Importantly, stress-promoted changes can be either global or local. In the latter case, they will occur preferentially at weak points in the system, that is, at the flaws.

8.3. Stress-Promoted Morphogenesis of Mitotic Chromosomes

Multiple observations suggest that chromatin pushing underlies basic events of chromosome morphogenesis in the mitotic cell cycle.

8.3.1. Perversions. Linear loop/axis arrays of mitotic chromosomes (**Figure 8*c***) exhibit regularly alternating tendencies for right and left helical handedness, revealed by defining the paths of the intensity-weighted centroids of chromosome axes (55) (**Figure 8*d–f***). Such handedness changes are called perversions. Properties of these perversions imply that they arise from internal mechanical stress, including their progressive emergence (**Figure 8*e***) and their highly dynamic readjustment (55). Perversions can be explained as deformations resulting from pushing between adjacent chromatin loops: Helicity will place adjacent loops out of phase, thus reducing adjacent pushing forces (54).

8.3.2. Late prophase sister separation, chromosome expansion, and bridge emergence. At late prophase, global cohesin is lost and the axes of mitotic sister chromatids separate in parallel. Concomitantly, total chromosome volume increases (213). This progression fits the paradigm of pushing-mediated autocatalytic loss of tethers (cohesins) with resultant release of intersister pushing forces (which separate sisters) and a concomitant chromatin volume increase. In addition, individual axes retain their perversions and become linked by evenly spaced interaxis bridges that comprise DNA and structural components, including residual cohesin (54, 55) (**Figure 8*e*,*g*,*b***). These bridges arise at the junctions between evenly spaced bubbles (**Figure 8*e***) whose size (and thus the distance between bridges) corresponds to two adjacent half-helices (**Figures 8*g***). These effects support a model in which bridges arise at positions where helical handedness changes, which are intrinsic weak points along the axes (**Figure 8*g***). Thus, bridge emergence can be explained by the combined effects of pushing-mediated axis perversions (generating weak points) and pushing-mediated separation of sister axes to create bubbles and accompanying bridges (**Figure 8*g***). Perversions and bridges remain present until anaphase, corresponding to the fact that metaphase chromosomes are not regularly helically coiled (for details see 54, 55) (**Figure 8*b***).

8.3.3. Pre-anaphase jumping apart. Immediately prior to the onset of anaphase, sister chromatids abruptly separate all along their lengths (56). This change is triggered by cleavage-mediated removal of cohesin from bridges and results in bridge elongation (but not removal). Prior to this transition, sister chromatid chromatin units point outward from bridges and thereafter rotate to a parallel disposition. These effects are expected if initial bridges keep sister chromatin units too close together along their axes, while release of cohesin allows those units to push one another into a less constrained conformation with concomitant/resultant bridge elongation. A global tendency for chromatin expansion precedes, and presumably enhances, these effects.

8.3.4. HEAT repeat proteins. Cohesin and condensin subunits prominently feature HEAT repeats, arrays of α-helix pairs that make a solenoidal shape (382). Molecular dynamics simulations suggest that HEAT repeats can sense and transduce mechanical stress (125).

8.4. Compaction/Expansion Stress Cycles

Inspection of spread budding yeast chromosomes at different stages of meiotic prophase revealed cyclic alternation between periods of chromatin compaction and chromatin diffuseness in correlation with classically defined stages (**Figure 9*a***). Such alternations are also seen in other organisms by other assays (**Figure 9*b***), pointing to a universal picture (186). We suggested that these cycles represent alternating accumulation and release of mechanical stress along/within chromosomes. Additionally, there were early hints that analogous cycles occurred during the mitotic program, with a specific relationship between the two programs. Subsequent studies have confirmed and extended these suggestions.

8.4.1. Cycles in the mitotic program. It is now possible to formulate a nearly complete description of the mitotic cycle as a series of compaction/expansion cycles (**Figure 9*c***). Periods of compaction and expansion can be attributed, specifically, to periods of installation and release of chromatin-constraining tethers, with corresponding resultant stress-promoted effects. Chromosomes become organized during G2 to mid-prophase, during which period linear loop/axis arrays arise and sister chromatids go from loosely to tightly juxtaposed via association of their respective axes. The mid-prophase compaction state, with accompanying development of perversions, is mediated by condensins and cohesins. It is followed by the late-prophase transition that includes

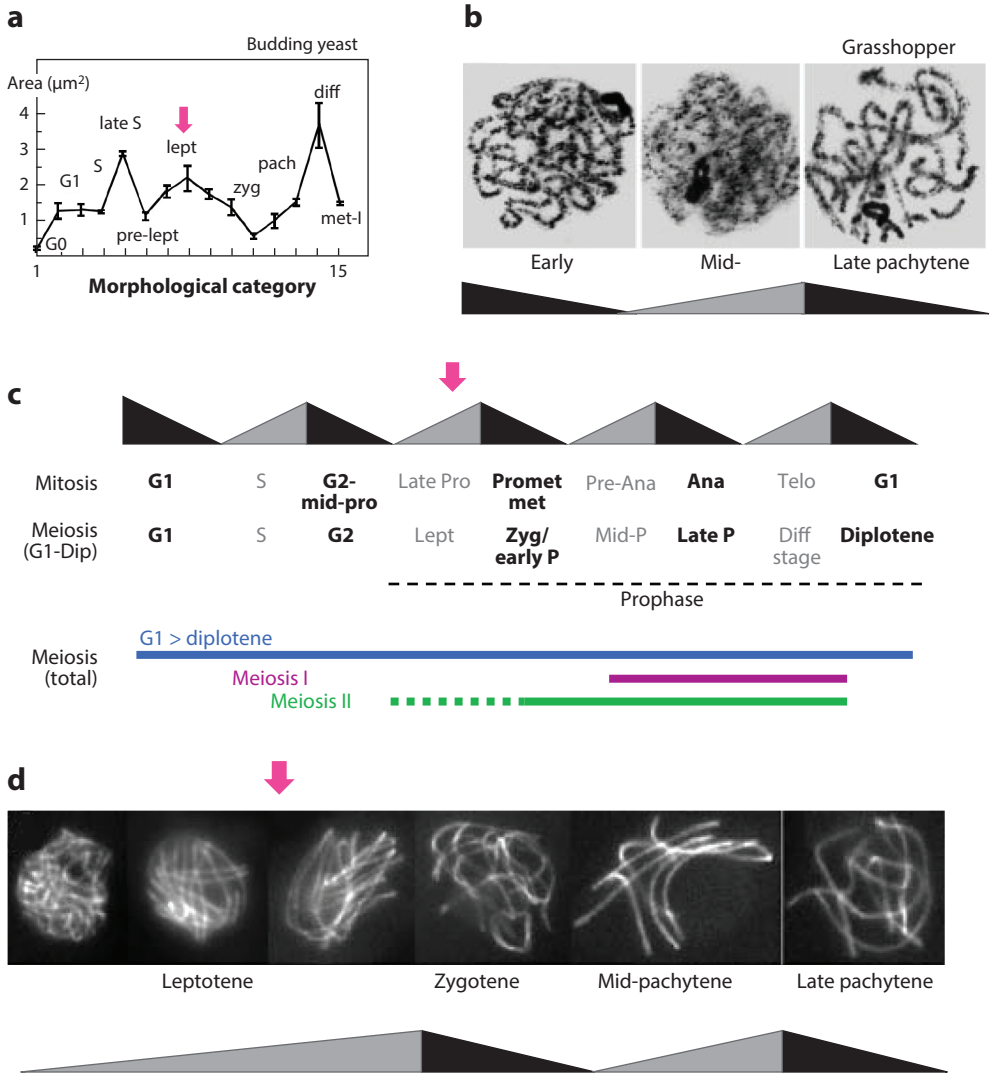

Figure 9

Chromatin compaction/expansion (stress) cycles link the mitotic and meiotic programs. (*a*) Cyclic variations in chromatin expansion/compaction status observed in spread budding yeast meiotic chromosomes in correlation with classical meiotic stages. (*b*) Cyclic variations in chromatin diffuseness during pachytene of grasshopper *Locusta migratoria*. (*c*) Chromosome compaction/expansion cycles (*black/gray triangles*) as defined for (*top*) the entire mitotic cell cycle and (*middle*) meiotic G1-prophase show direct correspondence. (*Bottom*) The entire meiotic program may comprise a triplication of the period of the mitotic cell cycle when chromosomes are individualized. (*d*) Axes of *Sordaria* prophase chromosomes (visualized by Spo76/Pds5-GFP) become more straight and more relaxed (more curved) in the expected correlation with chromatin expansion and compaction, which should give more and less distended axes. Panels *a*, *b*, and *d* adapted from Reference 186.

sister separation, chromatin expansion and bridge emergence enabled by bulk cohesin loss. Then ensues classical prometaphase compaction, which in turn is followed by the pre-anaphase jumping apart transition that includes further sister separation and chromatin expansion via further cohesin loss. Anaphase is then a major compaction stage, accompanied by increased condensin localization (243, 355). And at telophase, chromosomes dramatically expand into a diffuse stage, characterized

by the absence of any cohesin- or condensin-mediated organization (2). As chromosomes then enter G1 of the next cell cycle, they develop organization via large-scale cohesin-mediated loops (TADS) (257), implying compaction. They then progress to S phase, which, due to the requirement for disorganization, might be considered an expansion period. After S phase, chromosomes reenter G2 on their way to mid-prophase compaction.

8.4.2. Analogous cycles in the meiotic program imply an evolutionary relationship. Images of meiotic prophase chromosomes suggest that chromatin expands during leptotene; compacts during zygotene/early pachytene, with concomitant installation of the SC; expands again at mid-pachytene and compacts at late pachytene; expands dramatically at the postpachytene diffuse stage; and then compacts as chromosomes reform at diplotene (**Figure 9*a–c***).

These meiotic cycles appear to reflect modulations of stress, as inferred for mitotic chromosomes. Periods of expansion (compaction) include tendencies for increased (decreased) sister separation at the axis and/or chromatin levels plus tendencies for chromosomes to be longitudinally more (less) distended (e.g., **Figure 9*d***), all predicted effects of global interloop pushing between sister chromatids and along axes, respectively (186).

The meiotic prophase compaction/expansion cycles can be directly mapped to cycles seen for organized mitotic chromosomes by two anchor points. First, the late leptotene/zygotene cycle is closely analogous to mitotic late prophase/metaphase (**Figure 8*i,j***). Late leptotene and late mitotic prophase both exhibit a tendency for global sister separation, emergence of evenly spaced interaxis bridges, and a concomitant volume increase (77, 91). Additionally, the meiotic bridges are morphologically and structurally analogous to their mitotic counterparts but now link axes of homologs rather than sisters. Second, the meiotic diffuse stage is, by its intrinsic nature, analogous to mitotic telophase, another diffuse stage.

Given these anchor points, the meiotic prophase cycles from leptotene to diplotene should be analogous to the mitotic cycles from mid-prophase to prometaphase, thus pointing to a direct evolutionary relationship between the two periods. More generally, the entire meiotic program can be seen to comprise early events of the mitotic cell cycle (G1, S2, G2), followed by the above series of prophase cycles, followed by the two divisions, which can be directly related to the corresponding events of mitosis (**Figure 9*c***).

8.5. Functional Implications for Meiosis

The analogy between the meiotic leptotene/zygotene and mitotic prophase/prometaphase expansion/compaction cycles is particularly notable. In *Sordaria* and budding yeast, late leptotene is the time at which crossover interference is implemented (398) (see Section 6). More specifically, in *Sordaria*, interference mediates SC nucleation, which occurs at a subset of late leptotene bridges (91). The corresponding mitotic stage includes perversion-mediated emergence of bridges. This analogy supports the idea that bridge emergence and crossover/SC nucleation patterning comprise a single mechanical stress-promoted transition. Further, SC nucleation involves contraction along bridges (91). This effect could be a consequence of local relaxation resulting from a stress-promoted bridge defect, with global relaxation at zygotene allowing the completion of SC formation throughout the genome (25).

Recent findings support these interpretations. If bridge emergence is promoted by mechanical stress that is pushing on constraining components, it could be expected that loss of an axis component and/or intersister cohesin might cause chromosomes to blow up. In fact, in *Sordaria*, the absence of meiotic HORMAD protein Hop1, meiotic cohesin Rec8, or a meiosis-specific function of Spo76/Pds6 all result in dramatic destabilization of chromosomes, at both the axis and chromatin levels, exactly at this transition point.

8.6. Synthesis

The above considerations suggest that, during the critical leptotene/zygotene transition of meiosis, the mechanical effects that underlie mitotic chromosome morphogenesis drive fundamental events of the meiotic interhomolog interaction program. Importantly, during meiosis, these effects are targeted to sites of recombination interactions, which would thus function as weak points (flaws) along the axes. Given that meiotic and mitotic chromosomes exhibit analogous compaction/expansion cycles, the same principle should operate throughout the meiotic interhomolog interaction program. By this scenario, association of recombination complexes to chromosome axes/SCs is the critical evolved feature that enables coupling of mitotic morphogenetic effects to meiotic processes (**Figure 8*a***).

DISCLOSURE STATEMENT

The authors are not aware of any affiliations, memberships, funding, or financial holdings that might be perceived as affecting the objectivity of this review.

ACKNOWLEDGMENTS

The authors are grateful to our many colleagues in the fields of meiosis and mitosis for their observations, insights, and willingness to consider our ideas, even (especially) when they contradict their own preferences. We apologize for not having cited all their results/publications, but due to space limitations, we had to refer more often than wished to reviews. We also tried to cite very recent work that, among other advantages, will allow readers to trace prior foundational studies. We are especially grateful to Michael Lichten for extensive and friendly assistance at several levels. We thank the members of our laboratories, whose ideas underlie much of our thinking. Finally, we thank Janet Montgomery for invaluable help in manuscript preparation. N.K. and D.Z. are supported by grant R35-GM-136322 from the National Institutes of Health (NIH) to N.K. D.Z. is also supported by the CNRS (UMR 9198, I2BC). N.K. dedicates this article to Guido Guidotti (see also **https://nrs.harvard.edu/URN-3:HUL.INSTREPOS:37368811**).

LITERATURE CITED

1. Aanen D, Beekman M, Kokko H. 2016. Weird sex: the underappreciated diversity of sexual reproduction. *Philos. Trans. R. Soc. B* 371(1706):20160262
2. Abramo K, Valton AL, Venev SV, Ozadam H, Fox AN, Dekker J. 2019. A chromosome folding intermediate at the condensin-to-cohesin transition during telophase. *Nat. Cell Biol.* 21(11):1393–402
3. Adams EE, He Q, McKee BD. 2020. How noncrossover homologs are conjoined and segregated in Drosophila male meiosis I: Stable but reversible homolog linkers require a novel Separase target protein. *PLOS Genet*. 16(10):e1008997
4. Ahmed EA, Rosemann M, Scherthan H. 2018. NHEJ contributes to the fast repair of radiation-induced DNA double-strand breaks at late prophase I telomeres. *Health Phys.* 115(1):102–7
5. Ahuja JS, Harvey CS, Wheeler DL, Lichten M. 2021. Repeated strand invasion and extensive branch migration are hallmarks of meiotic recombination. *Mol. Cell* 81(20):4258–70
6. Ahuja JS, Sandhu R, Mainpal R, Lawson C, Henley H, et al. 2017. Control of meiotic pairing and recombination by chromosomally tethered 26S proteasome. *Science* 355(6323):408–11
7. Albini SM, Jones GH. 1987. Synaptonemal complex spreading in *Allium cepa* and *A. fistulosum*. I. The initiation and sequence of pairing. *Chromosoma* 95:324–38
8. Allers T, Lichten M. 2001. Differential timing and control of noncrossover and crossover recombination during meiosis. *Cell* 106(1):47–57
9. Alleva B, Brick K, Pratto F, Huang M, Camerini-Otero RD. 2021. Cataloging human *PRDM9* allelic variation using long-read sequencing reveals *PRDM9* population specificity and two distinct groupings of related alleles. *Front. Cell Dev. Biol.* 9:675286

10. Almanzar DE, Gordon SG, Rog O. 2021. Meiotic sister chromatid exchanges are rare in *C. elegans*. *Curr. Biol.* 31(7):1499–507
11. Altmannova V, Firlej M, Müller F, Janning P, Rauleder R, et al. 2023. Biochemical characterization of Mer3 helicase interactions and the protection of meiotic recombination intermediates. *Nucleic Acids Res.* 51(9):4363–84
12. Arbel-Eden A, Simchen G. 2019. Elevated mutagenicity in meiosis and its mechanism. *Bioessays* 41(4):e1800235
13. Arnould C, Rocher V, Finoux AL, Clouaire T, Li K, et al. 2021. Loop extrusion as a mechanism for formation of DNA damage repair foci. *Nature* 590(7847):660–65
14. Arora K, Corbett KD. 2019. The conserved XPF:ERCC1-like Zip2:Spo16 complex controls meiotic crossover formation through structure-specific DNA binding. *Nucleic Acids Res.* 47(5):2365–76
15. Axelsson E, Webster MT, Ratnakumar A, Ponting CP, Lindblad-Toh K. 2012. Death of *PRDM9* coincides with stabilization of the recombination landscape in the dog genome. *Genome Res.* 22(1):51–63
16. Bell JC, Kowalczykowski SC. 2016. RecA: regulation and mechanism of a molecular search engine. *Trends Biochem. Sci.* 41(6):491–507
17. Bell LR, Byers B. 1983. Homologous association of chromosomal DNA during yeast meiosis. *Cold Spring Harb. Symp. Quant. Biol.* 47(Part 2):829–40
18. Bernstein H, Bernstein C. 2017. Sexual communication in Archaea, the precursor to eukaryotic meiosis. In *Biocommunication of Archaea*, ed. G Witzany, pp. 103–17. Cham, Switz.: Springer
19. Bhagwat NR, Owens SN, Ito M, Boinapalli JV, Poa P, et al. 2021. SUMO is a pervasive regulator of meiosis. *eLife* 10:e57720
20. Bhattacharyya T, Walker M, Powers NR, Brunton C, Fine AD, et al. 2019. *Prdm9* and meiotic cohesin proteins cooperatively promote DNA double-strand break formation in mammalian spermatocytes. *Curr. Biol.* 29:1002–18.e7
21. Bisig CG, Guiraldelli MF, Kouznetsova A, Scherthan H, Höög C, et al. 2012. Synaptonemal complex components persist at centromeres and are required for homologous centromere pairing in mouse spermatocytes. *PLOS Genet.* 8(6):e1002701
22. Blat Y, Protacio RU, Hunter N, Kleckner N. 2002. Physical and functional interactions among basic chromosome organizational features govern early steps of meiotic chiasma formation. *Cell* 111(6):791–802
23. Bojko M. 1983. Human meiosis VIII. Chromosome pairing and formation of the synaptonemal complex in oocytes. *Carlsberg Res. Commun.* 48:457–83
24. Borde V, Goldman AS, Lichten M. 2000. Direct coupling between meiotic DNA replication and recombination initiation. *Science* 290(5492):806–9
25. Börner GV, Kleckner N, Hunter N. 2004. Crossover/noncrossover differentiation, synaptonemal complex formation, and regulatory surveillance at the leptotene/zygotene transition of meiosis. *Cell* 117(1):29–45
26. Borts RH, Lichten M, Hearn M, Davidow LS, Haber JE. 1984. Physical monitoring of meiotic recombination in *Saccharomyces cerevisiae*. *Cold Spring Harb. Symp. Quant. Biol.* 49:67–76
27. Boulton A, Myers RS, Redfield RJ. 1997. The hotspot conversion paradox and the evolution of meiotic recombination. *PNAS* 94(15):8058–63
28. Bozdag GO, Ono J, Denton JA, Karakoc E, Hunter N, et al. 2021. Breaking a species barrier by enabling hybrid recombination. *Curr. Biol.* 31(4):R180–81
29. Brick K, Pratto F, Camerini-Otero RD. 2020. After the break: DSB end processing in mouse meiosis. *Genes Dev.* 34(11–12):731–32
30. Brick K, Smagulova F, Khil P, Camerini-Otero RD, Petukhova GV. 2012. Genetic recombination is directed away from functional genomic elements in mice. *Nature* 485(7400):642–45
31. Brinkmeier J, Coelho S, de Massy B, Bourbon HM. 2022. Evolution and diversity of the TopoVI and TopoVI-like subunits with extensive divergence of the TOPOVIBL subunit. *Mol. Biol. Evol.* 39(11):msac227
32. Brown MS, Bishop DK. 2014. DNA strand exchange and RecA homologs in meiosis. *Cold Spring Harb. Perspect. Biol.* 7(1):a016659

33. Brown MS, Grubb J, Zhang A, Rust MJ, Bishop DK. 2015. Small Rad51 and Dmc1 complexes often co-occupy both ends of a meiotic DNA double strand break. *PLOS Genet*. 11(12):e1005653
34. Buhler C, Borde V, Lichten M. 2007. Mapping meiotic single-strand DNA reveals a new landscape of DNA double-strand breaks in *Saccharomyces cerevisiae*. *PLOS Biol*. 5(12):e324
35. Byers B, Goetsch L. 1975. Electron microscopic observations on the meiotic karyotype of diploid and tetraploid *Saccharomyces cerevisiae*. *PNAS* 72:5056–60
36. Bzymek M, Thayer NH, Oh SD, Kleckner N, Hunter N. 2010. Double Holliday junctions are intermediates of DNA break repair. *Nature* 464(7290):937–41
37. Cahoon CK, Hawley RS. 2013. Flies get a head start on meiosis. *PLOS Genet.* 9(12):e1004051
38. Cahoon CK, Helm JM, Libuda DE. 2019. Synaptonemal complex central region proteins promote localization of pro-crossover factors to recombination events during *Caenorhabditis elegans* meiosis. *Genetics* 213(2):395–409
39. Cannavo E, Sanchez A, Anand R, Ranjha L, Hugener J, et al. 2020. Regulation of the MLH1–MLH3 endonuclease in meiosis. *Nature* 586(7830):618–22
40. Capilla-Pérez L, Durand S, Hurel A, Lian Q, Chambon A, et al. 2021. The synaptonemal complex imposes crossover interference and heterochiasmy in *Arabidopsis*. *PNAS* 118(12):e2023613118
41. Carlton PM, Farruggio AP, Dernburg AF. 2006. A link between meiotic prophase progression and crossover control. *PLOS Genet*. 2(2):e12
42. Carpenter ATC. 1975. Electron microscopy of meiosis in *Drosophila melanogaster* females: II: The recombination nodule—a recombination-associated structure at pachytene? *PNAS* 72:3186–89
43. Cejka P, Symington LS. 2021. DNA end resection: mechanism and control. *Annu. Rev. Genet.* 55:285–307
44. Chacón MR, Delivani P, Tolić IM. 2016. Meiotic nuclear oscillations are necessary to avoid excessive chromosome associations. *Cell Rep.* 17(6):1632–45
45. Challa K, Lee M-S, Shinohara M, Kim KP, Shinohara A. 2016. Rad61/Wpl1 (Wapl), a cohesin regulator, controls chromosome compaction during meiosis. *Nucleic Acids Res.* 44(7):3190–203
46. Chan Y-L, Zhang A, Weissman BP, Bishop DK. 2019. RPA resolves conflicting activities of accessory proteins during reconstitution of Dmc1-mediated meiotic recombination. *Nucleic Acids Res.* 47(2):747–61
47. Chelysheva L, Vezon D, Chambon A, Gendrot G, Pereira L, et al. 2012. The *Arabidopsis* HEI10 is a new ZMM protein related to Zip3. *PLOS Genet*. 8(7):e1002799
48. Chen H, He C, Wang C, Wang X, Ruan F, et al. 2021. RAD51 supports DMC1 by inhibiting the SMC5/6 complex during meiosis. *Plant Cell* 33(8):2869–82
49. Chen SY, Tsubouchi T, Rockmill B, Sandler JS, Richards DR, et al. 2008. Global analysis of the meiotic crossover landscape. *Dev. Cell* 15(3):401–15
50. Chen X, Suhandynata RT, Sandhu R, Rockmill B, Mohibullah N, et al. 2015. Phosphorylation of the synaptonemal complex protein Zip1 regulates the crossover/noncrossover decision during yeast meiosis. *PLOS Biol*. 13(12):e1002329
51. Chen Y, Lyu R, Rong B, Zheng Y, Lin Z, et al. 2020. Refined spatial temporal epigenomic profiling reveals intrinsic connection between PRDM9-mediated H3K4me3 and the fate of double-stranded breaks. *Cell Res.* 30(3):256–68
52. Cheng CH, Lo YH, Liang SS, Ti SC, Lin FM, et al. 2006. SUMO modifications control assembly of synaptonemal complex and polycomplex in meiosis of *Saccharomyces cerevisiae*. *Genes Dev.* 20(15):2067–81
53. Cho NW, Dilley RL, Lampson MA, Greenberg RA. 2014. Interchromosomal homology searches drive directional ALT telomere movement and synapsis. *Cell* 159(1):108–21
54. Chu L, Liang Z, Mukhina MV, Fisher JK, Hutchinson JW, Kleckner NE. 2020. One-dimensional spatial patterning along mitotic chromosomes: a mechanical basis for macroscopic morphogenesis. *PNAS* 117(43):26749–55
55. Chu L, Liang Z, Mukhina MV, Fisher JK, Vincenten N, et al. 2020. The 3D topography of mitotic chromosomes. *Mol. Cell* 79(6):902–16
56. Chu L, Zhang Z, Mukhina M, Zickler D, Kleckner N. 2022. Sister chromatids separate during anaphase in a three-stage program as directed by interaxis bridges. *PNAS* 119(10):e2123363119

57. Chuang C-N, Cheng Y-H, Wang T-F. 2012. Mek1 stabilizes Hop1-Thr318 phosphorylation to promote interhomolog recombination and checkpoint responses during yeast meiosis. *Nucleic Acids Res.* 40(22):11416–27
58. Claeys Bouuaert C, Pu S, Wang J, Oger C, Daccache D, et al. 2021. DNA-driven condensation assembles the meiotic DNA break machinery. *Nature* 592(7852):144–49
59. Claeys Bouuaert C, Tischfield SE, Pu S, Mimitou EP, Arias-Palomo E, et al. 2021. Structural and functional characterization of the Spo11 core complex. *Nat. Struct. Mol. Biol.* 28(1):92–102
60. Cloud V, Chan YL, Grubb J, Budke B, Bishop DK. 2012. Rad51 is an accessory factor for Dmc1-mediated joint molecule formation during meiosis. *Science* 337(6099):1222–25
61. Codina-Pascual M, Campillo M, Kraus J, Speicher MR, Egozcue J, et al. 2006. Crossover frequency and synaptonemal complex length: their variability and effects on human male meiosis. *Mol. Hum. Reprod.* 12(2):123–33
62. Cole F, Baudat F, Grey C, Keeney S, de Massy B, Jasin M. 2014. Mouse tetrad analysis provides insights into recombination mechanisms and hotspot evolutionary dynamics. *Nat. Genet.* 46(10):1072–80
63. Cole F, Kauppi L, Lange J, Roig I, Wang R, et al. 2012. Homeostatic control of recombination is implemented progressively in mouse meiosis. *Nat. Cell Biol.* 14(4):424–30
64. Cole F, Keeney S, Jasin M. 2012. Preaching about the converted: how meiotic gene conversion influences genomic diversity. *Ann. N. Y. Acad. Sci.* 1267:95–102
65. Colombo PC, Jones GH. 1997. Chiasma interference is blind to centromeres. *Heredity* 79:214–27
66. Conrad MN, Lee C-Y, Chao G, Shinohara M, Kosaka H, et al. 2008. Rapid telomere movement in meiotic prophase is promoted by *NDJ1*, *MPS3*, and *CSM4* and is modulated by recombination. *Cell* 133(7):1175–87
67. Crismani W, Girard C, Froger N, Pradillo M, Santos JL, et al. 2012. FANCM limits meiotic crossovers. *Science* 336:1588–90
68. Crismani W, Girard C, Lloyd A. 2021. Crossover interference: Just ZYP it. *PNAS* 118(17):e2103433118
69. Croft JA, Jones GH. 1989. Meiosis in *Mesostoma ehrenbergii ehrenbergii*. IV. Recombination nodules in spermatocytes and a test of the correspondence of late recombination nodules and chiasmata. *Genetics* 121(2):255–62
70. Crown KN, Miller DE, Sekelsky J, Hawley RS. 2018. Local inversion heterozygosity alters recombination throughout the genome. *Curr. Biol.* 28(18):2984–90
71. Cutter DiPiazza AR, Taneja N, Dhakshnamoorthy J, Wheeler D, Holla S, Grewal SIS. 2021. Spreading and epigenetic inheritance of heterochromatin require a critical density of histone H3 lysine 9 tri-methylation. *PNAS* 118(22):e2100699118
72. Dai J, Sanchez A, Adam C, Ranjha L, Reginato G, et al. 2021. Molecular basis of the dual role of the Mlh1-Mlh3 endonuclease in MMR and in meiotic crossover formation. *PNAS* 118(23):e2022704118
73. Damm E, Odenthal-Hesse L. 2023. Orchestrating recombination initiation in mice and men. *Curr. Top. Dev. Biol.* 151:27–42
74. Darlington CD. 1937. *Recent Advances in Cytology*. Philadelphia: P. Blakiston's Son & Co. Inc. 2nd ed.
75. Davies B, Gupta Hinch A, Cebrian-Serrano A, Alghadban S, Becker PW, et al. 2021. Altering the binding properties of PRDM9 partially restores fertility across the species boundary. *Mol. Biol. Evol.* 38(12):5555–62
76. Davies B, Hatton E, Altemose N, Hussin JG, Pratto F, et al. 2016. Re-engineering the zinc fingers of PRDM9 reverses hybrid sterility in mice. *Nature* 530(7589):171–76
77. Dawe RK, Sedat JW, Agard DA, Cande WZ. 1994. Meiotic chromosome pairing in maize is associated with a novel chromatin organization. *Cell* 76(5):901–12
78. de Boer E, Dietrich AJ, Höög C, Stam P, Heyting C. 2007. Meiotic interference among MLH1 foci requires neither an intact axial element structure nor full synapsis. *J. Cell Sci.* 120(Part 5):731–36
79. de Boer E, Jasin M, Keeney S. 2015. Local and sex-specific biases in crossover versus noncrossover outcomes at meiotic recombination hot spots in mice. *Genes Dev.* 29(16):1721–33
80. de Boer E, Stam P, Dietrich AJ, Pastink A, Heyting C. 2006. Two levels of interference in mouse meiotic recombination. *PNAS* 103(25):9607–12
81. de la Fuente R, Parra MT, Viera A, Calvente A, Gómez R, et al. 2007. Meiotic pairing and segregation of achiasmate sex chromosomes in eutherian mammals: the role of SYCP3 protein. *PLOS Genet.* 3(11):e198

82. De Muyt A, Jessop L, Kolar E, Sourirajan A, Chen J, et al. 2012. BLM helicase ortholog Sgs1 is a central regulator of meiotic recombination intermediate metabolism. *Mol. Cell* 46(1):43–53
83. De Muyt A, Pyatnitskaya A, Andréani J, Ranjha L, Ramus C, et al. 2018 A meiotic XPF–ERCC1-like complex recognizes joint molecule recombination intermediates to promote crossover formation. *Genes Dev.* 32(3–4):283–96
84. De Muyt A, Zhang L, Piolot T, Kleckner N, Espagne E, Zickler D. 2014. E3 ligase Hei10: a multifaceted structure-based signaling molecule with roles within and beyond meiosis. *Genes Dev.* 28(10):1111–23
85. Dernburg AF, McDonald K, Moulder G, Barstead R, Dresser M, Villeneuve AM. 1998. Meiotic recombination in *C. elegans* initiates by a conserved mechanism and is dispensable for homologous chromosome synapsis. *Cell* 94(3):387–98
86. Desjardins SD, Simmonds J, Guterman I, Kanyuka K, Burridge AJ, et al. 2022. FANCM promotes class I interfering crossovers and suppresses class II non-interfering crossovers in wheat meiosis. *Nat. Commun.* 13(1):3644
87. Ding D-Q, Haraguchi T, Hiraoka Y. 2013. The role of chromosomal retention of noncoding RNA in meiosis. *Chromosome Res.* 21(6–7):665–72
88. Ding D-Q, Yamamoto A, Haraguchi T, Hiraoka Y. 2004. Dynamics of homologous chromosome pairing during meiotic prophase in fission yeast. *Dev. Cell* 6(3):329–41
89. Drouaud J, Khademian H, Giraut L, Zanni V, Bellalou S, et al. 2013. Contrasted patterns of crossover and non-crossover at *Arabidopsis thaliana* meiotic recombination hotspots. *PLOS Genet.* 9(11):e1003922
90. Drouaud J, Mercier R, Chelysheva L, Bérard A, Falque M, et al. 2007. Sex-specific crossover distributions and variations in interference level along *Arabidopsis thaliana* chromosome 4. *PLOS Genet.* 3(6):e106
91. Dubois E, De Muyt A, Soyer JL, Budin K, Legras M, et al. 2019. Building bridges to move recombination complexes. *PNAS* 116(25):12400–9
92. Durand S, Lian Q, Jing J, Ernst M, Grelon M, et al. 2022. Joint control of meiotic crossover patterning by the synaptonemal complex and HEI10 dosage. *Nat. Commun.* 13(1):5999
93. Duroc Y, Kumar R, Ranjha L, Adam C, Guérois R, et al. 2017. Concerted action of the MutLβ heterodimer and Mer3 helicase regulates the global extent of meiotic gene conversion. *eLife* 6:e21900
94. Dutreux F, Dutta A, Peltier E, Bibi-Triki S, Friedrich A, et al. 2023. Lessons from the meiotic recombination landscape of the ZMM deficient budding yeast *Lachancea waltii*. *PLOS Genet.* 19(1):e1010592
95. Egel R. 1978. Synaptonemal complex and crossing-over: structural support or interference? *Heredity* 41(2):233–37
96. Egel-Mitani M, Olson LW, Egel R. 1982. Meiosis in *Aspergillus nidulans*: another example for lacking synaptonemal complexes in the absence of crossover interference. *Hereditas* 97(2):179–87
97. Eyster C, Chuong HH, Lee CY, Pezza RJ, Dawson D. 2019. The pericentromeric heterochromatin of homologous chromosomes remains associated after centromere pairing dissolves in mouse spermatocyte meiosis. *Chromosoma* 128(3):355–67
98. Fellmeth JE, McKim KS. 2022. A brief history of *Drosophila* (female) meiosis. *Genes* 13(5):775
99. Fernandes JB, Séguéla-Arnaud M, Larchevêque C, Lloyd AH, Mercier R. 2018. Unleashing meiotic crossovers in hybrid plants. *PNAS* 115(10):2431–36
100. Ferreira MTM, Glombik M, Perničková K, Duchoslav M, Scholten O, et al. 2021. Direct evidence for crossover and chromatid interference in meiosis of two plant hybrids (*Lolium multiflorum* × *Festuca pratensis* and *Allium cepa* × *A. roylei*). *J. Exp. Bot.* 72(2):254–67
101. Firlej M, Weir JR. 2023. Unwinding during stressful times: mechanisms of helicases in meiotic recombination. *Curr. Top. Dev. Biol.* 151:191–215
102. Forejt J, Jansa P, Parvanov E. 2021. Hybrid sterility genes in mice (*Mus musculus*): a peculiar case of PRDM9 incompatibility. *Trends Genet.* 37(12):1095–108
103. Fozard JA, Morgan C, Howard M. 2023. Coarsening dynamics can explain meiotic crossover patterning in both the presence and absence of the synaptonemal complex. *eLife* 12:e79408
104. France MG, Enderle J, Röhrig S, Puchta H, Franklin FCH, Higgins JD. 2021. ZYP1 is required for obligate cross-over formation and cross-over interference in *Arabidopsis*. *PNAS* 118(14):e2021671118
105. Fraune J, Brochier-Armanet C, Alsheimer M, Volff JN, Schücker K, Benavente R. 2016. Evolutionary history of the mammalian synaptonemal complex. *Chromosoma* 125(3):355–60

106. Fujitani Y, Kawai J, Kobayashi I. 2010. Random-walk mechanism in the genetic recombination. *Adv. Exp. Med. Biol.* 680:275–82
107. Fujiwara Y, Horisawa-Takada Y, Inoue E, Tani N, Shibuya H, et al. 2020. Meiotic cohesins mediate initial loading of HORMAD1 to the chromosomes and coordinate SC formation during meiotic prophase. *PLOS Genet.* 16(9):e1009048
108. Fung JC, Rockmill B, Odell M, Roeder GS. 2004. Imposition of crossover interference through the nonrandom distribution of synapsis initiation complexes. *Cell* 116(6):795–802
109. Gao J, Colaiácovo MP. 2018. Zipping and unzipping: protein modifications regulating synaptonemal complex dynamics. *Trends Genet.* 34(3):232–45
110. Garcia V, Gray S, Allison RM, Cooper TJ, Neale MJ. 2015. Tel1^{ATM}-mediated interference suppresses clustered meiotic double-strand-break formation. *Nature* 520(7545):114–18
111. Gelei J. 1921. Weitere Studien über die Oogenese des *Dendrocoelum lacteum*. II. Die Längskonjugation der Chromosomen. *Arch. F. Zellforsch.* 16:88–169
112. Gergelits V, Parvanov E, Simecek P, Forejt J. 2021. Chromosome-wide characterization of meiotic noncrossovers (gene conversions) in mouse hybrids. *Genetics* 217(1):1–14
113. Gibcus JH, Samejima K, Goloborodko A, Samejima I, Naumova N, et al. 2018. A pathway for mitotic chromosome formation. *Science* 359(6376):eaao6135
114. Girard C, Budin K, Boisnard S, Zhang L, Debuchy R, et al. 2021. RNAi-related Dicer and Argonaute proteins play critical roles for meiocyte formation, chromosome-axes lengths and crossover patterning in the fungus *Sordaria macrospora*. *Front. Cell Dev. Biol.* 9:684108
115. Girard C, Zwicker D, Mercier R. 2023. The regulation of meiotic crossover distribution: a coarse solution to a century-old mystery? *Biochem. Soc. Trans.* 5:BST20221329
116. Giraut L, Falque M, Drouaud J, Pereira L, Martin OC, Mézard C. 2011. Genome-wide crossover distribution in *Arabidopsis thaliana* meiosis reveals sex-specific patterns along chromosomes. *PLOS Genet.* 7(11):e1002354
117. Goldfarb T, Lichten M. 2010. Frequent and efficient use of the sister chromatid for DNA double-strand break repair during budding yeast meiosis. *PLOS Biol.* 8(10):e1000520
118. Goldman ASH, Lichten M. 1996. The efficiency of meiotic recombination between dispersed sequences in *Saccharomyces cerevisiae* depends upon their chromosomal location. *Genetics* 144(1):43–55
119. Goldman ASH, Lichten M. 2000. Restriction of ectopic recombination by interhomolog interactions during *Saccharomyces cerevisiae* meiosis. *PNAS* 97(17):9537–42
120. Gorbsky GJ. 2015. The spindle checkpoint and chromosome segregation in meiosis. *FEBS J.* 282(13):2471–87
121. Gordon SG, Kursel LE, Xu K, Rog O. 2021. Synaptonemal complex dimerization regulates chromosome alignment and crossover patterning in meiosis. *PLOS Genet.* 17(3):e1009205
122. Gray S, Santiago ER, Chappie JS, Cohen PE. 2020. Cyclin N-terminal domain-containing-1 coordinates meiotic crossover formation with cell-cycle progression in a cyclin-independent manner. *Cell Rep.* 32(1):107858
123. Grey C, Baudat F, de Massy B. 2018. PRDM9, a driver of the genetic map. *PLOS Genet.* 14(8):e1007479
124. Grey C, de Massy B. 2021. Chromosome organization in early meiotic prophase. *Front. Cell Dev. Biol.* 9:688878
125. Grinthal A, Adamovic I, Weiner B, Karplus M, Kleckner N. 2010. PR65, the HEAT-repeat scaffold of phosphatase PP2A, is an elastic connector that links force and catalysis. *PNAS* 107(6):2467–72
126. Gruhn JR, Al-Asmar N, Fasnacht R, Maylor-Hagen H, Peinado V, et al. 2016. Correlations between synaptic initiation and meiotic recombination: a study of humans and mice. *Am. J. Hum. Genet.* 98(1):102–15
127. Gruhn JR, Hoffmann ER. 2022. Errors of the egg: the establishment and progression of human aneuploidy research in the maternal germline. *Annu. Rev. Genet.* 56:369–90
128. Gruhn JR, Rubio C, Broman KW, Hunt PA, Hassold T. 2013. Cytological studies of human meiosis: Sex-specific differences in recombination originate at, or prior to, establishment of double-strand breaks. *PLOS ONE* 8(12):e85075
129. Gu Y, Desai A, Corbett KD. 2022. Evolutionary dynamics and molecular mechanisms of HORMA domain protein signaling. *Annu. Rev. Biochem.* 91:541–69

130. Guillon H, Baudat F, Grey C, Liskay RM, de Massy B. 2005. Crossover and noncrossover pathways in mouse meiosis. *Mol. Cell* 20(4):563–73
131. Guo H, Stamper EL, Sato-Carlton A, Shimazoe MA, Li X, et al. 2022. Phosphoregulation of DSB-1 mediates control of meiotic double-strand break activity. *eLife* 11:e77956
132. Gyuricza MR, Manheimer KB, Apte V, Krishnan B, Joyce EF, et al. 2016. Dynamic and stable cohesins regulate synaptonemal complex assembly and chromosome segregation. *Curr. Biol.* 26(13):1688–98
133. Hartmann M, Kohl KP, Sekelsky J, Hatkevich T. 2019. Meiotic MCM proteins promote and inhibit crossovers during meiotic recombination. *Genetics* 212(2):461–68
134. Hassold T, Hunt P. 2001. To err (meiotically) is human: the genesis of human aneuploidy. *Nat. Rev. Genet.* 2(4):280–91
135. Hassold T, Maylor-Hagen H, Wood A, Gruhn J, Hoffmann E, et al. 2021. Failure to recombine is a common feature of human oogenesis. *Am. J. Hum. Genet.* 108(1):16–24
136. Hatkevich T, Miller DE, Turcotte CA, Miller MC, Sekelsky J. 2021. A pathway for error-free non-homologous end joining of resected meiotic double-strand breaks. *Nucleic Acids Res.* 49(2):879–90
137. Haversat J, Woglar A, Klatt K, Akerib CC, Roberts V, et al. 2022. Robust designation of meiotic crossover sites by CDK-2 through phosphorylation of the MutSγ complex. *PNAS* 119(21):e2117865119
138. He W, Rao HBDP, Tang S, Bhagwat N, Kulkarni DS, et al. 2020. Regulated proteolysis of MutSγ controls meiotic crossing over. *Mol. Cell* 78(1):168–83
139. He W, Verhees GF, Bhagwat N, Yang Y, Kulkarni DS, et al. 2021. SUMO fosters assembly and functionality of the MutSγ complex to facilitate meiotic crossing over. *Dev. Cell* 56(14):2073–88
140. Heldrich J, Milano CR, Markowitz TE, Ur SN, Vale-Silva LA, et al. 2022. Two pathways drive meiotic chromosome axis assembly in *Saccharomyces cerevisiae*. *Nucleic Acids Res.* 50(8):4545–56
141. Henderson IR, Bomblies K. 2021. Evolution and plasticity of genome-wide meiotic recombination rates. *Annu. Rev. Genet.* 55:23–43
142. Higgins JD, Osman K, Desjardins SD, Henderson IR, Edwards KJ, Franklin FCH. 2022. Unravelling mechanisms that govern meiotic crossover formation in wheat. *Biochem. Soc. Trans.* 50(4):1179–86
143. Higgins JD, Osman K, Jones GH, Franklin FC. 2014. Factors underlying restricted crossover localization in barley meiosis. *Annu. Rev. Genet.* 48:29–47
144. Higgins JD, Vignard J, Mercier R, Pugh AG, Franklin FC, Jones GH. 2008. AtMSH5 partners AtMSH4 in the class I meiotic crossover pathway in *Arabidopsis thaliana*, but is not required for synapsis. *Plant J.* 55(1):28–39
145. Hinch AG, Becker PW, Li T, Moralli D, Zhang G, et al. 2020. The configuration of RPA, RAD51, and DMC1 binding in meiosis reveals the nature of critical recombination intermediates. *Mol. Cell* 79(4):689–701
146. Hiraoka Y, Dernburg AF. 2009. The SUN rises on meiotic chromosome dynamics. *Dev. Cell* 17(5):598–605
147. Hollingsworth NM, Gaglione R. 2019. The meiotic-specific Mek1 kinase in budding yeast regulates interhomolog recombination and coordinates meiotic progression with double-strand break repair. *Curr. Genet.* 65(3):631–41
148. Holm PB, Rasmussen SW. 1980. Chromosome pairing, recombination nodules and chiasma formation in diploid Bombyx males. *Carlsberg Res. Commun.* 45(6):483–548
149. Hong S, Joo JH, Yun H, Kleckner N, Kim KP. 2019. Recruitment of Rec8, Pds5 and Rad61/Wapl to meiotic homolog pairing, recombination, axis formation and S-phase. *Nucleic Acids Res.* 47(22):11691–708
150. Hong S, Sung Y, Yu M, Lee M, Kleckner N, Kim KP. 2013. The logic and mechanism of homologous recombination partner choice. *Mol. Cell* 51(4):440–53
151. Hooker GW, Roeder GS. 2006. A role for SUMO in meiotic chromosome synapsis. *Curr. Biol.* 16(12):1238–43
152. Huang J, Wang C, Wang H, Lu P, Zheng B, et al. 2019. Meiocyte-specific and AtSPO11-1–dependent small RNAs and their association with meiotic gene expression and recombination. *Plant Cell* 31(2):444–64

153. Hughes SE, Gilliland WD, Cotitta JL, Takeo S, Collins KA, Hawley RS. 2009. Heterochromatic threads connect oscillating chromosomes during prometaphase I in *Drosophila* oocytes. *PLOS Genet*. 5(1):e1000348
154. Hultén MA. 2011. On the origin of crossover interference: a chromosome oscillatory movement (COM) model. *Mol. Cytogenet.* 8:4–10
155. Hunter N. 2015. Meiotic recombination: the essence of heredity. *Cold Spring Harb. Perspect. Biol.* 7(12):a016618
156. Hunter N, Kleckner N. 2001. The single-end invasion: an asymmetric intermediate at the double-strand break to double-Holliday junction transition of meiotic recombination. *Cell* 106(1):59–70
157. Hurlock ME, Čavka I, Kursel LE, Haversat J, Wooten M, et al. 2020. Identification of novel synaptonemal complex components in *C. elegans*. *J. Cell Biol.* 219(5):e201910043
158. Hurst LD, Nurse P. 1991. A note on the evolution of meiosis. *J. Theor. Biol.* 150(4):561–63
159. Ishiguro K, Kim J, Fujiyama-Nakamura S, Kato S, Watanabe Y. 2011. A new meiosis-specific cohesin complex implicated in the cohesin code for homologous pairing. *EMBO Rep*. 12(3):267–75
160. Ito M, Shinohara A. 2023. Chromosome architecture and homologous recombination in meiosis. *Front. Cell Dev. Biol.* 10:1097446
161. Ivanov V, Mizuuchi K. 2010. Multiple modes of interconverting dynamic pattern formation by bacterial cell division proteins. *PNAS* 107(18):8071–78
162. Jahns MT, Vezon D, Chambon A, Pereira L, Falque M, et al. 2014. Crossover localisation is regulated by the neddylation posttranslational regulatory pathway. *PLOS Biol*. 12(8):e1001930
163. Jing J, Mercier R. 2022. Meiosis: deciphering the dialog between recombination and the synaptonemal complex. *Curr. Biol.* 32(21):R1235–37
164. Johnson D, Crawford M, Cooper T, Claeys Bouuaert C, Keeney S, et al. 2021. Concerted cutting by Spo11 illuminates meiotic DNA break mechanics. *Nature* 594(7864):572–76
165. Johnson RD, Jasin M. 2001. Double-strand-break-induced homologous recombination in mammalian cells. *Biochem. Soc. Trans*. 29(Part 2):196–201
166. Jones GH, Franklin FC. 2006. Meiotic crossing-over: obligation and interference. *Cell* 126(2):246–48
167. Joyce EF, Apostolopoulos N, Beliveau BJ, Wu CT. 2013. Germline progenitors escape the widespread phenomenon of homolog pairing during *Drosophila* development. *PLOS Genet*. 9(12):e1004013
168. Joyce EF, McKim KS. 2011. Meiotic checkpoints and the interchromosomal effect on crossing over in *Drosophila* females. *Fly* 5(2):134–40
169. Kabakci Z, Reichle HE, Lemke B, Rousova D, Gupta S, et al. 2022. Homologous chromosomes are stably conjoined for *Drosophila* male meiosis I by SUM, a multimerized protein assembly with modules for DNA-binding and for separase-mediated dissociation co-opted from cohesin. *PLOS Genet*. 18(12):e1010547
170. Kar FM, Hochwagen A. 2021. Phospho-regulation of meiotic prophase. *Front. Cell Dev. Biol.* 9:667073
171. Kariyazono R, Oda A, Yamada T, Ohta K. 2019. Conserved HORMA domain-containing protein Hop1 stabilizes interaction between proteins of meiotic DNA break hotspots and chromosome axis. *Nucleic Acids Res.* 47(19):10166–80
172. Kauppi L, Jasin M, Keeney S. 2012. The tricky path to recombining X and Y chromosomes in meiosis. *Ann. N. Y. Acad. Sci.* 1267:18–23
173. Kaur H, De Muyt A, Lichten M. 2015. Top3-Rmi1 DNA single-strand decatenase is integral to the formation and resolution of meiotic recombination intermediates. *Mol. Cell* 57(4):583–94
174. Keeney S, Giroux CN, Kleckner N. 1997. Meiosis-specific DNA double-strand breaks are catalyzed by Spo11, a member of a widely conserved protein family. *Cell* 88(3):375–84
175. Keeney S, Kleckner N. 1996. Communication between homologous chromosomes: Genetic alterations at a nuclease-hypersensitive site can alter mitotic chromatin structure at that site both in *cis* and in *trans*. *Genes Cells* 1(5):475–89
176. Keeney S, Lange J, Mohibullah N. 2014. Self-organization of meiotic recombination initiation: general principles and molecular pathways. *Annu. Rev. Genet.* 48:187–214
177. Kelly KO, Dernburg AF, Stanfield GM, Villeneuve AM. 2000. *Caenorhabditis elegans msh-5* is required for both normal and radiation-induced meiotic crossing over but not for completion of meiosis. *Genetics* 156(2):617–30

178. Keyl HG. 1975. Lampbrush chromosomes in spermatocytes of *Chironomus*. *Chromosoma* 51:75–91
179. Keymakh M, Dau J, Hu J, Ferlez B, Lisby M, Crickard JB. 2022. Rdh54 stabilizes Rad51 at displacement loop intermediates to regulate genetic exchange between chromosomes. *PLOS Genet*. 18(9):e1010412
180. Kim KP, Mirkin EV. 2018. So similar yet so different: the two ends of a double strand break. *Mutat. Res.* 809:70–80
181. Kim KP, Weiner BM, Zhang L, Jordan A, Dekker J, Kleckner N. 2010. Sister cohesion and structural axis components mediate homolog bias of meiotic recombination. *Cell* 143(6):924–37
182. King JS, Mortimer RK. 1990. A polymerization model of chiasma interference and corresponding computer simulation. *Genetics* 126(4):1127–38
183. Kleckner N. 1996. Meiosis: How could it work? *PNAS* 93(16):8167–74
184. Kleckner N. 2006. Chiasma formation: chromatin/axis interplay and the role(s) of the synaptonemal complex. *Chromosoma* 115(3):175–94
185. Kleckner N, Storlazzi A, Zickler D. 2003. Coordinate variation in meiotic pachytene SC length and total crossover/chiasma frequency under conditions of constant DNA length. *Trends Genet.* 19(11):623–28
186. Kleckner N, Zickler D, Jones GH, Dekker J, Padmore R, et al. 2004. A mechanical basis for chromosome function. *PNAS* 101(34):12592–97
187. Klutstein M, Cooper JP. 2014. The chromosomal courtship dance—homolog pairing in early meiosis. *Curr. Opin. Cell Biol.* 26:123–31
188. Knoll A, Higgins JD, Seeliger K, Reha SJ, Dangel NJ, et al. 2012. The Fanconi anemia ortholog FANCM ensures ordered homologous recombination in both somatic and meiotic cells in *Arabidopsis*. *Plant Cell* 24:1448–64
189. Köhler S, Wojcik M, Xu K, Dernburg AF. 2017. Superresolution microscopy reveals the three-dimensional organization of meiotic chromosome axes in intact *Caenorhabditis elegans* tissue. *PNAS* 114(24):E4734–43
190. Kopecký D, Lukaszewski AJ, Dolezel J. 2008. Meiotic behaviour of individual chromosomes of *Festuca pratensis* in tetraploid *Lolium multiflorum*. *Chromosome Res.* 16(7):987–98
191. Koszul R, Kim KP, Prentiss M, Kleckner N, Kameoka S. 2008. Meiotic chromosomes move by linkage to dynamic actin cables with transduction of force through the nuclear envelope. *Cell* 133(7):1188–201
192. Koszul R, Kleckner N. 2009. Dynamic chromosome movements during meiosis: a way to eliminate unwanted connections? *Cell Biol.* 19(12):716–24
193. Koszul R, Meselson M, Van Doninck K, Vandenhaute J, Zickler D. 2012. The centenary of Janssens's chiasmatype theory. *Genetics* 191(2):309–17
194. Kulkarni DS, Owens SN, Honda M, Ito M, Yang Y, et al. 2020. PCNA activates the MutLγ endonuclease to promote meiotic crossing over. *Nature* 586(7830):623–27
195. Kuo P, Da Ines O, Lambing C. 2021. Rewiring meiosis for crop improvement. *Front. Plant Sci.* 12:708948
196. Kurdzo EL, Obeso D, Chuong H, Dawson DS. 2017. Meiotic centromere coupling and pairing function by two separate mechanisms in *Saccharomyces cerevisiae*. *Genetics* 205(2):657–71
197. Lai CL, Chen C, Ou SC, Prentiss M, Pettitt BM. 2020. Interactions between identical DNA double helices. *Phys. Rev. E* 101:032414
198. Lake CM, Hawley RS. 2021. Synaptonemal complex. *Curr. Biol.* 31(5):R225–27
199. Lam I, Keeney S. 2014. Mechanism and regulation of meiotic recombination initiation. *Cold Spring Harb. Perspect. Biol.* 7(1):a016634
200. Lam I, Keeney S. 2015. Nonparadoxical evolutionary stability of the recombination initiation landscape in yeast. *Science* 350(6263):932–37
201. Lambing C, Kuo P, Kim J, Osman K, Whitbread AL, et al. 2022. Differentiated function and localisation of SPO11-1 and PRD3 on the chromosome axis during meiotic DSB formation in *Arabidopsis thaliana*. *PLOS Genet*. 18(7):e1010298
202. Lan W-H, Lin S-Y, Kao C-Y, Chang W-H, Yeh H-Y, et al. 2020. Rad51 facilitates filament assembly of meiosis-specific Dmc1 recombinase. *PNAS* 117(21):11257–64
203. Lande R, Stahl FW. 1993. Chiasma interference and the distribution of exchanges in *Drosophila melanogaster*. *Cold Spring Harb. Symp. Quant. Biol.* 58:543–52
204. Lange J, Yamada S, Tischfield SE, Pan J, Kim S, et al. 2016. The landscape of mouse meiotic double-strand break formation, processing, and repair. *Cell* 167(3):695–708

205. Lao JP, Cloud V, Huang CC, Grubb J, Thacker D, et al. 2013. Meiotic crossover control by concerted action of Rad51-Dmc1 in homolog template bias and robust homeostatic regulation. *PLOS Genet.* 9(12):e1003978
206. Lao JP, Oh SD, Shinohara M, Shinohara A, Hunter N. 2008. Rad52 promotes postinvasion steps of meiotic double-strand-break repair. *Mol. Cell* 29(4):517–24
207. Láscarez-Lagunas LI, Nadarajan S, Martinez-Garcia M, Quinn JN, Todisco E, et al. 2022. ATM/ATR kinases link the synaptonemal complex and DNA double-strand break repair pathway choice. *Curr. Biol.* 32(21):4719–26
208. Lee CY, Bisig CG, Conrad MN, Ditamo Y, Previato de Almeida L, et al. 2020. Telomere-led meiotic chromosome movements: recent update in structure and function. *Nucleus* 11(9):111–16
209. Lee MS, Higashide MT, Choi H, Li K, Hong S, et al. 2021. The synaptonemal complex central region modulates crossover pathways and feedback control of meiotic double-strand break formation. *Nucleic Acids Res.* 49(13):7537–53
210. Lemmens BB, Johnson NM, Tijsterman M. 2013. COM-1 promotes homologous recombination during *Caenorhabditis elegans* meiosis by antagonizing Ku-mediated non-homologous end joining. *PLOS Genet.* 9(2):e1003276
211. Lenormand T, Engelstädter J, Johnston SE, Wijnker E, Haag CR. 2016. Evolutionary mysteries in meiosis. *Philos. Trans. R. Soc. B* 371(1706):20160001
212. Lhuissier FG, Offenberg HH, Wittich PE, Vischer NO, Heyting C. 2007. The mismatch repair protein MLH1 marks a subset of strongly interfering crossovers in tomato. *Plant Cell* 19(3):862–76
213. Liang Z, Zickler D, Prentiss M, Chang FS, Witz G, et al. 2015. Chromosomes progress to metaphase in multiple discrete steps via global compaction/expansion cycles. *Cell* 161(5):1124–37
214. Libuda DE, Uzawa S, Meyer BJ, Villeneuve AM. 2013. Meiotic chromosome structures constrain and respond to designation of crossover sites. *Nature* 502(7473):703–6
215. Lichten M, Borts RH, Haber JE. 1987. Meiotic gene conversion and crossing over between dispersed homologous sequences occurs frequently in *Saccharomyces cerevisiae*. *Genetics* 115(2):233–46
216. Lichten M, Goldman AS. 1995. Meiotic recombination hotspots. *Annu. Rev. Genet.* 29:423–44
217. Lin F-M, Lai Y-J, Shen H-J, Cheng Y-H, Wang T-F. 2010. Yeast axial-element protein, Red1, binds SUMO chains to promote meiotic interhomologue recombination and chromosome synapsis. *EMBO J.* 29(3):586–96
218. Link J, Jantsch V. 2019. Meiotic chromosomes in motion: a perspective from *Mus musculus* and *Caenorhabditis elegans*. *Chromosoma* 128(3):317–30
219. Liu H, Gordon SG, Rog O. 2021. Heterologous synapsis in *C. elegans* is regulated by meiotic double-strand breaks and crossovers. *Chromosoma* 130(4):237–50
220. Lloyd A, Morgan C, Franklin FCH, Bomblies K. 2018. Plasticity of meiotic recombination rates in response to temperature in *Arabidopsis*. *Genetics* 208(4):1409–20
221. Loidl J. 2021. *Tetrahymena* meiosis: simple yet ingenious. *PLOS Genet.* 17(7):e1009627
222. Loidl J, Scherthan H. 2004. Organization and pairing of meiotic chromosomes in the ciliate *Tetrahymena thermophila*. *J. Cell Sci.* 117(Part 24):5791–801
223. Lukaszewicz A, Lange J, Keeney S, Jasin M. 2018. Control of meiotic double-strand-break formation by ATM: local and global views. *Cell Cycle* 17(10):1155–72
224. Lukaszewicz A, Lange J, Keeney S, Jasin M. 2021. De novo deletions and duplications at recombination hotspots in mouse germlines. *Cell* 184(24):5970–84
225. Maguire MP, Reiss RW. 1996. The coupling of crossing over and synapsis in maize inversions. *Genetica* 98:263–72
226. Manhart CM, Alani E. 2016. Roles for mismatch repair family proteins in promoting meiotic crossing over. *DNA Repair* 38:84–93
227. Marko JF, Siggia ED. 1997. Polymer models of meiotic and mitotic chromosomes. *Mol. Biol. Cell* 8(11):2217–31
228. Marsolier-Kergoat MC, Khan MM, Schott J, Zhu X, Llorente B. 2018. Mechanistic view and genetic control of DNA recombination during meiosis. *Mol. Cell* 70(1):9–20

229. Martinez-Garcia M, Schubert V, Osman K, Darbyshire A, Sanchez-Moran E, Franklin FCH. 2018. TOPII and chromosome movement help remove interlocks between entangled chromosomes during meiosis. *J. Cell Biol.* 217(12):4070–79
230. Martini E, Borde V, Legendre M, Audic S, Regnault B, et al. 2011. Genome-wide analysis of heteroduplex DNA in mismatch repair-deficient yeast cells reveals novel properties of meiotic recombination pathways. *PLOS Genet*. 7(9):e1002305
231. Martini E, Diaz RL, Hunter N, Keeney S. 2006. Crossover homeostasis in yeast meiosis. *Cell* 126(2):285–95
232. Mazur AK, Gladyshev E. 2023. C-DNA may facilitate homologous DNA pairing. *Trends Genet*. 39(7):575–85
233. McDonald MJ, Rice DP, Desai MM. 2016. Sex speeds adaptation by altering the dynamics of molecular evolution. *Nature* 531(7593):233–36
234. Mercier R, Mézard C, Jenczewski E, Macaisne N, Grelon M. 2015. The molecular biology of meiosis in plants. *Annu. Rev. Plant Biol.* 66:297–327
235. Mhaskar AN, Koornneef L, Zelensky AN, Houtsmuller AB, Baarends WM. 2021. High resolution view on the regulation of recombinase accumulation in mammalian meiosis. *Front. Cell Dev. Biol.* 9:672191
236. Mirny L, Slutsky M, Wunderlich Z, Tafvizi A, Leith J, Kosmrlj A. 2009. How a protein searches for its site on DNA: the mechanism of facilitated diffusion. *J. Phys. A Math. Theor.* 42:434013
237. Mitchison TJ. 2020. Beyond Langmuir: surface-bound macromolecule condensates. *Mol. Biol. Cell* 31(23):2502–8
238. Miyoshi T, Ito M, Kugou K, Yamada S, Furuichi M, et al. 2012. A central coupler for recombination initiation linking chromosome architecture to S phase checkpoint. *Mol. Cell* 47(5):722–33
239. Mizuuchi K, Vecchiarelli AG. 2018. Mechanistic insights of the Min oscillator via cell-free reconstitution and imaging. *Phys. Biol.* 15(3):031001
240. Moens PB, Kolas NK, Tarsounas M, Marcon E, Cohen PE, Spyropoulos B. 2002. The time course and chromosomal localization of recombination-related proteins at meiosis in the mouse are compatible with models that can resolve the early DNA-DNA interactions without reciprocal recombination. *J. Cell Sci.* 115:1611–22
241. Moens PB, Marcon E, Shore JS, Kochakpour N, Spyropoulos B. 2007. Initiation and resolution of interhomolog connections: crossover and non-crossover sites along mouse synaptonemal complexes. *J. Cell Sci.* 120(6):1017–27
242. Moens PB, Pearlman RE. 1988. Chromatin organization at meiosis. *Bioessays* 9:151–53
243. Mora-Bermúdez F, Gerlich D, Ellenberg J. 2007. Maximal chromosome compaction occurs by axial shortening in anaphase and depends on Aurora kinase. *Nat. Cell Biol.* 9(7):822–31
244. Morgan C, Fozard JA, Hartley M, Henderson IR, Bomblies K, Howard M. 2021. Diffusion-mediated HEI10 coarsening can explain meiotic crossover positioning in *Arabidopsis*. *Nat. Commun.* 12(1):4674
245. Morgan C, Nayak A, Hosoya N, Smith GR, Lambing C. 2023. Meiotic chromosome organization and its role in recombination and cancer. *Curr. Top. Dev. Biol.* 151:91–126
246. Morgan C, White MA, Franklin FCH, Zickler D, Kleckner N, Bomblies K. 2021. Evolution of crossover interference enables stable autopolyploidy by ensuring pairwise partner connections in *Arabidopsis arenosa*. *Curr. Biol.* 31(21):4713–26
247. Morgan CH, Zhang H, Bomblies K. 2017. Are the effects of elevated temperature on meiotic recombination and thermotolerance linked via the axis and synaptonemal complex? *Philos. Trans. R. Soc. B* 372(1736):20160470
248. Mu X, Murakami H, Mohibullah N, Keeney S. 2020. Chromosome-autonomous feedback downregulates meiotic DNA break competence upon synaptonemal complex formation. *Genes Dev.* 34(23–24):1605–18
249. Muller HJ. 1916. The mechanism of crossing-over. I–IV. *Am. Nat.* 50:193–434
250. Murakami H, Keeney S. 2008. Regulating the formation of DNA double-strand breaks in meiosis. *Genes Dev.* 22(3):286–92
251. Murakami H, Keeney S. 2014. DDK links replication and recombination in meiosis. *Cell Cycle* 13(23):3621–22

252. Murakami H, Mu X, Keeney S. 2021. How do small chromosomes know they are small? Maximizing meiotic break formation on the shortest yeast chromosomes. *Curr. Genet.* 67(3):431–37
253. Neale MJ, Pan J, Keeney S. 2005. Endonucleolytic processing of covalent protein-linked DNA double-strand breaks. *Nature* 436(7053):1053–57
254. Nebel BR, Coulon EM. 1962. The fine structure of chromosomes in pigeon spermatocytes. *Chromosoma* 13:272–91
255. Nguyen H, Labella S, Silva N, Jantsch V, Zetka M. 2018. *C. elegans* ZHP-4 is required at multiple distinct steps in the formation of crossovers and their transition to segregation competent chiasmata. *PLOS Genet.* 14(10):e1007776
256. Ninan CA. 1958. Studies on the cytology and phylogeny of the Pteridophytes. VI. Observations on the Ophioglossaceae. *Cytologia* 23:291–316
257. Nora EP, Dekker J, Heard E. 2013. Segmental folding of chromosomes: a basis for structural and regulatory chromosomal neighborhoods? *Bioessays* 35(9):818–28
258. Novak I, Wang H, Revenkova E, Jessberger R, Scherthan H, Höög C. 2008. Cohesin Smc1β determines meiotic chromatin axis loop organization. *J. Cell Biol.* 180(1):83–90
259. Nozaki T, Chang F, Weiner B, Kleckner N. 2021. High temporal resolution 3D live-cell imaging of budding yeast meiosis defines discontinuous actin/telomere-mediated chromosome motion, correlated nuclear envelope deformation and actin filament dynamics. *Front. Cell Dev. Biol.* 9:687132
260. Oh SD, Lao JP, Hwang PYH, Taylor AF, Smith GR, Hunter N. 2007. BLM ortholog, Sgs1, prevents aberrant crossing-over by suppressing formation of multichromatid joint molecules. *Cell* 130(2):259–72
261. Oh SD, Lao JP, Taylor AF, Smith GR, Hunter N. 2008. RecQ helicase, Sgs1, and XPF family endonuclease, Mus81-Mms4, resolve aberrant joint molecules during meiotic recombination. *Mol. Cell* 31(3):324–36
262. Ohta K, Wu TC, Lichten M, Shibata T. 1999. Competitive inactivation of a double-strand DNA break site involves parallel suppression of meiosis-induced changes in chromatin configuration. *Nucleic Acids Res.* 27(10):2175–80
263. Oliver-Bonet M, Campillo M, Turek PJ, Ko E, Martin RH. 2007. Analysis of replication protein A (RPA) in human spermatogenesis. *Mol. Hum. Reprod.* 13:837–44
264. Oomen ME, Hedger AK, Watts JK, Dekker J. 2020. Detecting chromatin interactions between and along sister chromatids with SisterC. *Nat. Methods* 17(10):1002–9
265. Osman K, Algopishi U, Higgins JD, Henderson IR, Edwards KJ, et al. 2021. Distal bias of meiotic crossovers in hexaploid bread wheat reflects spatio-temporal asymmetry of the meiotic program. *Front. Plant Sci.* 12:631323
266. Osman K, Sanchez-Moran E, Higgins JD, Jones GH, Franklin FC. 2006. Chromosome synapsis in *Arabidopsis*: analysis of the transverse filament protein ZYP1 reveals novel functions for the synaptonemal complex. *Chromosoma* 115(3):212–19
267. Osman K, Sanchez-Moran E, Mann SC, Jones GH, Franklin FC. 2009. Replication protein A (AtRPA1a) is required for class I crossover formation but is dispensable for meiotic DNA break repair. *EMBO J.* 28(4):394–404
268. Ottolini CS, Newnham L, Capalbo A, Natesan SA, Joshi HA, et al. 2015. Genome-wide maps of recombination and chromosome segregation in human oocytes and embryos show selection for maternal recombination rates. *Nat. Genet.* 47(7):727–35
269. Owens S, Tang S, Hunter N. 2018. Monitoring recombination during meiosis in budding yeast. *Methods Enzymol.* 601:275–307
270. Padmore R, Cao L, Kleckner N. 1991. Temporal comparison of recombination and synaptonemal complex formation during meiosis in *S. cerevisiae*. *Cell* 66(6):1239–56
271. Page SL, Hawley RS. 2001. *c(3)G* encodes a *Drosophila* synaptonemal complex protein. *Genes Dev.* 15(23):3130–43
272. Paigen K, Petkov PM. 2018. PRDM9 and its role in genetic recombination. *Trends Genet.* 34(4):291–300
273. Pan J, Sasaki M, Kniewel R, Murakami H, Blitzblau HG, et al. 2011. A hierarchical combination of factors shapes the genome-wide topography of yeast meiotic recombination initiation. *Cell* 144(5):719–31
274. Panizza S, Mendoza MA, Berlinger M, Huang L, Nicolas A, et al. 2011. Spo11-accessory proteins link double-strand break sites to the chromosome axis in early meiotic recombination. *Cell* 146(3):372–83

275. Paouneskou D, Jantsch V. 2019. Meiotic chromosome movement: What's lamin got to do with it? *Nucleus* 10(1):1–6
276. Pazhayam NM, Turcotte CA, Sekelsky J. 2021. Meiotic crossover patterning. *Front. Cell Dev. Biol.* 9:681123
277. Petkov PM, Broman KW, Szatkiewicz JP, Paigen K. 2007. Crossover interference underlies sex differences in recombination rates. *Trends Genet.* 23(11):539–42
278. Piazza A, Heyer WD. 2018. Multi-invasion-induced rearrangements as a pathway for physiological and pathological recombination. *Bioessays* 40(5):e1700249
279. Ponting CP. 2011. What are the genomic drivers of the rapid evolution of PRDM9? *Trends Genet.* 27(5):165–71
280. Pratto F, Brick K, Cheng G, Lam KG, Cloutier JM, et al. 2021. Meiotic recombination mirrors patterns of germline replication in mice and humans. *Cell* 184(16):4251–67
281. Previato de Almeida L, Evatt JM, Chuong HH, Kurdzo EL, Eyster CA, et al. 2019. Shugoshin protects centromere pairing and promotes segregation of nonexchange partner chromosomes in meiosis. *PNAS* 116(19):9417–22
282. Prieler S, Chen D, Huang L, Mayrhofer E, Zsótér S, et al. 2021. Spo11 generates gaps through concerted cuts at sites of topological stress. *Nature* 594(7864):577–82
283. Prince JP, Martinez-Perez E. 2022. Functions and regulation of meiotic HORMA-domain proteins. *Genes* 13(5):777
284. Protacio RU, Davidson MK, Wahls WP. 2022. Adaptive control of the meiotic recombination landscape by DNA site-dependent hotspots with implications for evolution. *Front. Genet.* 13:947572
285. Pyatnitskaya A, Andreani J, Guérois R, De Muyt A, Borde V. 2022. The Zip4 protein directly couples meiotic crossover formation to synaptonemal complex assembly. *Genes Dev.* 36(1–2):53–69
286. Pyatnitskaya A, Borde V, De Muyt A. 2019. Crossing and zipping: molecular duties of the ZMM proteins in meiosis. *Chromosoma* 128(3):181–98
287. Qiao H, Chen JK, Reynolds A, Höög C, Paddy M, Hunter N. 2012. Interplay between synaptonemal complex, homologous recombination, and centromeres during mammalian meiosis. *PLOS Genet.* 8(6):e1002790
288. Qiao H, Rao HBDP, Yang Y, Fong JH, Cloutier JM, et al. 2014. Antagonistic roles of ubiquitin ligase HEI10 and SUMO ligase RNF212 regulate meiotic recombination. *Nat. Genet.* 46(2):194–99
289. Rao HBDP, Qiao H, Bhatt SK, Bailey LR, Tran HD, et al. 2017. A SUMO-ubiquitin relay recruits proteasomes to chromosome axes to regulate meiotic recombination. *Science* 355(6323):403–7
290. Rao HBDP, Sato T, Challa K, Fujita Y, Shinohara M, Shinohara A. 2021. Phosphorylation of luminal region of the SUN-domain protein Mps3 promotes nuclear envelope localization during meiosis. *eLife* 10:e63119
291. Rasmussen SW. 1977. Meiosis in *Bombyx mori* females. *Philos. Trans. R. Soc. B* 277(955):343–50
292. Rasmussen SW. 1986. Initiation of synapsis and interlocking of chromosomes during zygotene in *Bombyx* spermatocytes. *Carlsberg Res. Commun.* 1(6):401–32
293. Rasmussen SW, Holm PB. 1978. Human meiosis II. Chromosome pairing and recombination nodules in human spermatocytes. *Carlsberg Res. Commun.* 43(5):275–327
294. Reitz D, Grubb J, Bishop DK. 2019. A mutant form of Dmc1 that bypasses the requirement for accessory protein Mei5-Sae3 reveals independent activities of Mei5-Sae3 and Rad51 in Dmc1 filament stability. *PLOS Genet.* 15(12):e1008217
295. Reynolds A, Qiao H, Yang Y, Chen JK, Jackson N, et al. 2013. RNF212 is a dosage-sensitive regulator of crossing-over during mammalian meiosis. *Nat. Genet.* 45(3):269–78
296. Rhoades N, Nguyen T-S, Witz G, Cecere G, Hammond T, et al. 2021. Recombination-independent recognition of DNA homology for meiotic silencing in *Neurospora crassa*. *PNAS* 118(33):e2108664118
297. Robert T, Vrielynck N, Mézard C, de Massy B, Grelon M. 2016. A new light on the meiotic DSB catalytic complex. *Semin. Cell Dev. Biol.* 54:165–76
298. Rog O, Dernburg AF. 2013. Chromosome pairing and synapsis during *Caenorhabditis elegans* meiosis. *Curr. Opin. Cell Biol.* 25(3):349–56
299. Rog O, Köhler S, Dernburg AF. 2017. The synaptonemal complex has liquid crystalline properties and spatially regulates meiotic recombination factors. *eLife* 6:e21455

300. Rousová D, Nivsarkar V, Altmannova V, Raina VB, Funk SK, et al. 2021. Novel mechanistic insights into the role of Mer2 as the keystone of meiotic DNA break formation. *eLife* 10:e72330
301. Rubin T, Macaisne N, Vallés AM, Guilleman C, Gaugué I, et al. 2022. Premeiotic pairing of homologous chromosomes during *Drosophila* male meiosis. *PNAS* 119(47):e2207660119
302. Saitoh Y, Laemmli UK. 1994. Metaphase chromosome structure: Bands arise from a differential folding path of the highly AT-rich scaffold. *Cell* 76(4):609–22
303. Sakuno T, Tashiro S, Tanizawa H, Iwasaki O, Ding D-Q, et al. 2022. Rec8 cohesin-mediated axis-loop chromatin architecture is required for meiotic recombination. *Nucleic Acids Res.* 50(7):3799–816
304. Sandhu R, Monge Neria F, Monge Neria J, Chen X, Hollingsworth NM, Börner GV. 2020. DNA helicase Mph1^{FANCM} ensures meiotic recombination between parental chromosomes by dissociating precocious displacement loops. *Dev. Cell* 53(4):458–72.e5
305. Sarens M, Copenhaver GP, De Storme N. 2021. The role of chromatid interference in determining meiotic crossover patterns. *Front. Plant Sci.* 12:656691
306. Schalbetter SA, Fudenberg G, Baxter J, Pollard KS, Neale MJ. 2019. Principles of meiotic chromosome assembly revealed in *S. cerevisiae*. *Nat. Commun.* 10(1):4795
307. Scherthan H. 2001. A bouquet makes ends meet. *Nat. Rev. Mol. Cell Biol.* 2(8):621–27
308. Scherthan H, Schöfisch K, Dell T, Illner D. 2014. Contrasting behavior of heterochromatic and euchromatic chromosome portions and pericentric genome separation in pre-bouquet spermatocytes of hybrid mice. *Chromosoma* 123(6):609–24
309. Scherthan H, Sfeir A, de Lange T. 2011. Rap1-independent telomere attachment and bouquet formation in mammalian meiosis. *Chromosoma* 120(2):151–57
310. Scherthan H, Wang H, Adelfalk C, White EJ, Cowan C, et al. 2007. Chromosome mobility during meiotic prophase in *Saccharomyces cerevisiae*. *PNAS* 104(43):16934–39
311. Schield DR, Pasquesi GIM, Perry BW, Adams RH, Nikolakis ZL, et al. 2020. Snake recombination landscapes are concentrated in functional regions despite PRDM9. *Mol. Biol. Evol.* 37(5):1272–94
312. Schlecht HB, Lichten M, Goldman AS. 2004. Compartmentalization of the yeast meiotic nucleus revealed by analysis of ectopic recombination. *Genetics* 168(3):1189–203
313. Senmatsu S, Asada R, Oda A, Hoffman CS, Ohta K, Hirota K. 2021. lncRNA transcription induces meiotic recombination through chromatin remodeling in fission yeast. *Commun. Biol.* 4(1):295
314. Serra H, Lambing C, Griffin CH, Topp SD, Nageswaran DC, et al. 2018. Massive crossover elevation via combination of *HEI10* and *recq4a recq4b* during *Arabidopsis* meiosis. *PNAS* 115(10):2437–42
315. Serrentino ME, Chaplais E, Sommermeyer V, Borde V. 2013. Differential association of the conserved SUMO ligase Zip3 with meiotic double-strand break sites reveals regional variations in the outcome of meiotic recombination. *PLOS Genet.* 9(4):e1003416
316. Shinohara M, Hayashihara K, Grubb JT, Bishop DK, Shinohara A. 2015. DNA damage response clamp 9-1-1 promotes assembly of ZMM proteins for formation of crossovers and synaptonemal complex. *J. Cell Sci.* 128(8):1494–506
317. Shinohara M, Oh SD, Hunter N, Shinohara A. 2008. Crossover assurance and crossover interference are distinctly regulated by the ZMM proteins during yeast meiosis. *Nat. Genet.* 40(3):299–309
318. Shinohara M, Sakai K, Shinohara A, Bishop DK. 2003. Crossover interference in *Saccharomyces cerevisiae* requires a *TID1/RDH54*- and *DMC1*-dependent pathway. *Genetics* 163(4):1273–86
319. Sims J, Rabanal FA, Elgert C, von Haeseler A, Schlögelhofer P. 2021. It is just a matter of time: balancing homologous recombination and non-homologous end joining at the rDNA locus during meiosis. *Front. Plant Sci.* 12:773052
320. Singh DK, Gamboa RS, Singh AK, Walkemeier B, Van Leene J, et al. 2023. The FANCC–FANCE–FANCF complex is evolutionarily conserved and regulates meiotic recombination. *Nucleic Acids Res.* 51(6):2516–28
321. Singhal S, Leffler EM, Sannareddy K, Turner I, Venn O, et al. 2015. Stable recombination hotspots in birds. *Science* 350(6263):928–32
322. Slotman JA, Paul MW, Carofiglio F, de Gruiter HM, Vergroesen T, et al. 2020. Super-resolution imaging of RAD51 and DMC1 in DNA repair foci reveals dynamic distribution patterns in meiotic prophase. *PLOS Genet.* 16(6):e1008595

323. Song M, Zhai B, Yang X, Tan T, Wang Y, et al. 2021 Interplay between Pds5 and Rec8 in regulating chromosome axis length and crossover frequency. *Sci. Adv.* 7(11):eabe7920
324. Spruce C, Dlamini S, Ananda G, Bronkema N, Tian H, et al. 2020. HELLS and PRDM9 form a pioneer complex to open chromatin at meiotic recombination hot spots. *Genes Dev*. 34(5–6):398–412
325. Storlazzi A, Gargano S, Ruprich-Robert G, Falque M, David M, et al. 2010. Recombination proteins mediate meiotic spatial chromosome organization and pairing. *Cell* 141(1):94–106
326. Storlazzi A, Xu L, Schwacha A, Kleckner N. 1996. Synaptonemal complex (SC) component Zip1 plays a role in meiotic recombination independent of SC polymerization along the chromosomes. *PNAS* 93(17):9043–48
327. Subramanian VV, Zhu X, Markowitz TE, Vale-Silva LA, San-Segundo PA, et al. 2019. Persistent DNA-break potential near telomeres increases initiation of meiotic recombination on short chromosomes. *Nat. Commun.* 10(1):970
328. Sun X, Huang L, Markowitz TE, Blitzblau HG, Chen D, et al. 2015. Transcription dynamically patterns the meiotic chromosome-axis interface. *eLife* 4:e07424
329. Taagen E, Bogdanove AJ, Sorrells ME. 2020. Counting on crossovers: controlled recombination for plant breeding. *Trends Plant Sci.* 25(5):455–65
330. Taagen E, Jordan K, Akhunov E, Sorrells ME, Jannink JL. 2022. If it ain't broke, don't fix it: evaluating the effect of increased recombination on response to selection for wheat breeding. *G3* 12(12):jkac291
331. Tan R, Lam AJ, Tan T, Han J, Nowakowski DW, et al. 2019. Microtubules gate tau condensation to spatially regulate microtubule functions. *Nat. Cell Biol.* 21(9):1078–85
332. Tang S, Wu MKY, Zhang R, Hunter N. 2015. Pervasive and essential roles of the Top3-Rmi1 decatenase orchestrate recombination and facilitate chromosome segregation in meiosis. *Mol. Cell* 57(4):607–21
333. Tease C, Jones GH. 1995. Do chiasmata disappear? An examination of whether closely spaced chiasmata are liable to reduction or loss. *Chromosome Res.* 3:162–68
334. Tessé S, Bourbon HM, Debuchy R, Budin K, Dubois E, et al. 2017. Asy2/Mer2: an evolutionarily conserved mediator of meiotic recombination, pairing, and global chromosome compaction. *Genes Dev*. 31(18):1880–93
335. Tessé S, Storlazzi A, Kleckner N, Gargano S, Zickler D. 2003. Localization and roles of Ski8p protein in *Sordaria* meiosis and delineation of three mechanistically distinct steps of meiotic homolog juxtaposition. *PNAS* 100(22):12865–70
336. Thacker D, Mohibullah N, Zhu X, Keeney S. 2014. Homologue engagement controls meiotic DNA break number and distribution. *Nature* 510(7504):241–46
337. Tian H, Billings T, Petkov PM. 2021. EWSR1 affects PRDM9-dependent histone 3 methylation and provides a link between recombination hotspots and the chromosome axis protein REC8. *Mol. Biol. Cell* 32(1):1–14
338. Tock AJ, Henderson IR. 2018. Hotspots for initiation of meiotic recombination. *Front. Genet.* 9:521
339. Tsubouchi H. 2023. The Hop2-Mnd1 complex and its regulation of homologous recombination. *Biomolecules* 13(4):662
340. Tsubouchi H, Argunhan B, Ito K, Takahashi M, Iwasaki H. 2020. Two auxiliary factors promote Dmc1-driven DNA strand exchange via stepwise mechanisms. *PNAS* 117(22):12062–70
341. Tsubouchi H, Argunhan B, Tsubouchi T. 2016. Shaping meiotic chromosomes with SUMO: A feedback loop controls the assembly of the synaptonemal complex in budding yeast. *Microb. Cell* 3(3):126–28
342. Tsubouchi T, Zhao H, Roeder GS. 2006. The meiosis-specific Zip4 protein regulates crossover distribution by promoting synaptonemal complex formation together with Zip2. *Dev. Cell* 10(6):809–19
343. Uanschou C, Ronceret A, Von Harder M, De Muyt A, Vezon D, et al. 2013. Sufficient amounts of functional HOP2/MND1 complex promote interhomolog DNA repair but are dispensable for intersister DNA repair during meiosis in *Arabidopsis*. *Plant Cell* 25(12):4924–40
344. Underwood CJ, Mercier R. 2022. Engineering apomixis: clonal seeds approaching the fields. *Annu. Rev. Plant Biol.* 73:201–25
345. Ur SN, Corbett KD. 2021. Architecture and dynamics of meiotic chromosomes. *Annu. Rev. Genet.* 55:497–526

346. Vasnier C, de Muyt A, Zhang L, Tessé S, Kleckner NE, et al. 2014. Absence of SUN-domain protein Slp1 blocks karyogamy and switches meiotic recombination and synapsis from homologs to sister chromatids. *PNAS* 111(38):E4015–23
347. Veller C, Kleckner N, Nowak MA. 2019. A rigorous measure of genome-wide genetic shuffling that takes into account crossover positions and Mendel's second law. *PNAS* 116(5):1659–68
348. Veller C, Wang S, Zickler D, Zhang L, Kleckner N. 2022. Limitations of gamete sequencing for crossover analysis. *Nature* 606(7913):E1–3
349. Vernekar DV, Reginato G, Adam C, Ranjha L, Dingli F, et al. 2021. The Pif1 helicase is actively inhibited during meiotic recombination which restrains gene conversion tract length. *Nucleic Acids Res.* 49(8):4522–33
350. Viera A, Santos JL, Parra MT, Calvente A, Gómez R, et al. 2010. Incomplete synapsis and chiasma localization: the chicken or the egg? *Cytogenet. Genome Res.* 128(1–3):139–51
351. Vincenten N, Kuhl L-M, Lam I, Oke A, Kerr ARW, et al. 2015. The kinetochore prevents centromere-proximal crossover recombination during meiosis. *eLife* 4:e10850
352. von Diezmann L, Rog O. 2021. Let's get physical—mechanisms of crossover interference. *J. Cell Sci.* 134(10):jcs255745
353. von Wettstein D, Rasmussen SW, Holm PB. 1984. The synaptonemal complex in genetic segregation. *Annu. Rev. Genet.* 18:331–413
354. Vrielynck N, Schneider K, Rodriguez M, Sims J, Chambon A, et al. 2021. Conservation and divergence of meiotic DNA double strand break forming mechanisms in *Arabidopsis thaliana*. *Nucleic Acids Res.* 49(17):9821–35
355. Walther N, Hossain MJ, Politi AZ, Koch B, Kueblbeck M, et al. 2018. A quantitative map of human condensins provides new insights into mitotic chromosome architecture. *J. Cell Biol.* 217(7):2309–28
356. Wang CR, Carlton PM, Golubovskaya IN, Cande WZ. 2009. Interlock formation and coiling of meiotic chromosome axes during synapsis. *Genetics* 183(3):905–15
357. Wang S, Hassold T, Hunt P, White MA, Zickler D, et al. 2017. Inefficient crossover maturation underlies elevated aneuploidy in human female meiosis. *Cell* 168(6):977–89
358. Wang S, Kleckner N, Zhang L. 2017. Crossover maturation inefficiency and aneuploidy in human female meiosis. *Cell Cycle* 16(11):1017–19
359. Wang S, Veller C, Sun F, Ruiz-Herrera A, Shang Y, et al. 2019. Per-nucleus crossover covariation and implications for evolution. *Cell* 177(2):326–38
360. Wang S, Zickler D, Kleckner N, Zhang L. 2015. Meiotic crossover patterns: obligatory crossover, interference and homeostasis in a single process. *Cell Cycle* 14(3):305–14
361. Wang Y, Li S-Y, Wang Y-Z, He Y. 2023. ZmASY1 interacts with ZmPRD3 and is crucial for meiotic double-strand break formation in maize. *New Phytol.* 237(2):454–70
362. Wang Y, Zhai B, Tan T, Yang X, Zhang J, et al. 2021. ESA1 regulates meiotic chromosome axis and crossover frequency via acetylating histone H4. *Nucleic Acids Res.* 49(16):9353–73
363. Wartosch L, Schindler K, Schuh M, Gruhn JR, Hoffmann ER, et al. 2021. Origins and mechanisms leading to aneuploidy in human eggs. *Prenat. Diagn.* 41(5):620–30
364. West AM, Rosenberg SC, Ur SN, Lehmer MK, Ye Q, et al. 2019. A conserved filamentous assembly underlies the structure of the meiotic chromosome axis. *eLife* 8:e40372
365. Wilkins AS, Holliday R. 2009. The evolution of meiosis from mitosis. *Genetics* 181(1):3–12
366. Woglar A, Jantsch V. 2014. Chromosome movement in meiosis I prophase of *Caenorhabditis elegans*. *Chromosoma* 123(1–2):15–24
367. Woglar A, Villeneuve AM. 2018. Dynamic architecture of DNA repair complexes and the synaptonemal complex at sites of meiotic recombination. *Cell* 173(7):1678–91
368. Woglar A, Yamaya K, Roelens B, Boettiger A, Köhler S, Villeneuve AM. 2020. Quantitative cytogenetics reveals molecular stoichiometry and longitudinal organization of meiotic chromosome axes and loops. *PLOS Biol.* 18(8):e3000817
369. Wooldridge LK, Dumont BL. 2023. Rapid evolution of the fine-scale recombination landscape in wild house mouse (*Mus musculus*) populations. *Mol. Biol. Evol.* 40(1):msac267
370. Wu FL, Strand AI, Cox LA, Ober C, Wall JD, et al. 2020. A comparison of humans and baboons suggests germline mutation rates do not track cell divisions. *PLOS Biol.* 18(8):e3000838

371. Wynne DJ, Rog O, Carlton PM, Dernburg AF. 2012. Dynein-dependent processive chromosome motions promote homologous pairing in *C. elegans* meiosis. *J. Cell Biol.* 196(1):47–64
372. Xaver M, Huang L, Chen D, Klein F. 2013. Smc5/6-Mms21 prevents and eliminates inappropriate recombination intermediates in meiosis. *PLOS Genet.* 9(12):e1004067
373. Xu L, Kleckner N. 1995. Sequence non-specific double-strand breaks and interhomolog interactions prior to double-strand break formation at a meiotic recombination hot spot in yeast. *EMBO J.* 14(20):5115–28
374. Yadav VK, Claeys Bouuaert C. 2021. Mechanism and control of meiotic DNA double-strand break formation in *S. cerevisiae*. *Front. Cell Dev. Biol.* 9:642737
375. Yamada S, Hinch AG, Kamido H, Zhang Y, Edelmann W, Keeney S. 2020. Molecular structures and mechanisms of DNA break processing in mouse meiosis. *Genes Dev.* 34(11–12):806–18
376. Yancey-Wrona JE, Camerini-Otero RD. 1995. The search for DNA homology does not limit stable homologous pairing promoted by RecA protein. *Curr. Biol.* 5(10):1149–58
377. Yang D, Boyer B, Prévost C, Danilowicz C, Prentiss M. 2015. Integrating multi-scale data on homologous recombination into a new recognition mechanism based on simulations of the RecA-ssDNA/dsDNA structure. *Nucleic Acids Res.* 43(21):10251–63
378. Yang X, Song M, Wang Y, Tan T, Tian Z, et al. 2022. The ubiquitin–proteasome system regulates meiotic chromosome organization. *PNAS* 119(17):e2106902119
379. Yang X, Zhai B, Wang S, Kong X, Tan Y, et al. 2021. RNA-DNA hybrids regulate meiotic recombination. *Cell Rep.* 37(10):110097
380. Yokoo R, Zawadzki KA, Nabeshima K, Drake M, Arur S, Villeneuve AM. 2012. COSA-1 reveals robust homeostasis and separable licensing and reinforcement steps governing meiotic crossovers. *Cell* 149(1):75–87
381. Yoon S-W, Lee M-S, Xaver M, Zhang L, Hong S-G, et al. 2016. Meiotic prophase roles of Rec8 in crossover recombination and chromosome structure. *Nucleic Acids Res.* 44(19):9296–314
382. Yoshimura SH, Hirano T. 2016. HEAT repeats—versatile arrays of amphiphilic helices working in crowded environments? *J. Cell Sci.* 129(21):3963–70
383. Yun H, Kim K. 2019. Ku complex suppresses recombination in the absence of MRX activity during budding yeast meiosis. *BMB Rep.* 52(10):607–12
384. Zakharyevich K, Tang S, Ma Y, Hunter N. 2012. Delineation of joint molecule resolution pathways in meiosis identifies a crossover-specific resolvase. *Cell* 149(2):334–47
385. Zelazowski MJ, Cole F. 2016. X marks the spot: PRDM9 rescues hybrid sterility by finding hidden treasure in the genome. *Nat. Struct. Mol. Biol.* 23(4):267–69
386. Zelazowski MJ, Sandoval M, Paniker L, Hamilton HM, Han J, et al. 2017. Age-dependent alterations in meiotic recombination cause chromosome segregation errors in spermatocytes. *Cell* 171(3):601–14
387. Zetka M, Paouneskou D, Jantsch V. 2020. The nuclear envelope, a meiotic jack-of-all-trades. *Curr. Opin. Cell Biol.* 64:34–42
388. Zhang L, Espagne E, de Muyt A, Zickler D, Kleckner NE. 2014. Interference-mediated synaptonemal complex formation with embedded crossover designation. *PNAS* 111(47):E5059–68
389. Zhang L, Kim KP, Kleckner NE, Storlazzi A. 2011. Meiotic double-strand breaks occur once per pair of (sister) chromatids and, via Mec1/ATR and Tel1/ATM, once per quartet of chromatids. *PNAS* 108(50):20036–41
390. Zhang L, Köhler S, Rillo-Bohn R, Dernburg AF. 2018. A compartmentalized signaling network mediates crossover control in meiosis. *eLife* 7:e30789
391. Zhang L, Liang Z, Hutchinson J, Kleckner N. 2014. Crossover patterning by the beam-film model: analysis and implications. *PLOS Genet.* 10(1):e1004042
392. Zhang L, Wang S, Yin S, Hong S, Kim KP, Kleckner N. 2014. Topoisomerase II mediates meiotic crossover interference. *Nature* 511(7511):551–56
393. Zhang Z, Xie S, Wang R, Guo S, Zhao Q, et al. 2020. Multivalent weak interactions between assembly units drive synaptonemal complex formation. *J. Cell Biol.* 219(5):e201910086
394. Zickler D. 1977. Development of the synaptonemal complex and the "recombination nodules" during meiotic prophase in the seven bivalents of the fungus *Sordaria macrospora* Auersw. *Chromosoma* 61(4):289–316

395. Zickler D. 2006. From early homologue recognition to synaptonemal complex formation. *Chromosoma* 115(3):158–74
396. Zickler D, Kleckner N. 1998. The leptotene-zygotene transition of meiosis. *Annu. Rev. Genet.* 32:619–97
397. Zickler D, Kleckner N. 1999. Meiotic chromosomes: integrating structure and function. *Annu. Rev. Genet.* 33:603–754
398. Zickler D, Kleckner N. 2015. Recombination, pairing, and synapsis of homologs during meiosis. *Cold Spring Harb. Perspect. Biol.* 7(6):a016626
399. Zwettler FU, Spindler M-C, Reinhard S, Klein T, Kurz A, et al. 2020. Tracking down the molecular architecture of the synaptonemal complex by expansion microscopy. *Nat. Commun.* 11(1):3222